New diaryl-1,2,4-triazolo[3,4-a]pyrimidine hybrids as selective COX-2/sEH dual inhibitors with potent analgesic/anti-inflammatory and cardioprotective properties

Lamya H. Al-Wahaibi[1], Mostafa H. Abdel-Rahman[2], Khaled El-Adl[3,4], Bahaa G.M. Youssif[5]*, Stefan Bräse[6]*, Salah A. Abdel-Aziz[7,8]*

[1]Department of Chemistry, College of Sciences, Princess Nourah bint Abdulrahman University, Riyadh 11671, Saudi Arabia; [2]Department of Pharmaceutical Organic Chemistry, Faculty of Pharmacy(Boys), Al-Azhar University, Assiut 71524, Egypt; [3]Department of Chemistry, Faculty of Pharmacy, Heliopolis University for Sustainable Development, Cairo, Egypt. [4]Department of Pharmaceutical Medicinal Chemistry and Drug Design, Faculty of Pharmacy (Boys) Al-Azhar University Cairo Egypt. [5]Department of Pharmaceutical Organic Chemistry, Faculty of Pharmacy, Assiut University, Assiut 71526, Egypt; [6]Institute of Biological and Chemical Systems, IBCS-FMS, Karlsruhe Institute of Technology, 76131 Karlsruhe, Germany; [7]Department of Pharmaceutical Medicinal Chemistry and Drug Design, Faculty of Pharmacy (Boys) Al-Azhar University Assiut 71524, Egypt; [8]Department of Pharmaceutical Chemistry, Faculty of Pharmacy, Deraya University, Minia 61519, Egypt.

**To whom correspondence should be addressed:*

Bahaa G. M. Youssif, Ph.D. Pharmaceutical Organic Chemistry Department, Faculty of Pharmacy, Assiut University, Assiut 71526, Egypt.

Tel.: (002)-01098294419

E-mail address: bgyoussif2@gmail.com

Salah A. Abdel-Aziz, Ph.D., Pharmaceutical Medicinal Chemistry and Drug Design Department, Faculty of Pharmacy (Boys) Al-Azhar University Assiut 71524, Egypt

E-mail address: salahabdel-aziz@azhar.edu.eg

S. Bräse

Institute of Biological and Chemical Systems, IBCS-FMS, Karlsruhe Institute of Technology, 76131 Karlsruhe, Germany. E-mail: braese@kit.edu

Contents:

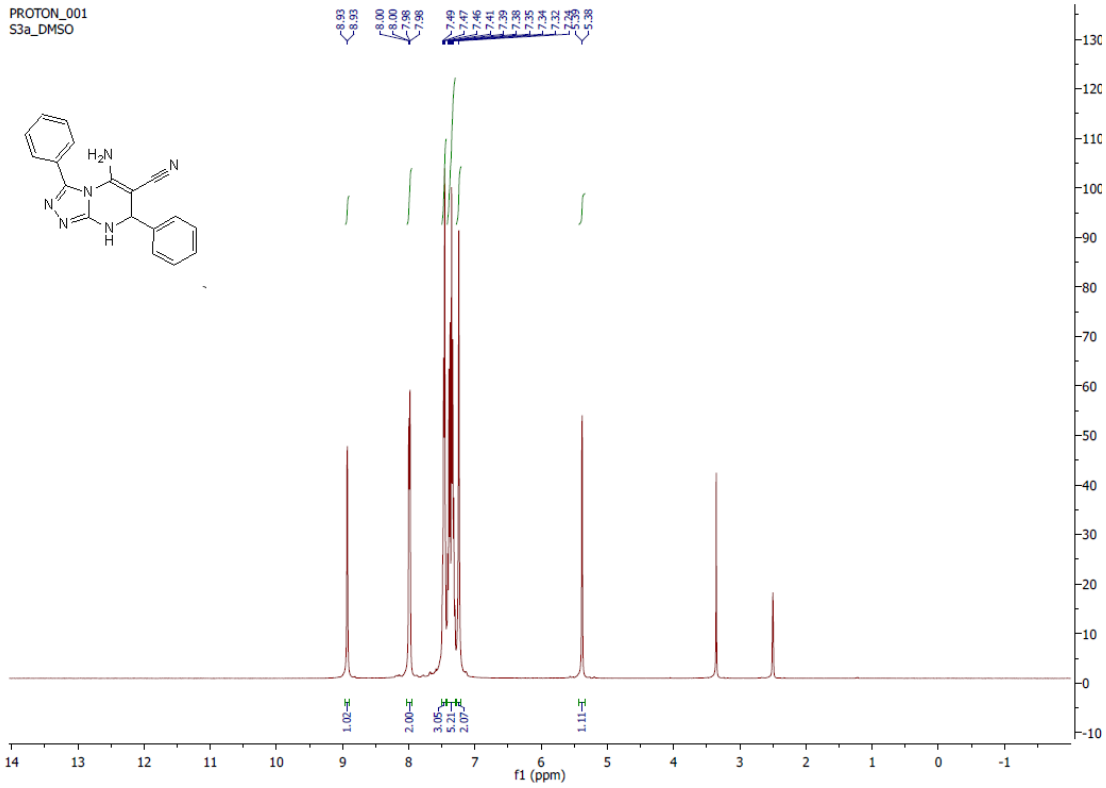

Fig. S1a: ^{1}H-NMR of compound 8a

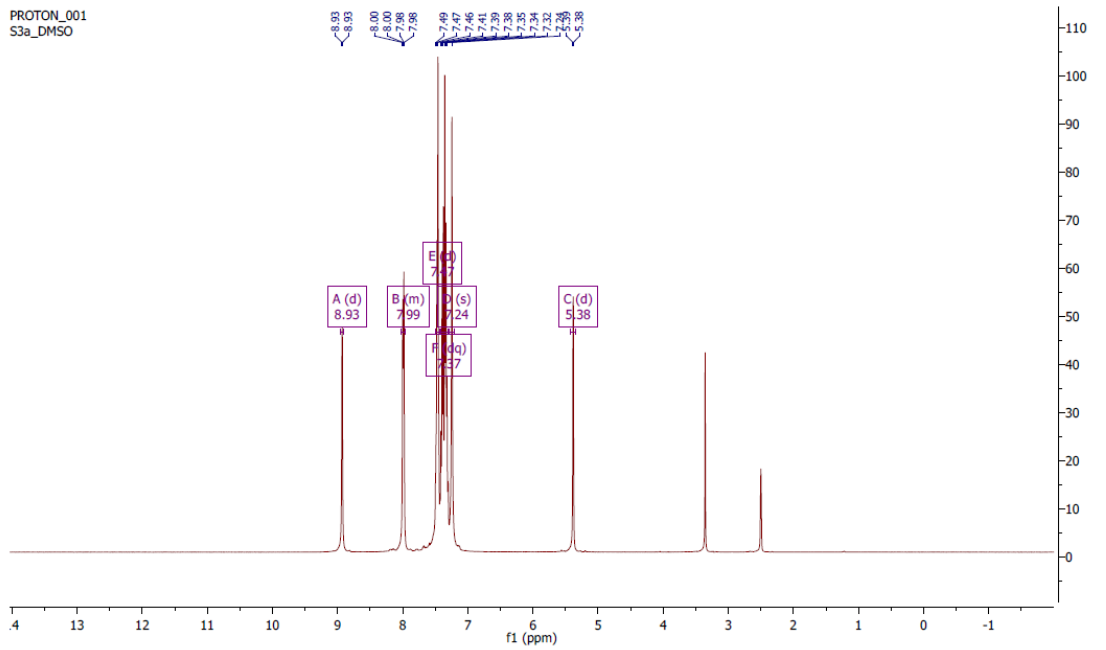

^{1}H NMR (400 MHz, DMSO-d_6) δ 8.93 (d, J = 2.7 Hz, 1H), 8.01 - 7.96 (m, 2H), 7.50 - 7.44 (m, 3H), 7.41 - 7.31 (m, 5H), 7.24 (s, 2H), 5.38 (d, J = 2.5 Hz, 1H).

Fig. S1b: ^{1}H-NMR of compound 8a

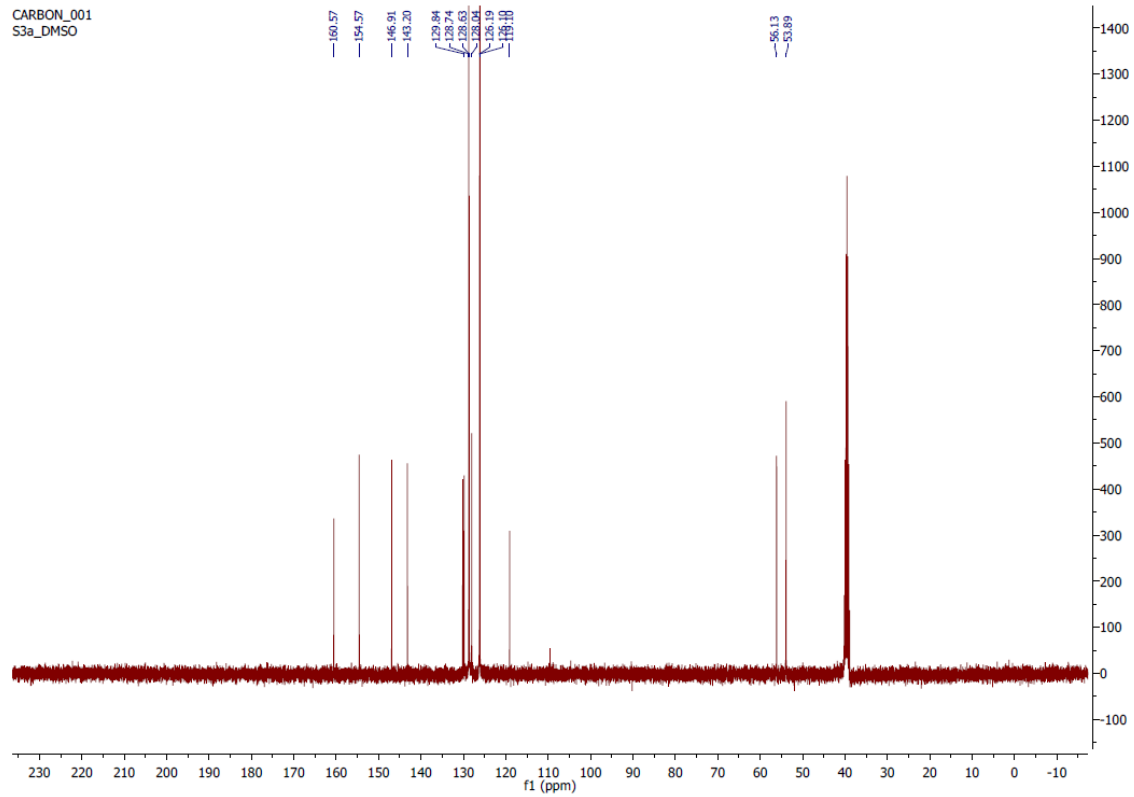

Fig. S2a: ^{13}C-NMR of compound 8a

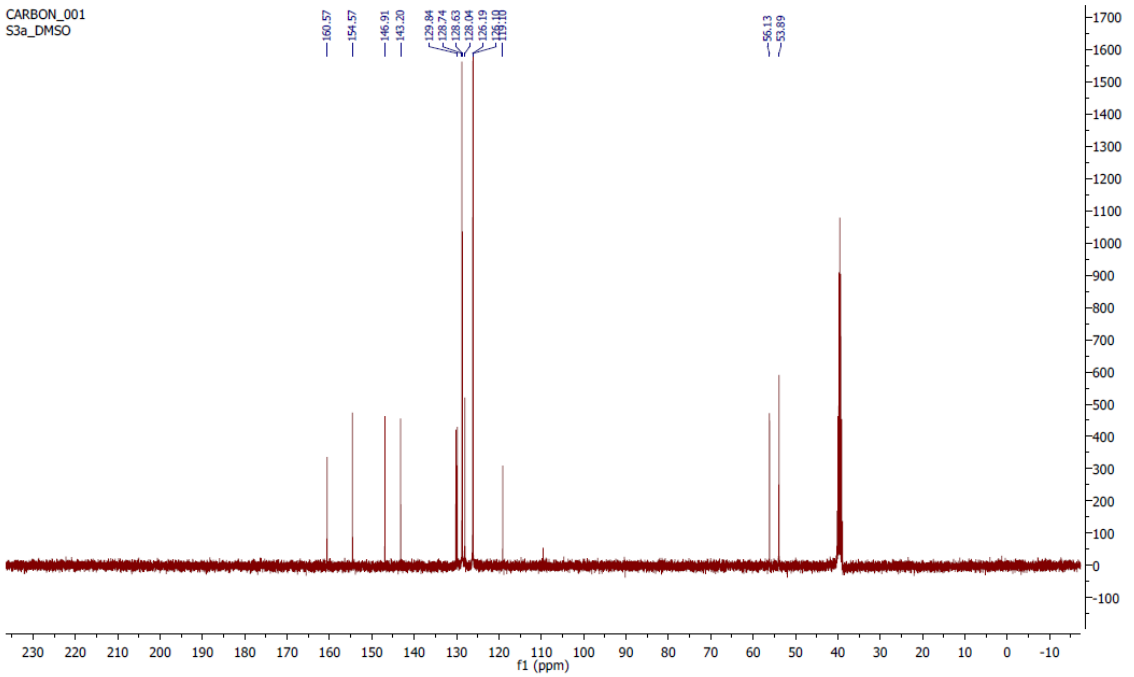

^{13}C NMR (101 MHz, dmso) δ 160.57, 154.57, 146.91, 143.20, 130.16, 129.84, 128.74, 128.63, 128.04, 126.19, 126.10, 119.10, 56.13, 53.89.

Fig. S2b: ^{13}C-NMR of compound 8a

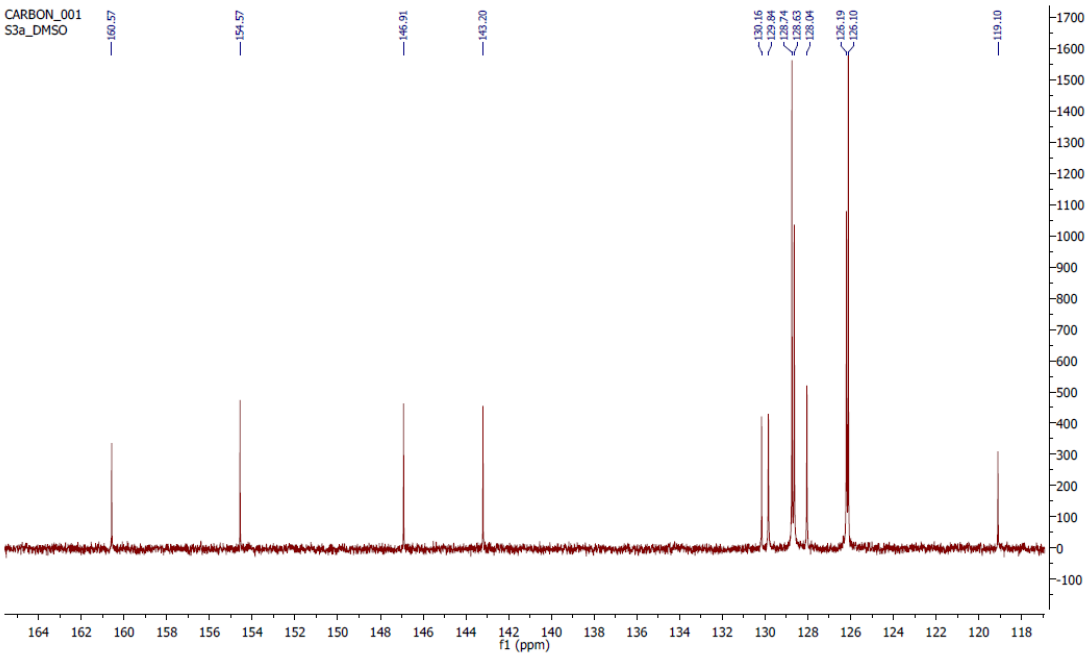

^{13}C NMR (101 MHz, dmso) δ 160.57, 154.57, 146.91, 143.20, 130.16, 129.84, 128.74, 128.63, 128.04, 126.19, 126.10, 119.10, 56.13, 53.89.

Fig. S2c: ^{13}C-NMR of compound 8a

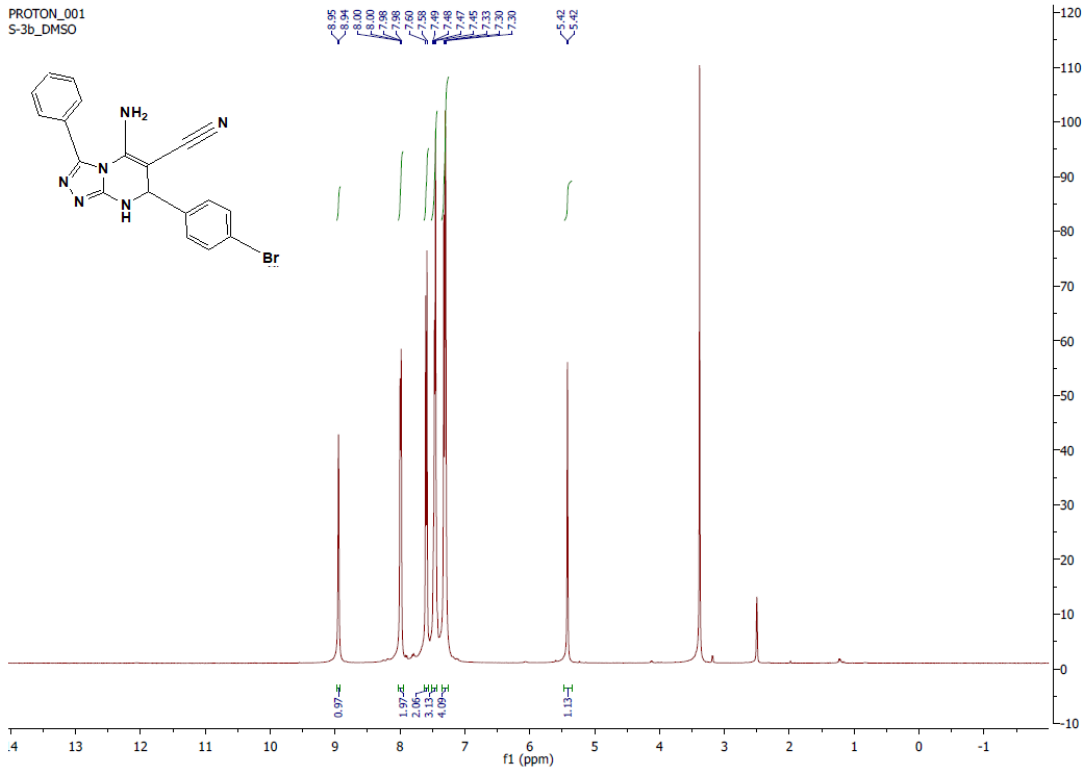

Fig. S3a: ^{1}H-NMR of compound 8b

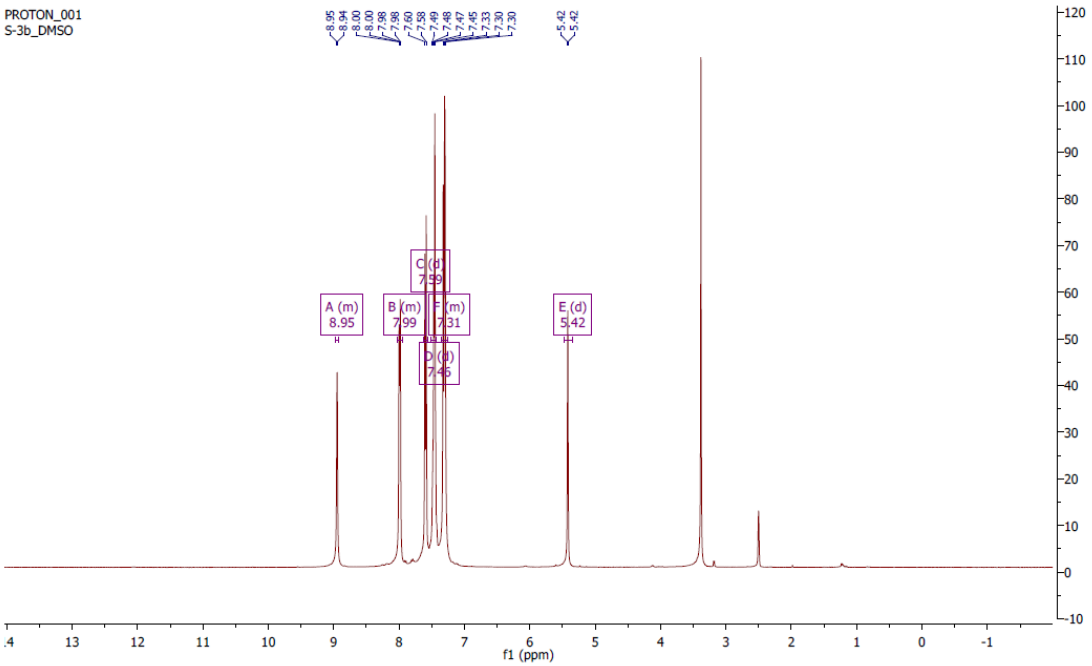

^{1}H NMR (400 MHz, DMSO-d_6) δ 8.95 (s, 1H), 8.03 – 7.95 (m, 2H), 7.59 (d, J = 8.1 Hz, 2H), 7.50 - 7.43 (m, 3H), 7.36 – 7.25 (m, 4H), 5.42 (d, J = 2.0 Hz, 1H).

Fig. S3b: ^{1}H-NMR of compound 8b

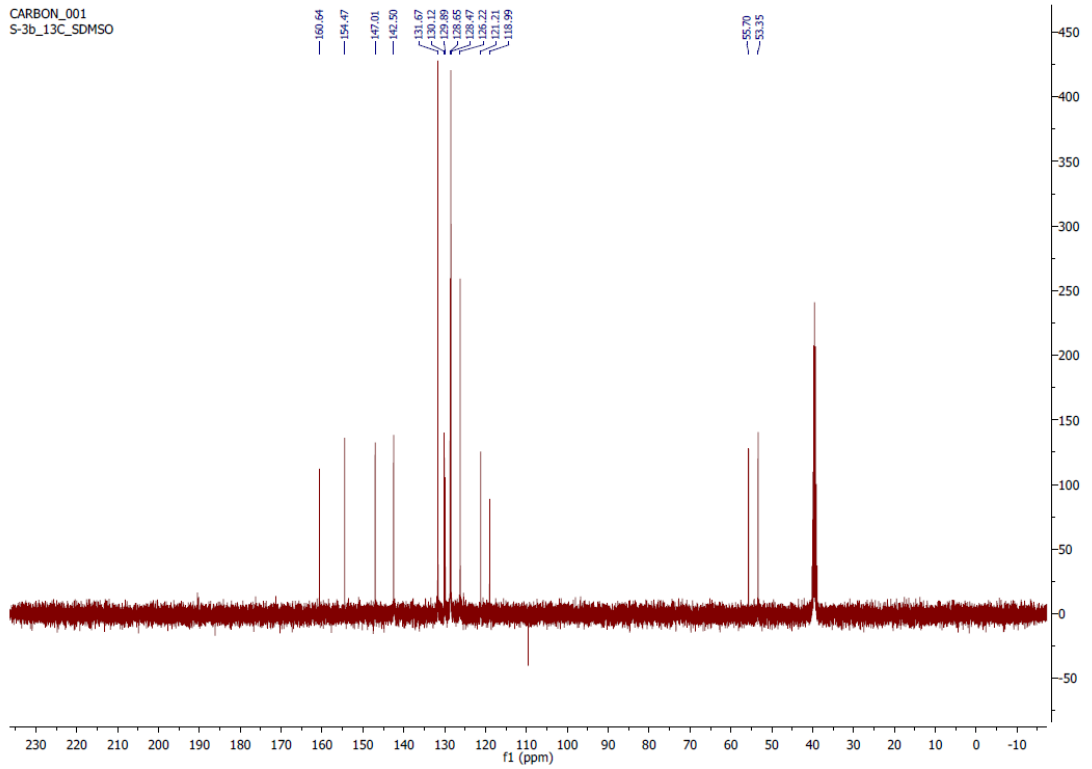

Fig. S4a: ^{13}C-NMR of compound 8b

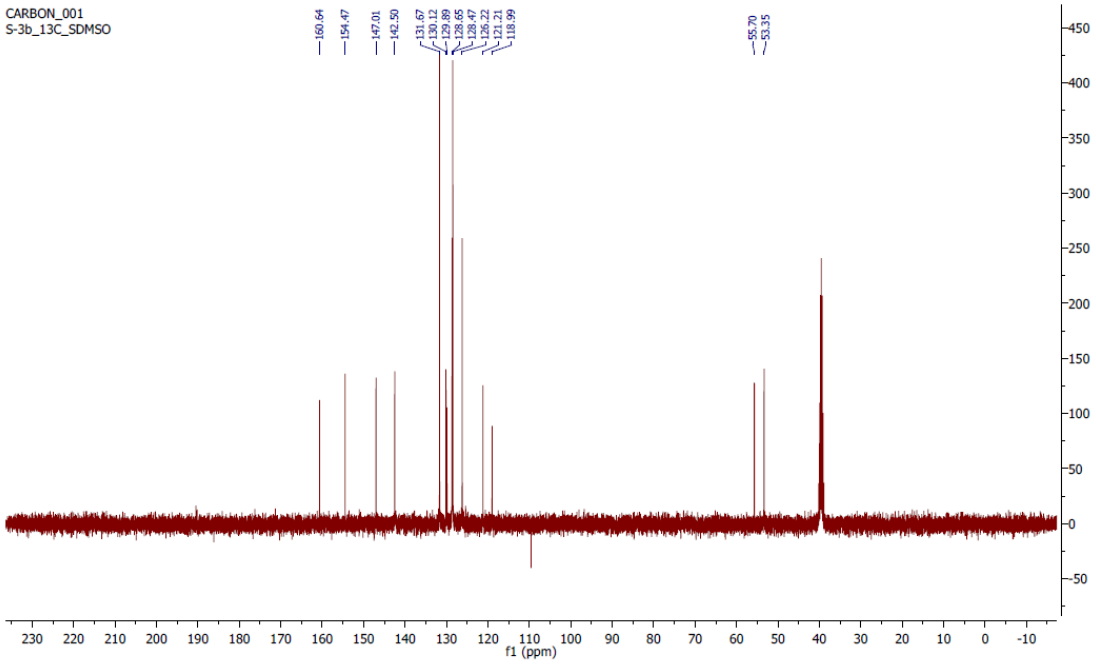

^{13}C NMR (101 MHz, dmso) δ 160.64, 154.47, 147.01, 142.50, 131.67, 130.12, 129.89, 128.65, 128.47, 126.22, 121.21, 118.99, 55.70, 53.35.

Fig. S4b: ^{13}C-NMR of compound 8b

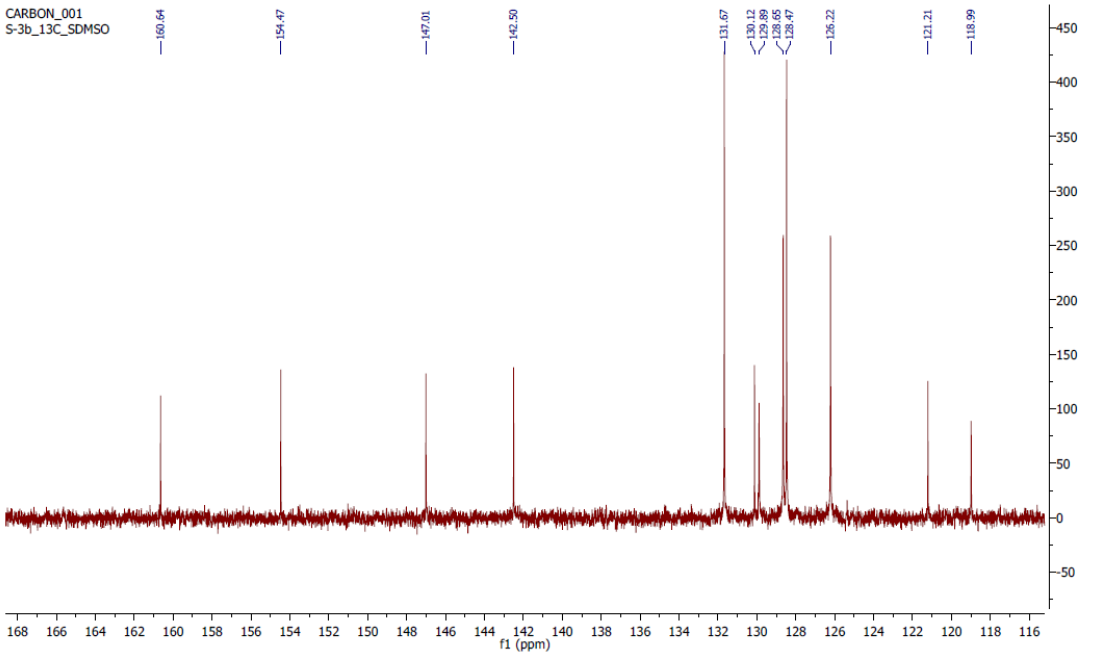

^{13}C NMR (101 MHz, dmso) δ 160.64, 154.47, 147.01, 142.50, 131.67, 130.12, 129.89, 128.65, 128.47, 126.22, 121.21, 118.99, 55.70, 53.35.

Fig. S4c: ^{13}C-NMR of compound 8b

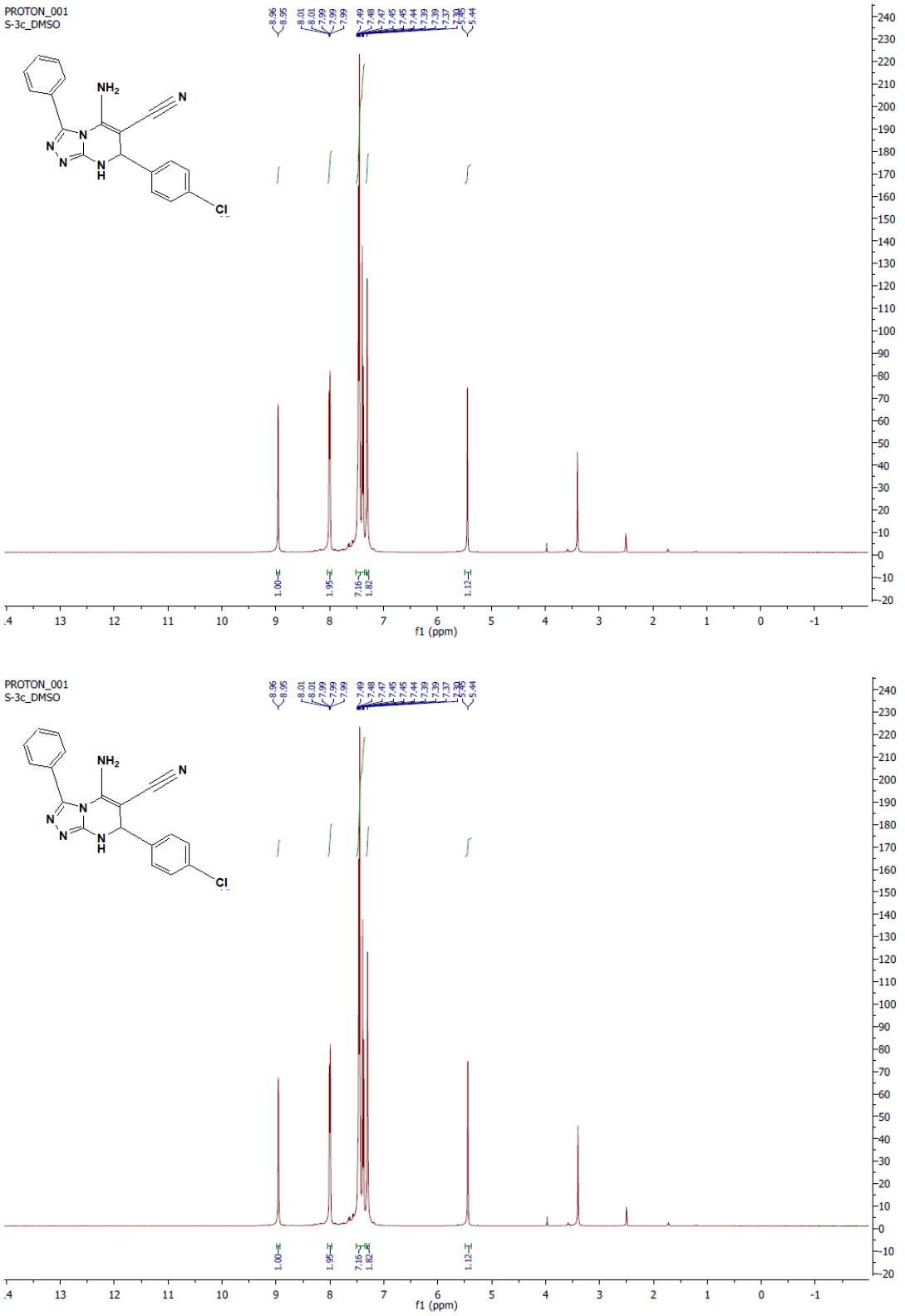

Fig. S5a: ^{1}H-NMR of compound 8c

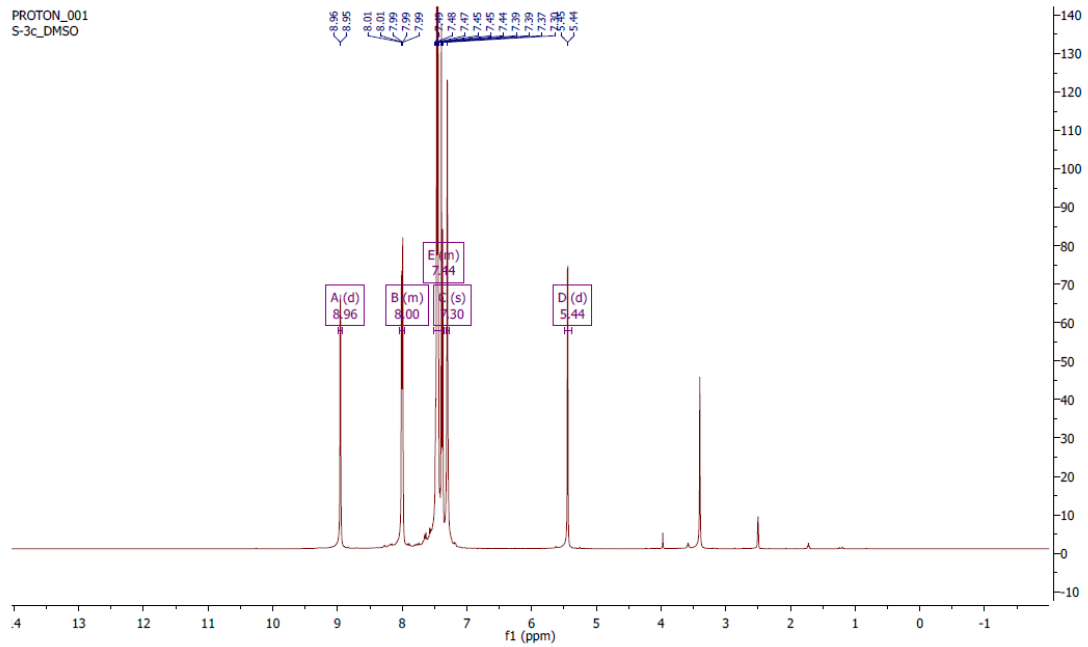

^{1}H NMR (400 MHz, DMSO-d_6) δ 8.96 (d, J = 2.6 Hz, 1H), 8.03 - 7.96 (m, 2H), 7.51 – 7.35 (m, 7H), 7.30 (s, 2H), 5.44 (d, J = 2.4 Hz, 1H).

Fig. S5b: ^{1}H-NMR of compound 8c

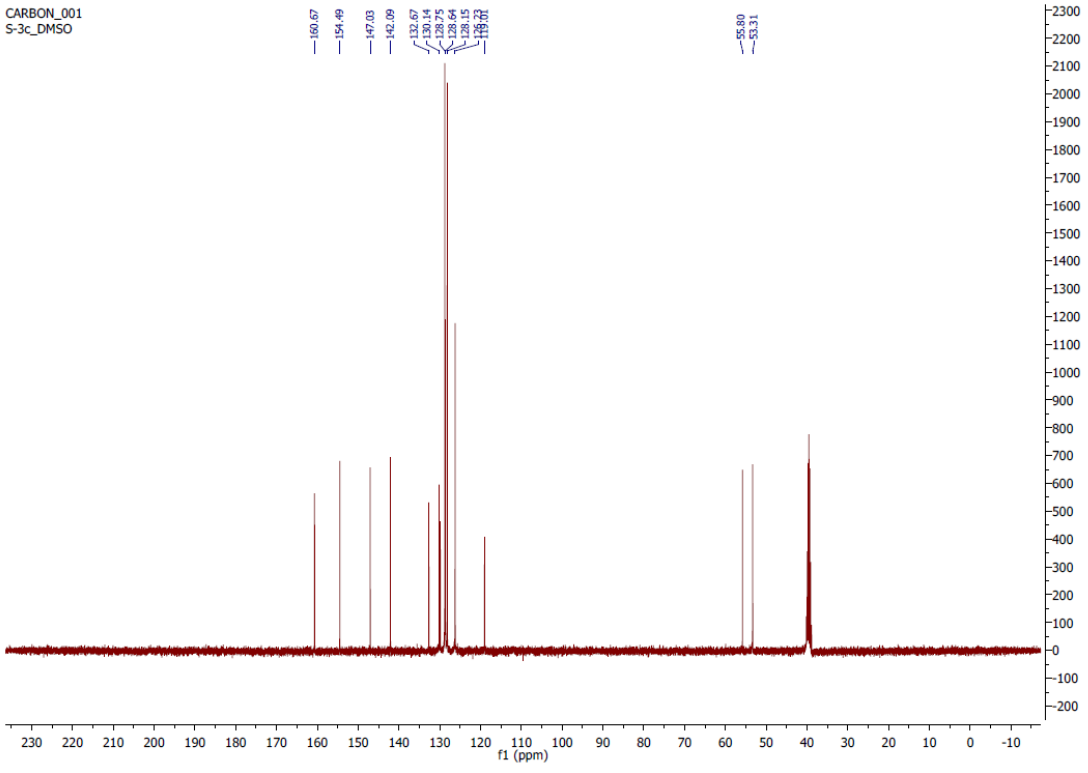

Fig. S6a: ^{13}C-NMR of compound 8c

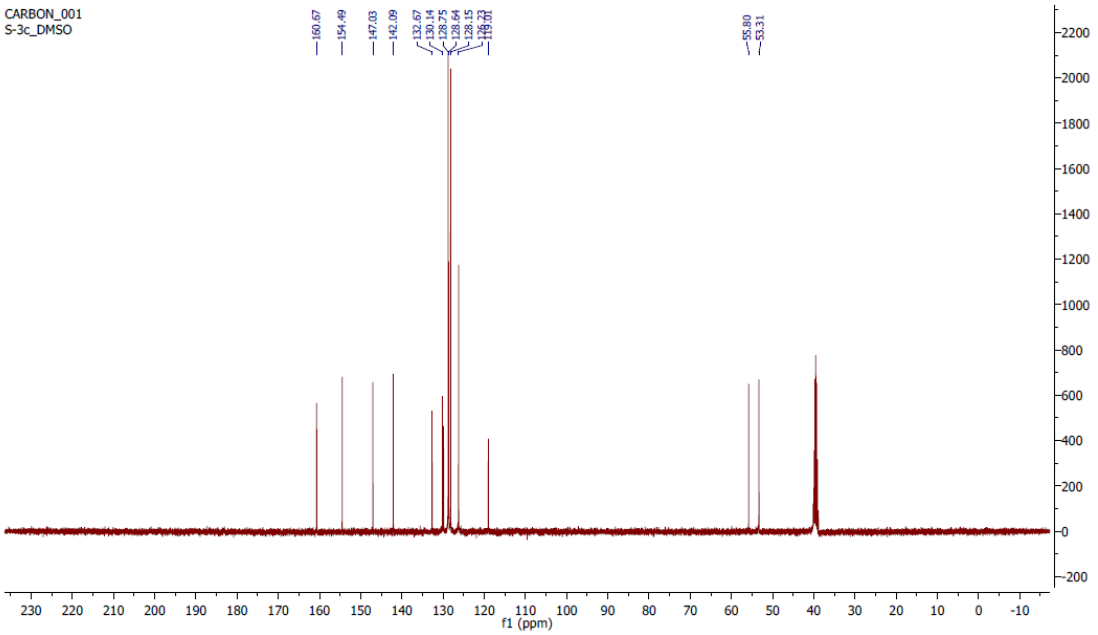

^{13}C NMR (101 MHz, dmso) δ 160.67, 154.49, 147.03, 142.09, 132.67, 130.14, 129.88, 128.75, 128.64, 128.15, 126.23, 119.01, 55.80, 53.31.

Fig. S6b: ^{13}C-NMR of compound 8c

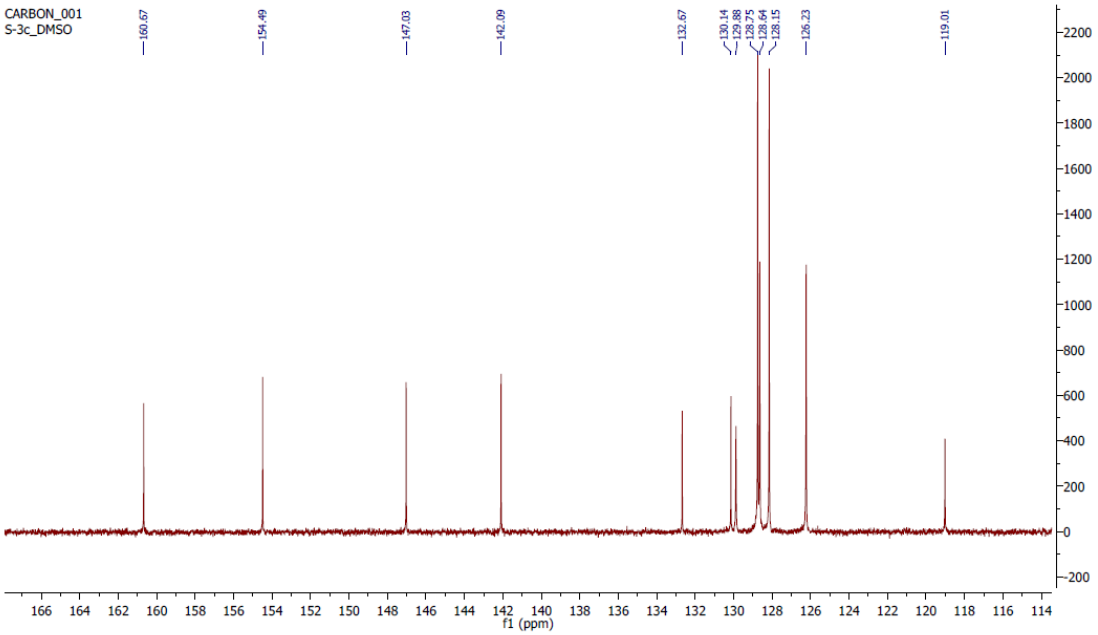

^{13}C NMR (101 MHz, dmso) δ 160.67, 154.49, 147.03, 142.09, 132.67, 130.14, 129.88, 128.75, 128.64, 128.15, 126.23, 119.01, 55.80, 53.31.

Fig. S6c: ^{13}C-NMR of compound 8c

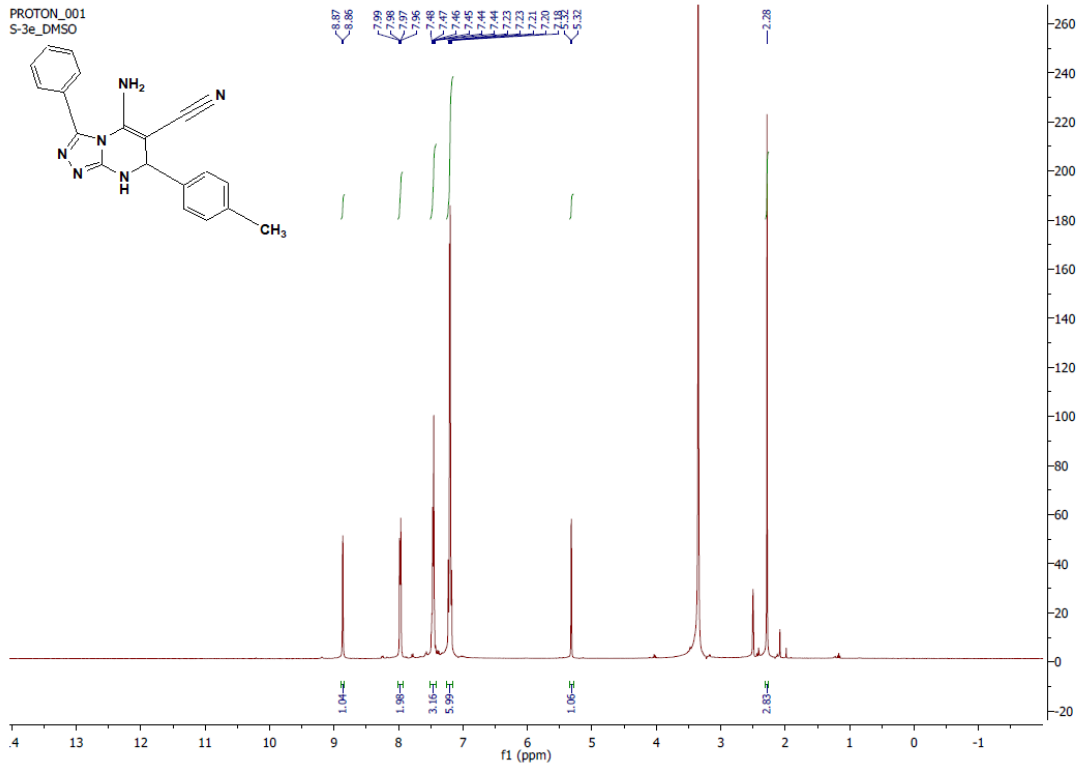

Fig. S7a: ^{1}H-NMR of compound 8d

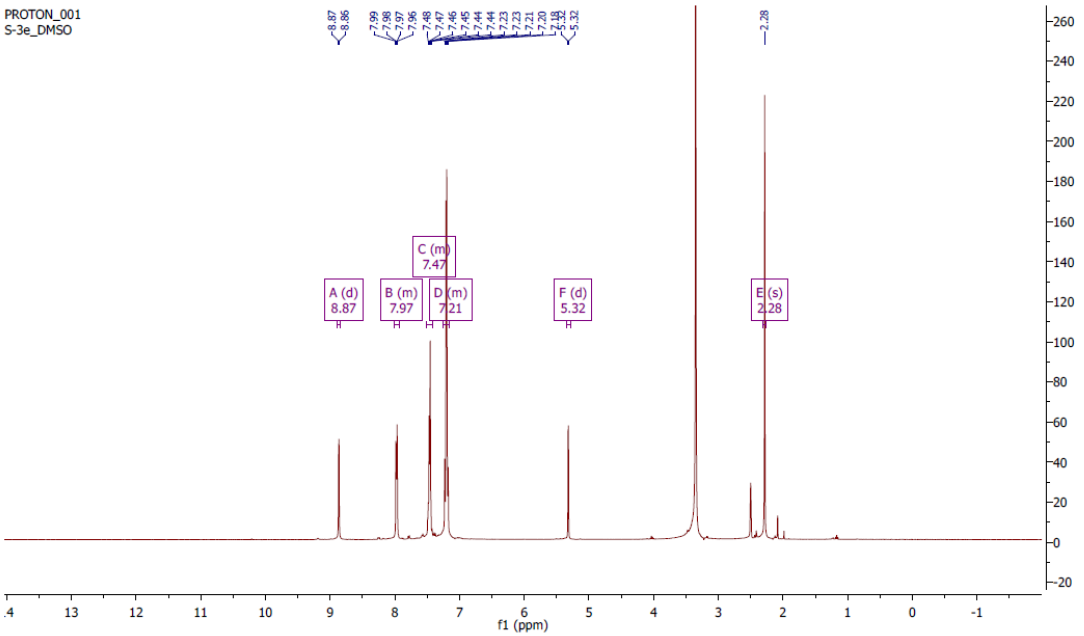

^{1}H NMR (400 MHz, DMSO-d_6) δ 8.87 (d, J = 2.5 Hz, 1H), 8.01 - 7.95 (m, 2H), 7.51 – 7.41 (m, 3H), 7.26 – 7.15 (m, 6H), 5.32 (d, J = 2.5 Hz, 1H), 2.28 (s, 3H).

Fig. S7b: ^{1}H-NMR of compound 8d

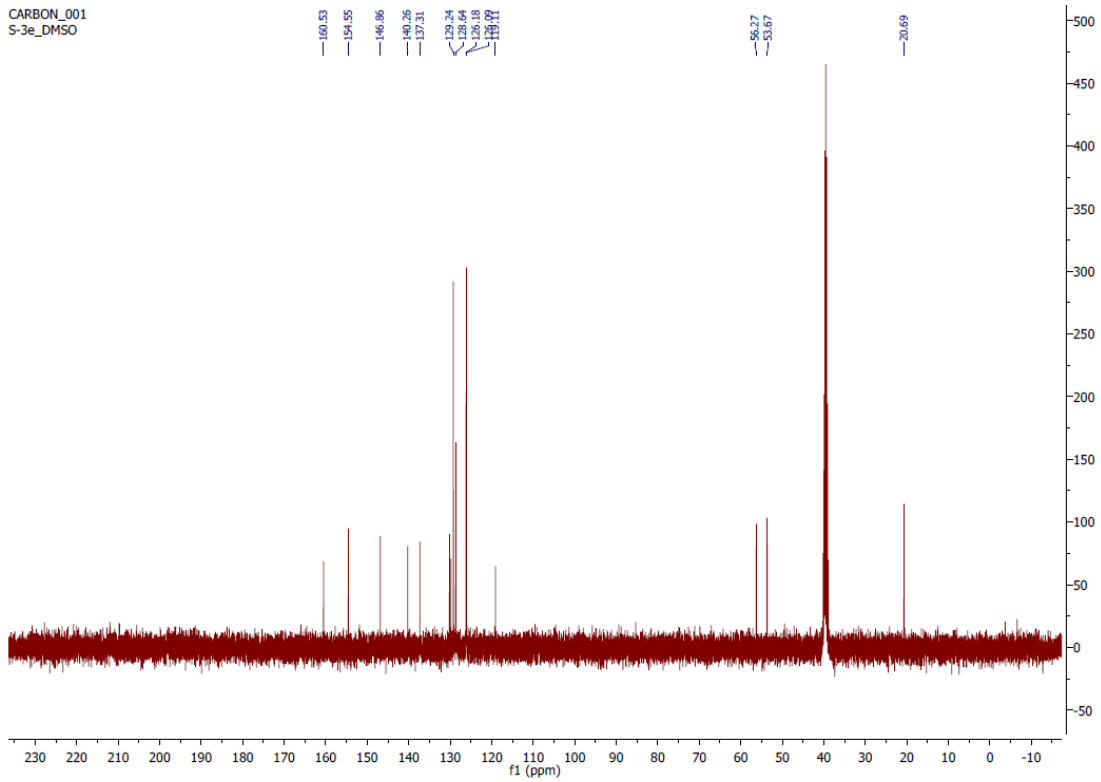

Fig. S8a: ^{13}C-NMR of compound 8d

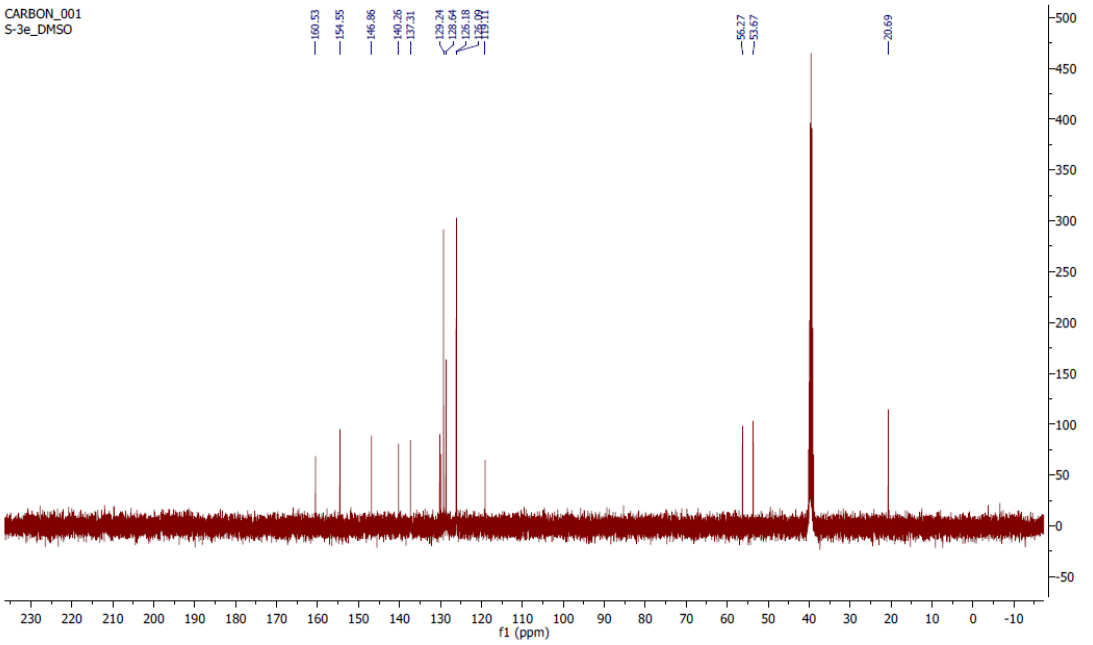

^{13}C NMR (101 MHz, dmso) δ 160.53, 154.55, 146.86, 140.26, 137.31, 130.17, 129.84, 129.24, 128.64, 126.18, 126.09, 119.11, 56.27, 53.67, 20.69.

Fig. S8b: ^{13}C-NMR of compound 8d

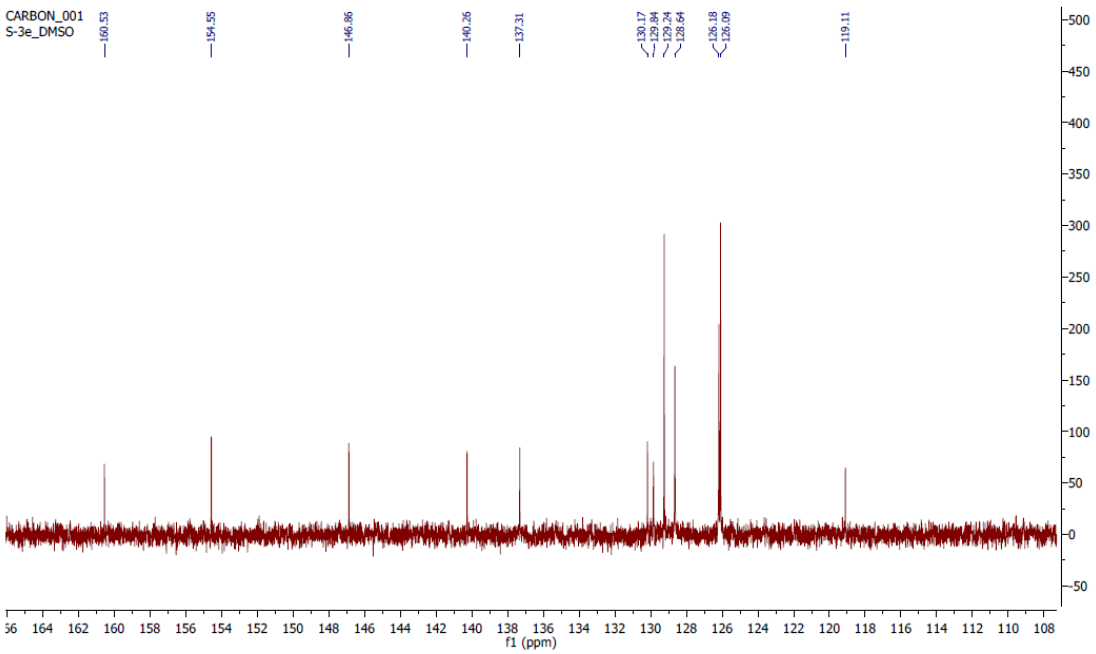

^{13}C NMR (101 MHz, dmso) δ 160.53, 154.55, 146.86, 140.26, 137.31, 130.17, 129.84, 129.24, 128.64, 126.18, 126.09, 119.11, 56.27, 53.67, 20.69.

Fig. S8c: ^{13}C-NMR of compound 8d

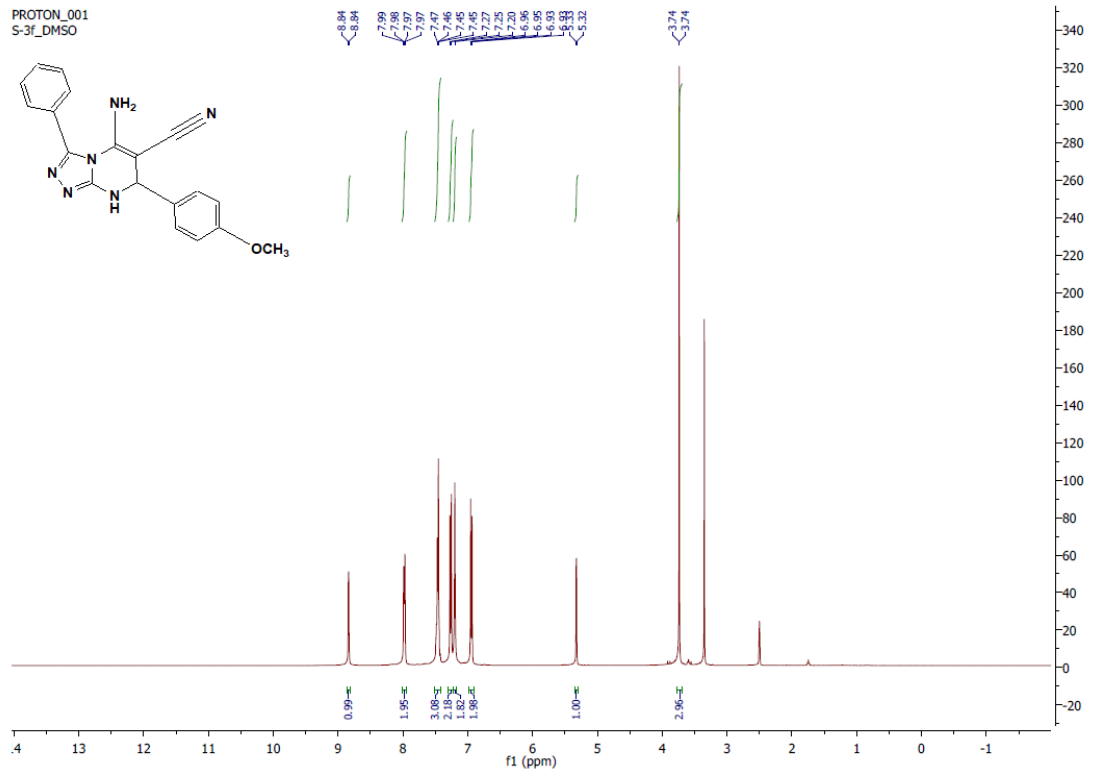

Fig. S9a: ^{1}H-NMR of compound 8e

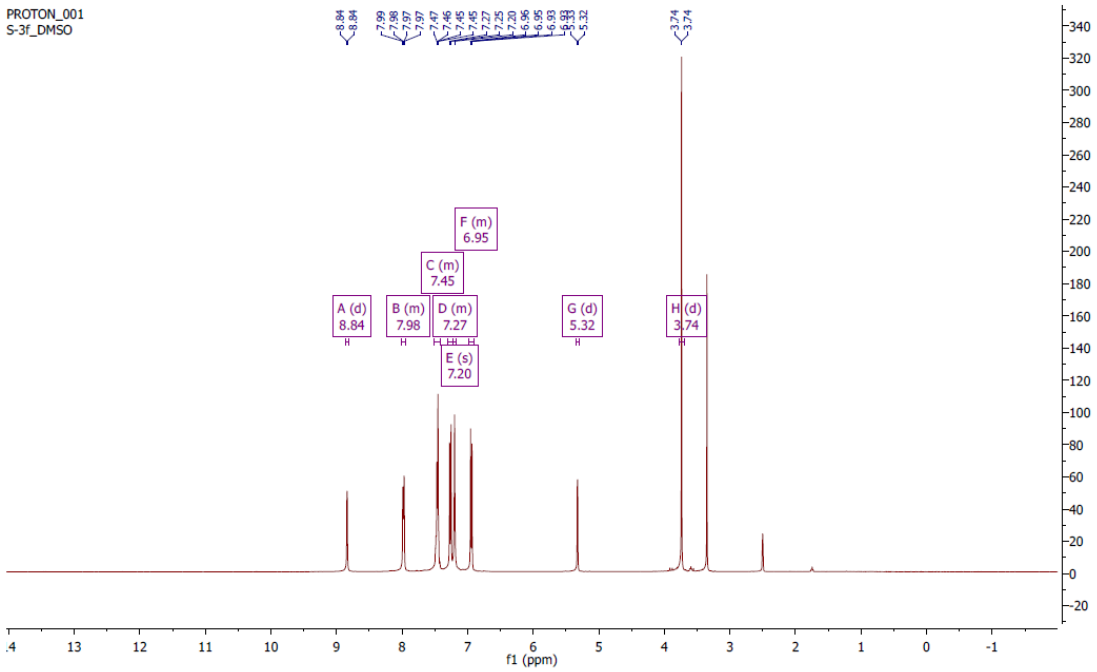

^{1}H NMR (400 MHz, DMSO-d_6) δ 8.84 (d, J = 2.4 Hz, 1H), 8.00 - 7.95 (s, 2H), 7.51 – 7.41 (m, 3H), 7.27 (d, J = 8.5 Hz, 2H), 7.20 (s, 2H), 6.95 (d, J = 8.5 Hz, 2H), 5.32 (d, J = 2.5 Hz, 1H), 3.74 (s, 3H).

Fig. S9b: ^{1}H-NMR of compound 8e

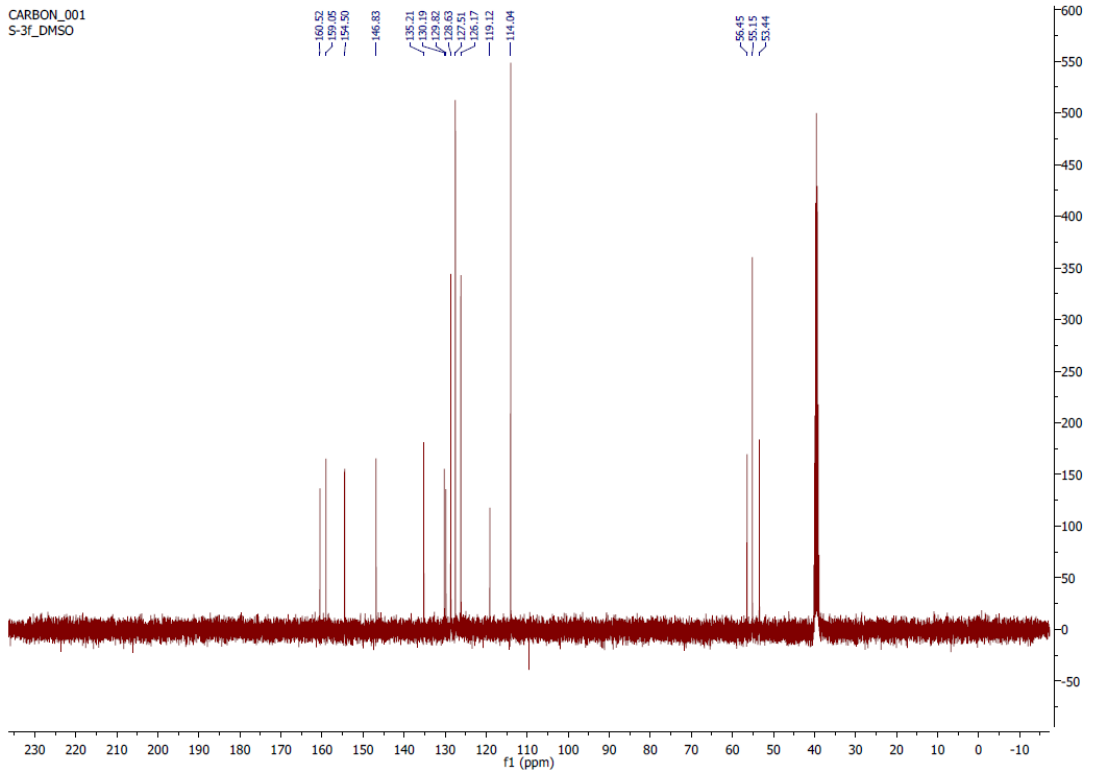

Fig. S10a: ^{13}C-NMR of compound 8e

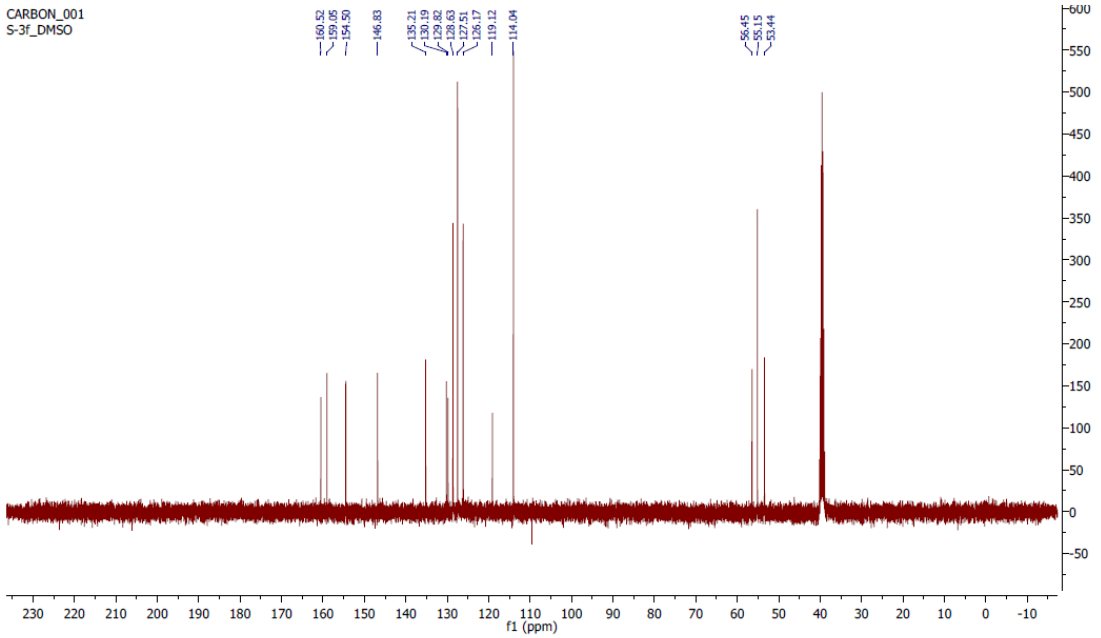

^{13}C NMR (101 MHz, dmso) δ 160.52, 159.05, 154.50, 146.83, 135.21, 130.19, 129.82, 128.63, 127.51, 126.17, 119.12, 114.04, 56.45, 55.15, 53.44.

Fig. S10b: ^{13}C-NMR of compound 8e

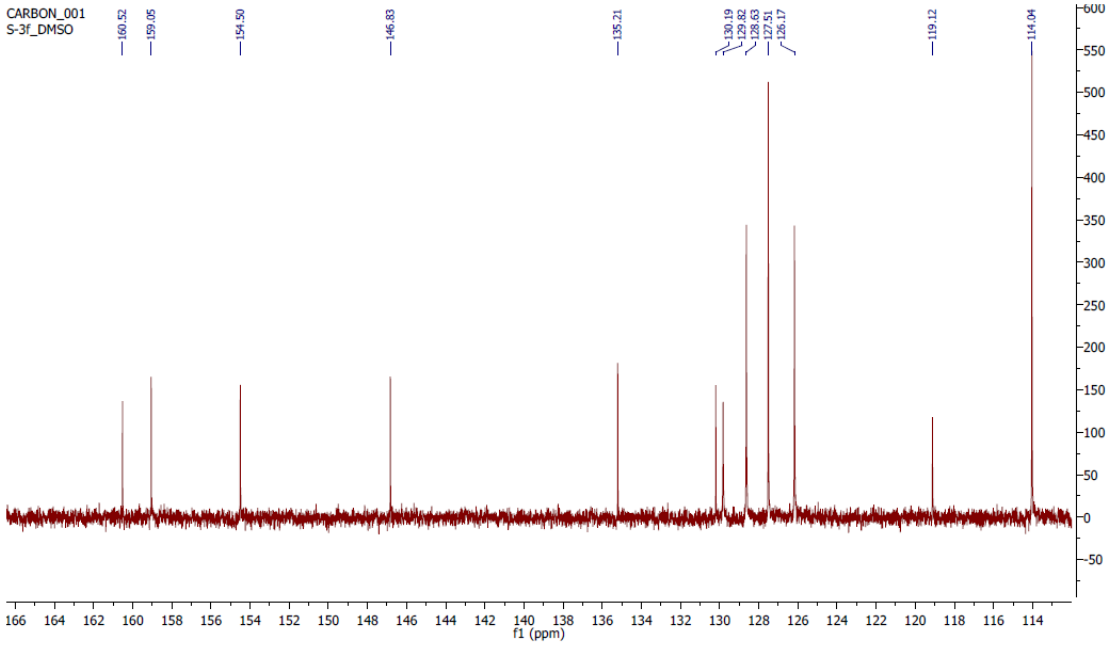

^{13}C NMR (101 MHz, dmso) δ 160.52, 159.05, 154.50, 146.83, 135.21, 130.19, 129.82, 128.63, 127.51, 126.17, 119.12, 114.04, 56.45, 55.15, 53.44.

Fig. S10c: ^{13}C-NMR of compound 8e

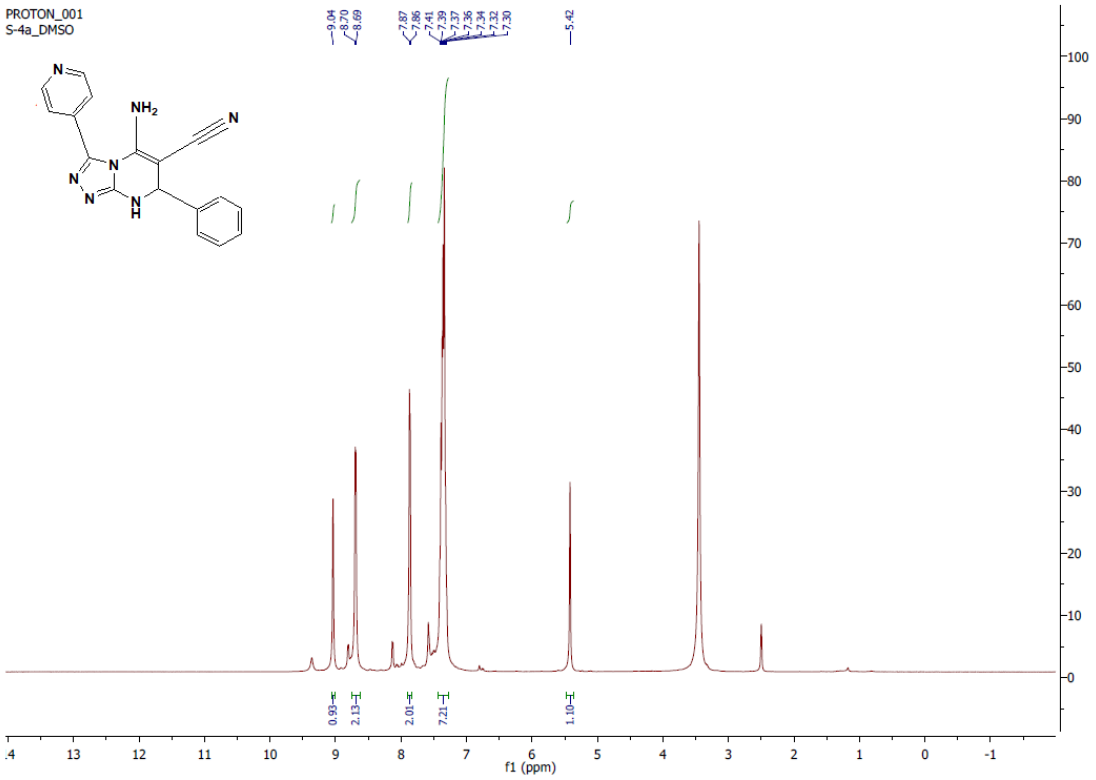

Fig. S11a: ^{1}H-NMR of compound 8f

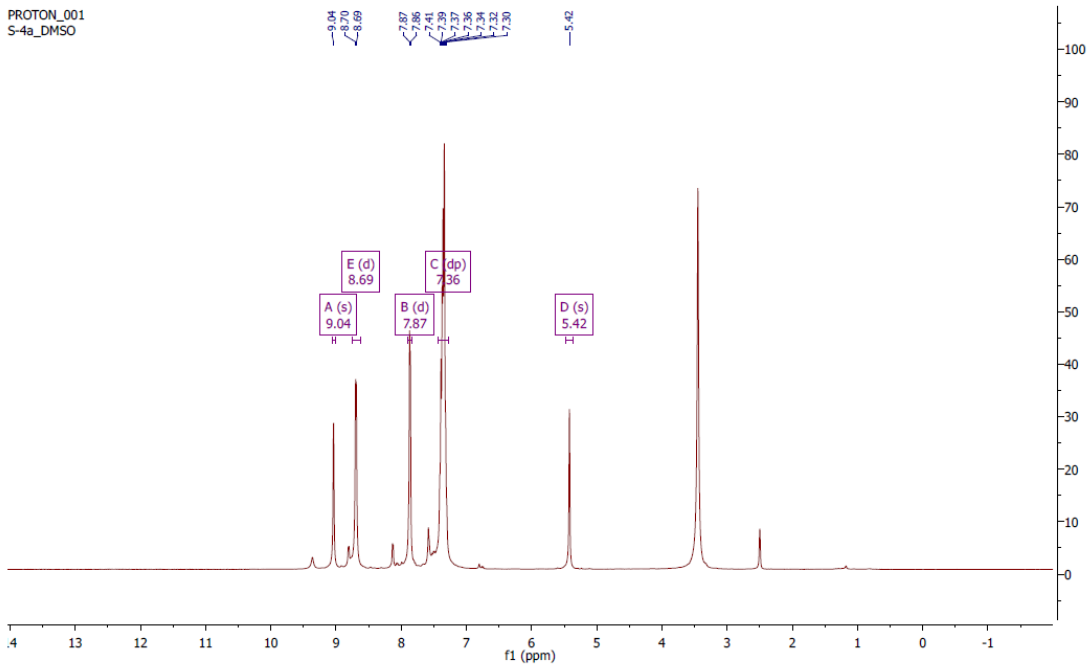

^{1}H NMR (400 MHz, DMSO-d_6) δ 9.04 (s, 1H), 8.69 (d, J = 5.0 Hz, 2H), 7.87 (d, J = 5.1 Hz, 2H), 7.42 - 7.28 (m, 7H), 5.42 (s, 1H).

Fig. S11b: ^{1}H-NMR of compound 8f

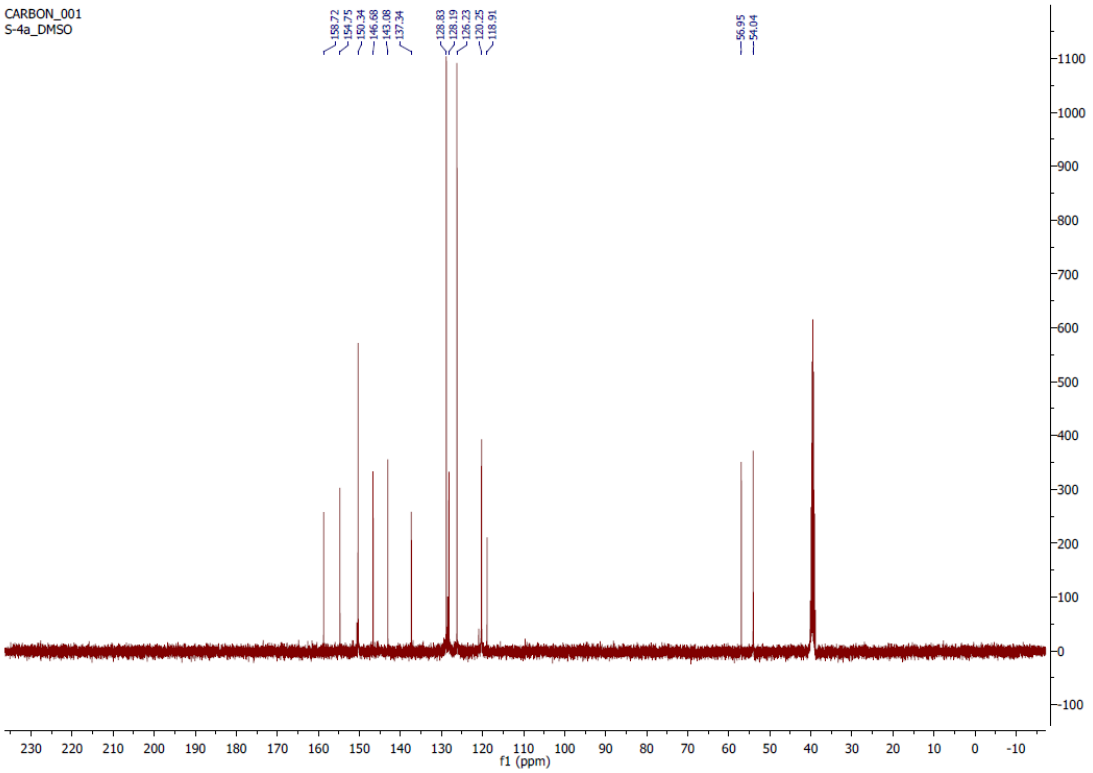

Fig. S12a: ^{13}C-NMR of compound 8f

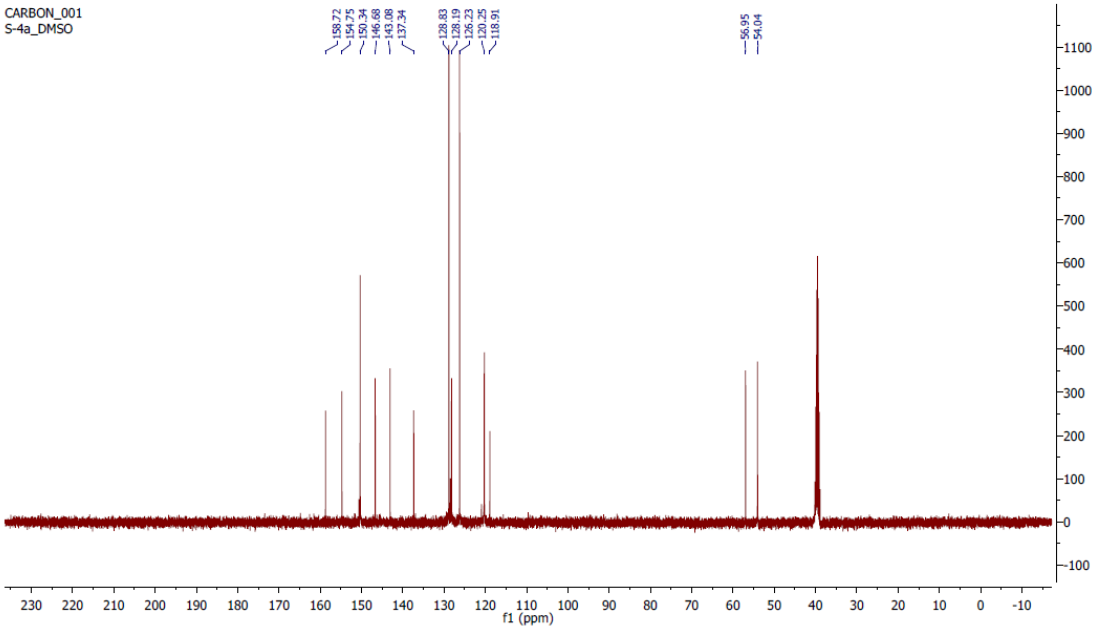

^{13}C NMR (101 MHz, dmso) δ 158.72, 154.75, 150.34, 146.68, 143.08, 137.34, 128.83, 128.19, 126.23, 120.25, 118.91, 56.95, 54.04.

Fig. S12b: ^{13}C-NMR of compound 8f

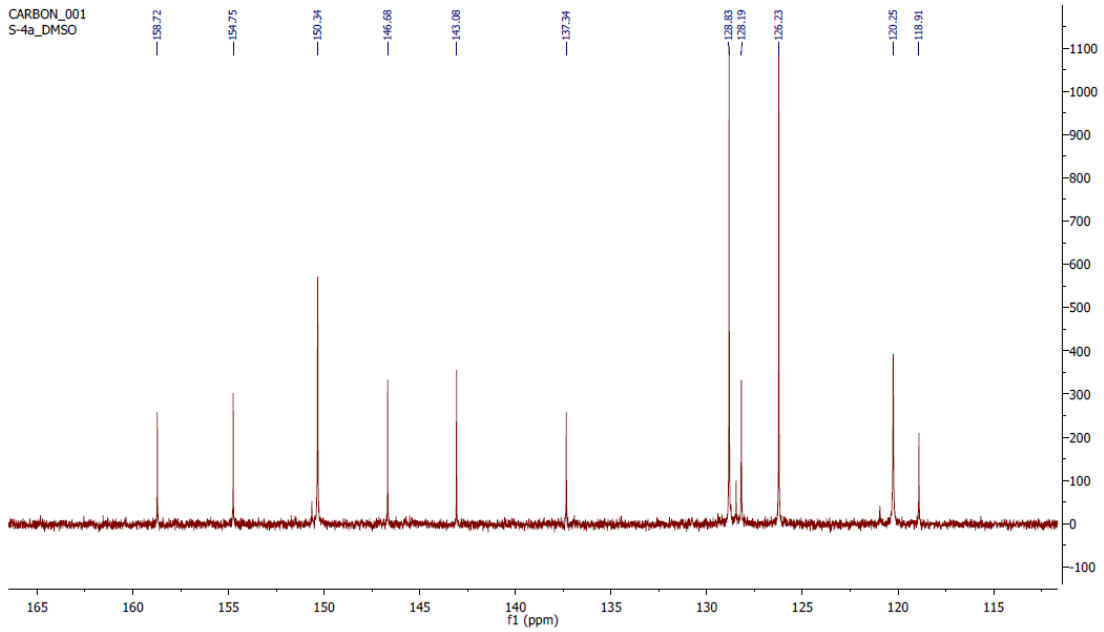

^{13}C NMR (101 MHz, dmso) δ 158.72, 154.75, 150.34, 146.68, 143.08, 137.34, 128.83, 128.19, 126.23, 120.25, 118.91, 56.95, 54.04.

Fig. S12c: ^{13}C-NMR of compound 8f

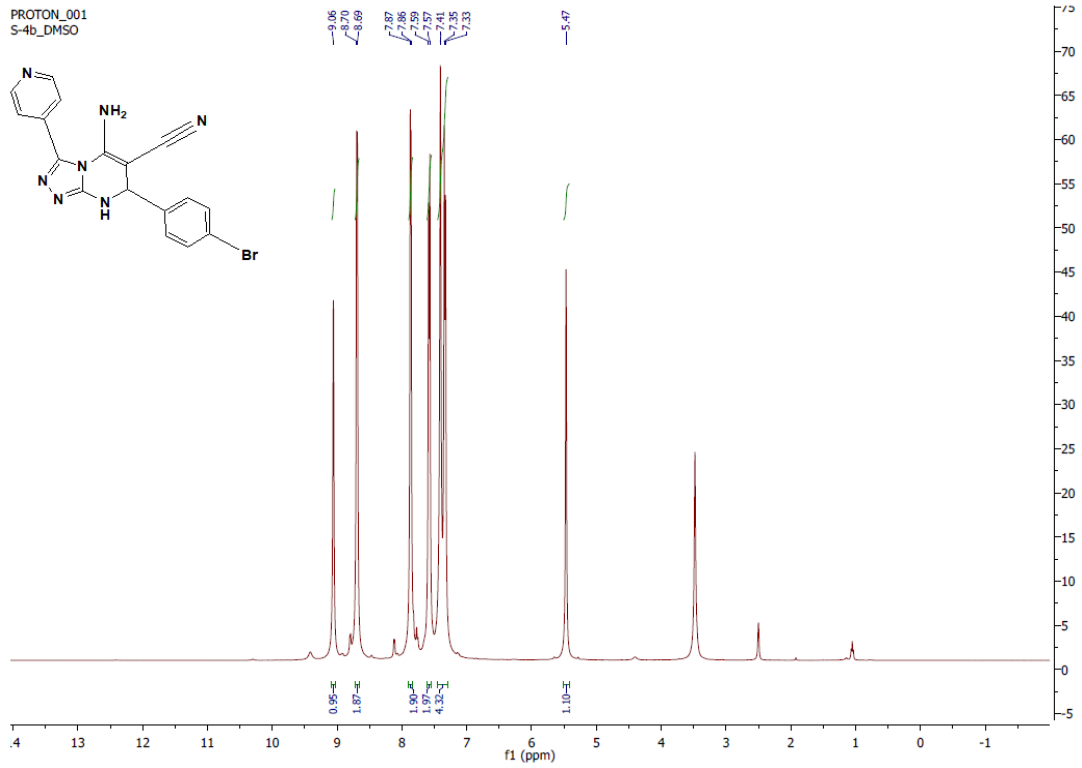

Fig. S13a: ^{1}H-NMR of compound 8g

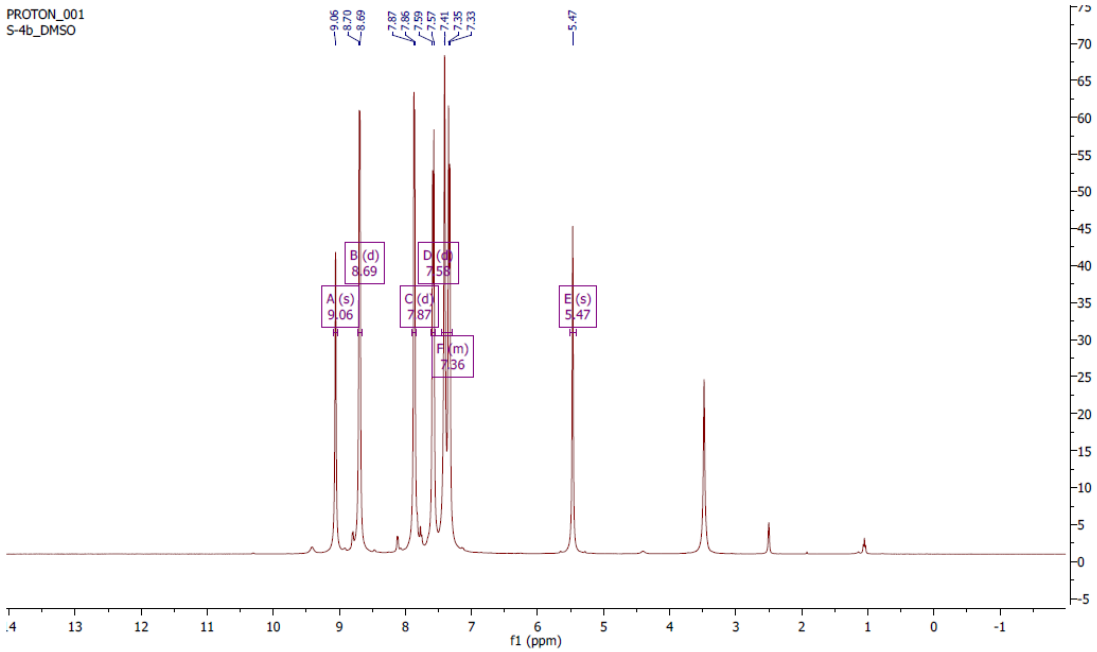

^{1}H NMR (400 MHz, DMSO-d_6) δ 9.06 (s, 1H), 8.69 (d, J = 5.2 Hz, 2H), 7.87 (d, J = 5.2 Hz, 2H), 7.58 (d, J = 8.1 Hz, 2H), 7.45 – 7.29 (m, 4H), 5.47 (s, 1H).

Fig. S13b: ^{1}H-NMR of compound 8g

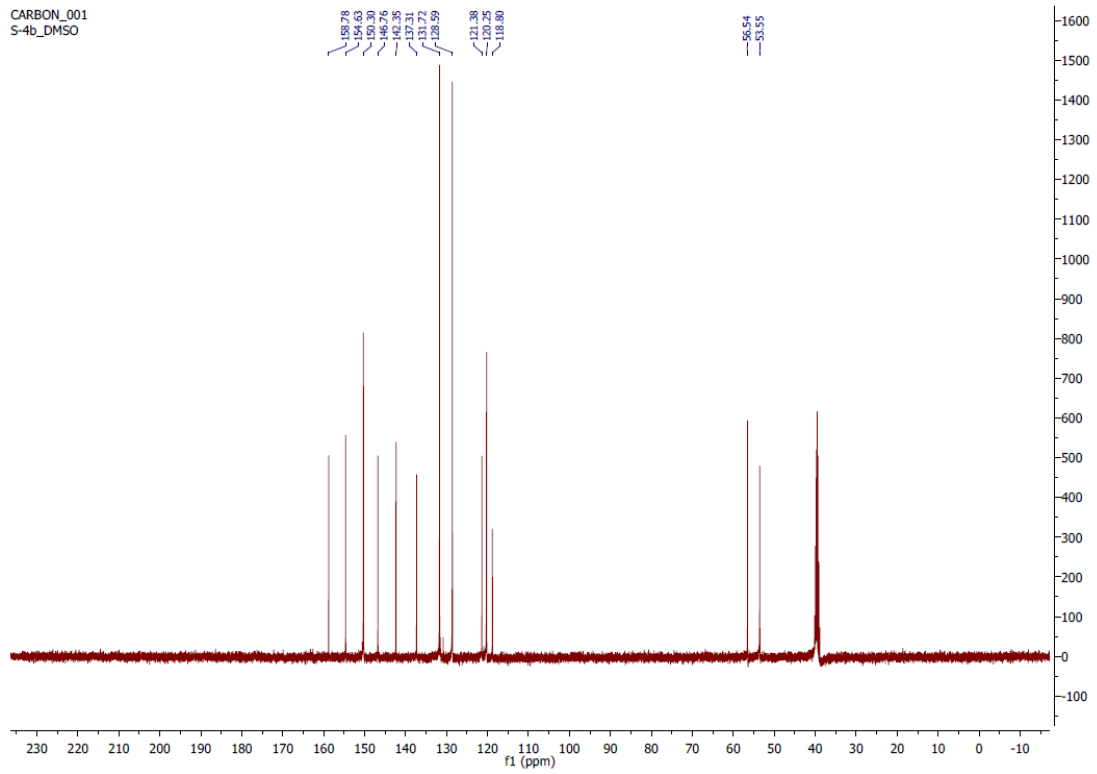

Fig. S14a: ^{13}C-NMR of compound 8g

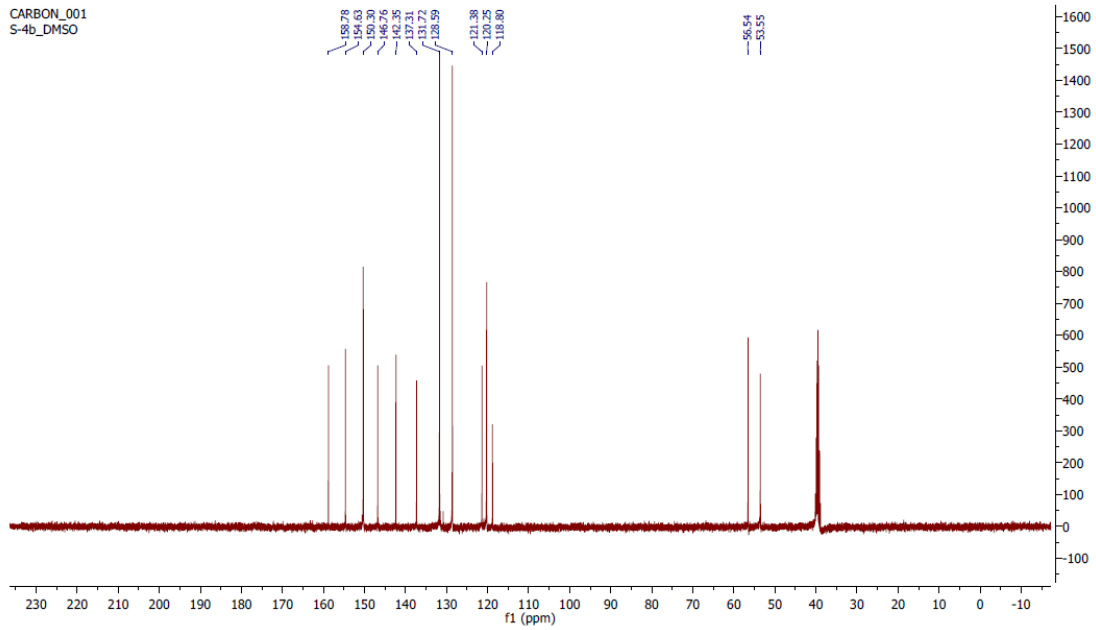

^{13}C NMR (101 MHz, dmso) δ 158.78, 154.63, 150.30, 146.76, 142.35, 137.31, 131.72, 128.59, 121.38, 120.25, 118.80, 56.54, 53.55.

Fig. S14b: ^{13}C-NMR of compound 8g

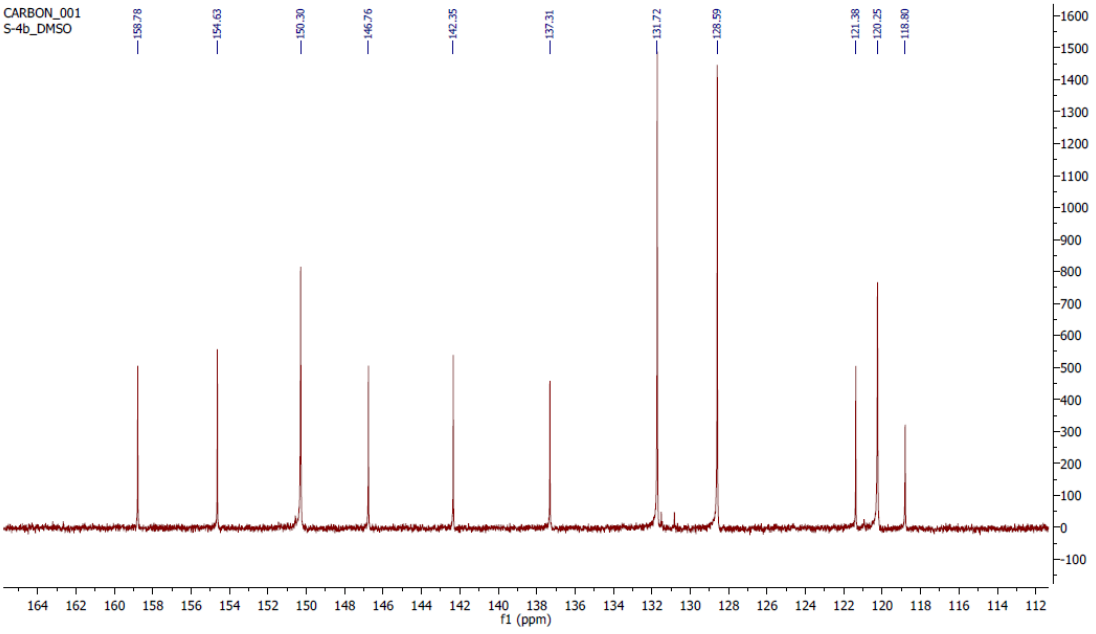

^{13}C NMR (101 MHz, dmso) δ 158.78, 154.63, 150.30, 146.76, 142.35, 137.31, 131.72, 128.59, 121.38, 120.25, 118.80, 56.54, 53.55.

Fig. S14c: ^{13}C-NMR of compound 8g

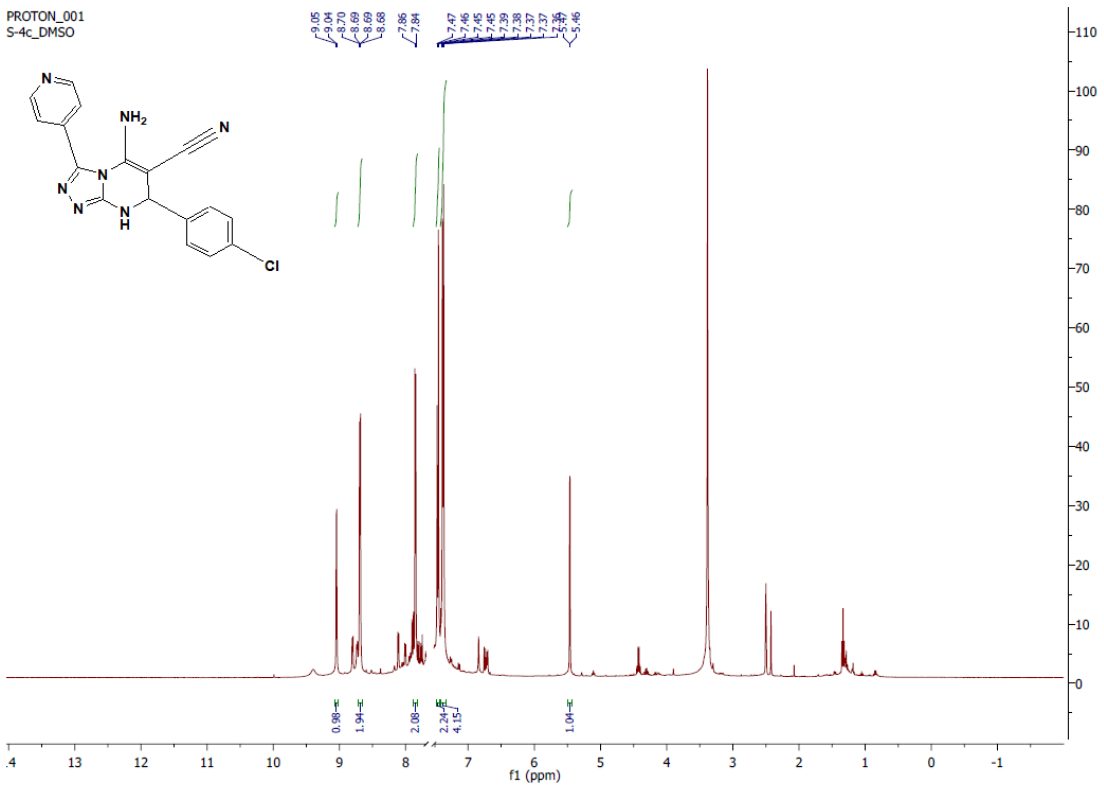

Fig. S15a: ^{1}H-NMR of compound 8h

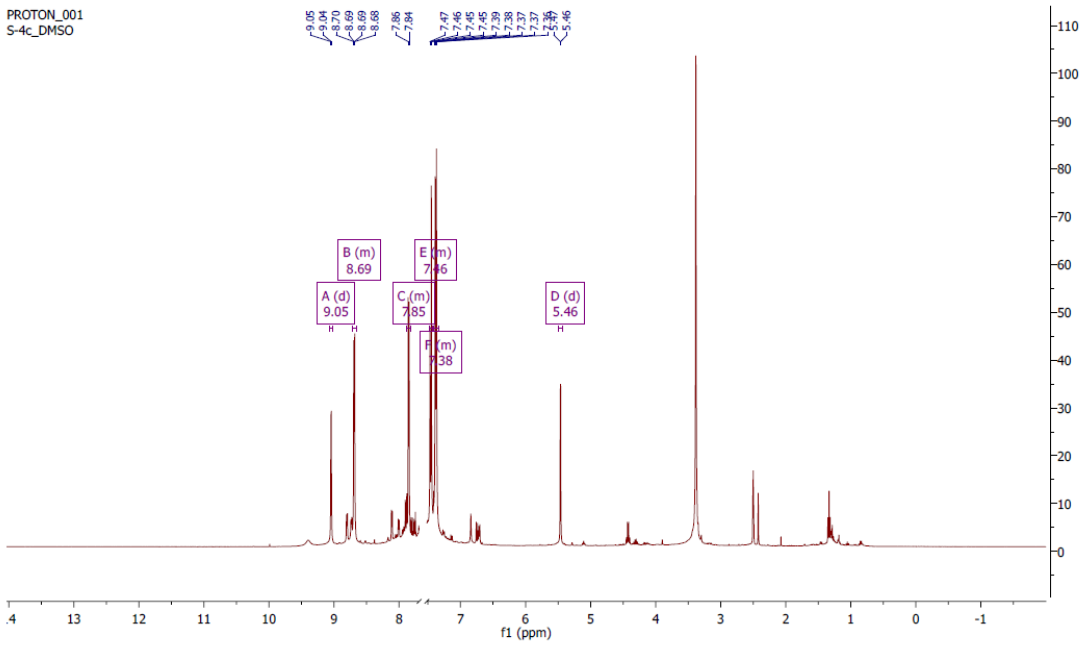

^{1}H NMR (400 MHz, DMSO-d_6) δ 9.05 (d, J = 2.6 Hz, 1H), 8.69 (d, J = 5.2 Hz, 2H), 7.85 (d, J = 5.2 Hz, 2H), 7.46 (d, J = 8.4 Hz, 2H), 7.42 – 7.33 (m, 4H), 5.46 (d, J = 2.3 Hz, 1H).

Fig. S15b: ^{1}H-NMR of compound 8h

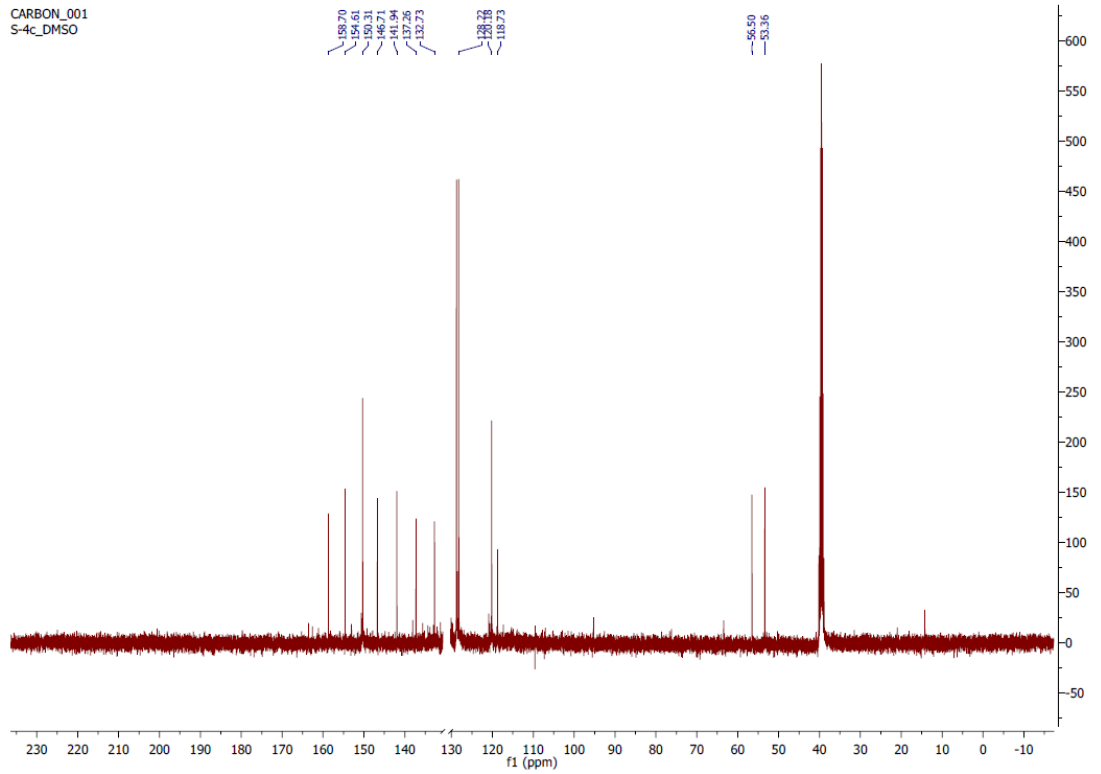

Fig. S16a: ^{13}C-NMR of compound 8h

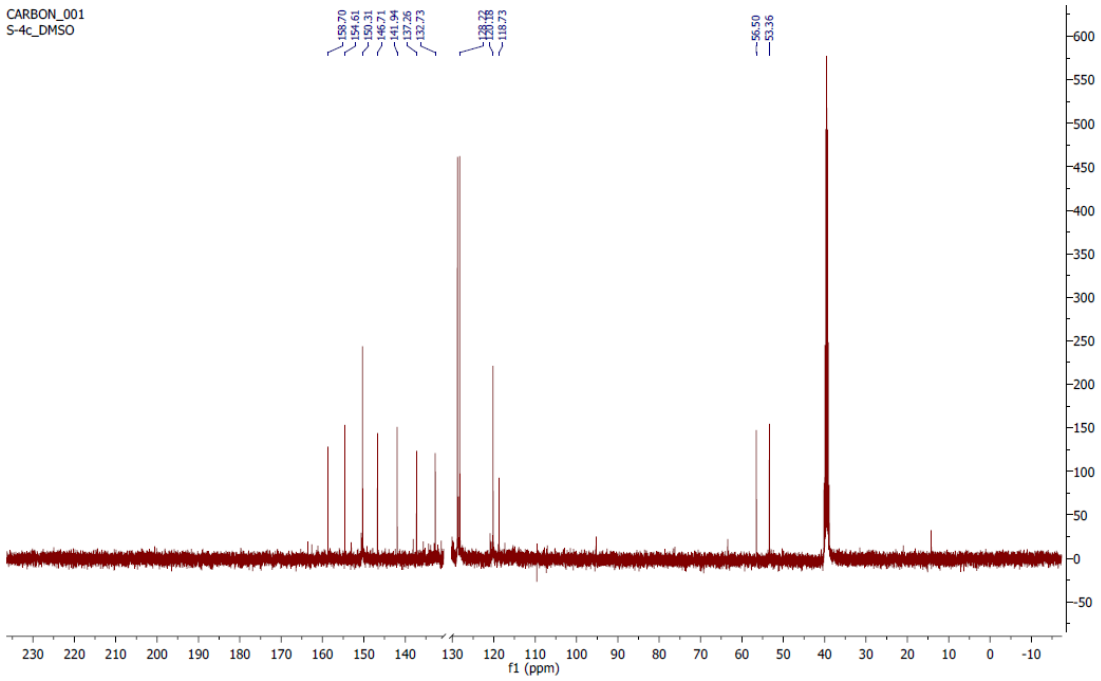

^{13}C NMR (101 MHz, dmso) δ 158.70, 154.61, 150.31, 146.71, 141.94, 137.26, 132.73, 128.78, 128.22, 120.18, 118.73, 56.50, 53.36.

Fig. S16b: ^{13}C-NMR of compound 8h

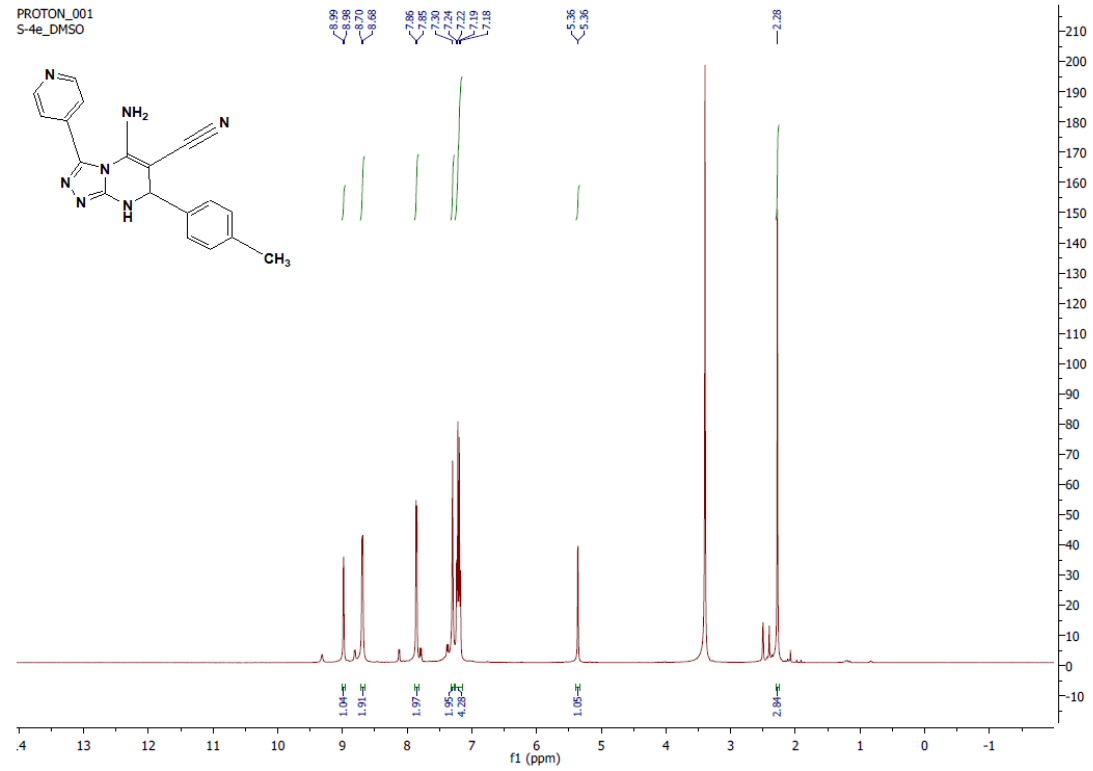

Fig. S17a: ^{1}H-NMR of compound 8i

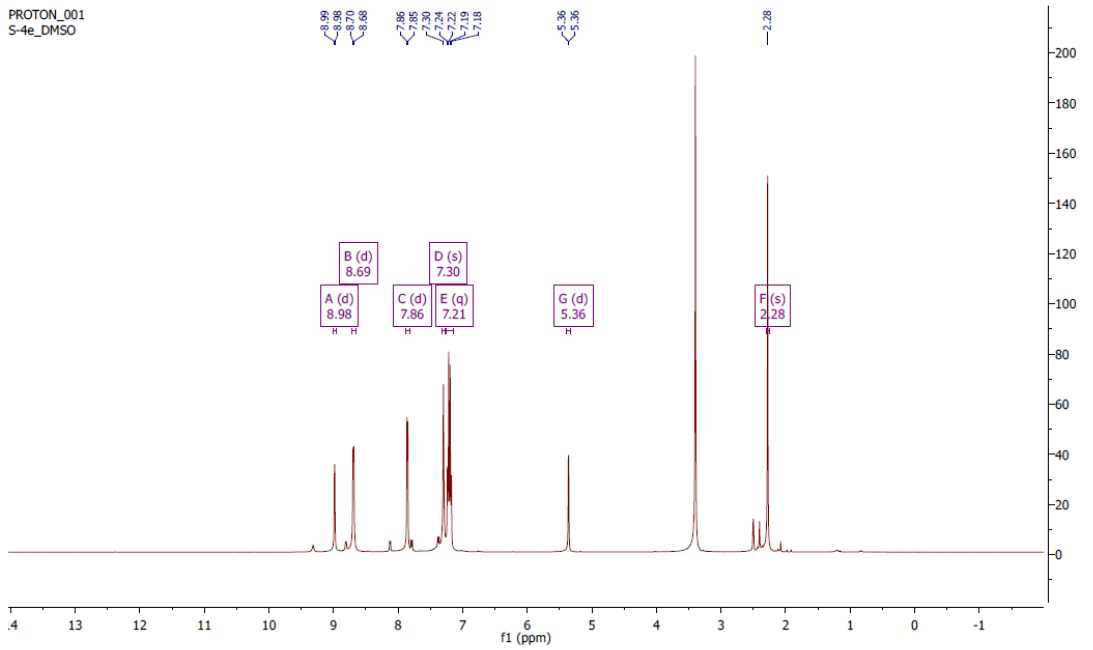

^{1}H NMR (400 MHz, DMSO-d_6) δ 8.98 (d, J = 2.6 Hz, 1H), 8.69 (d, J = 5.1 Hz, 2H), 7.86 (d, J = 5.0 Hz, 2H), 7.30 (s, 2H), 7.25 - 7.16 (m, 4H), 5.36 (d, J = 2.5 Hz, 1H), 2.28 (s, 3H).

Fig. S17b: ^{1}H-NMR of compound 8i

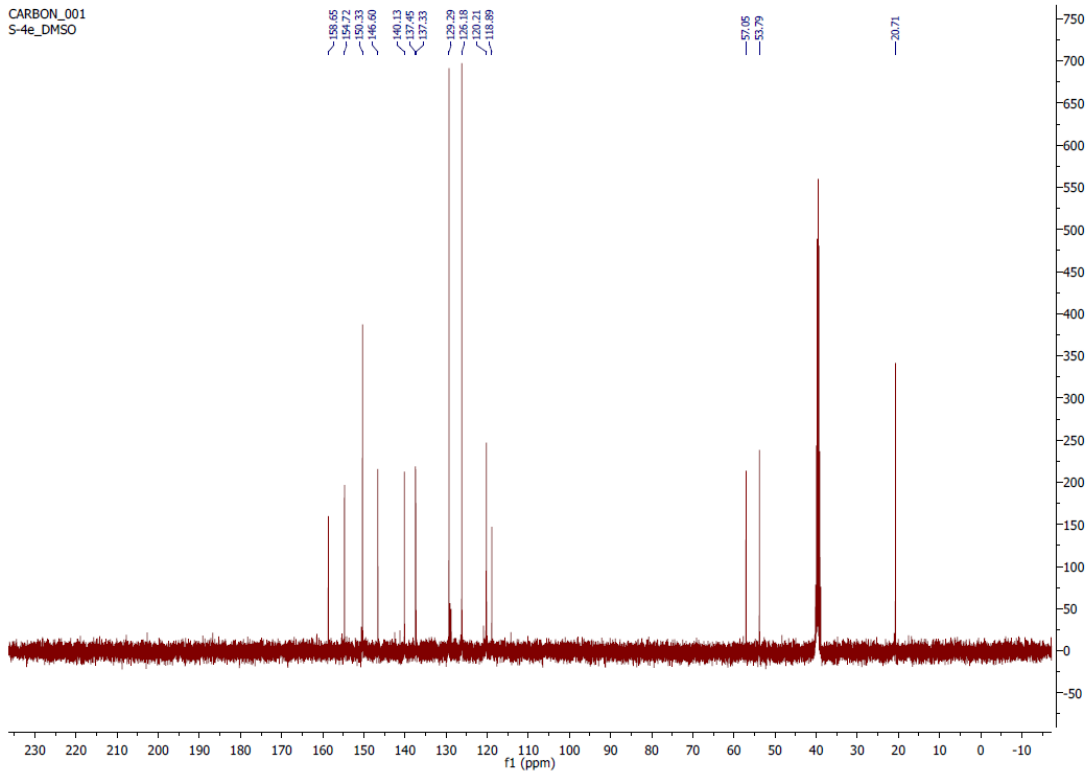

Fig. S18a: ^{13}C-NMR of compound 8i

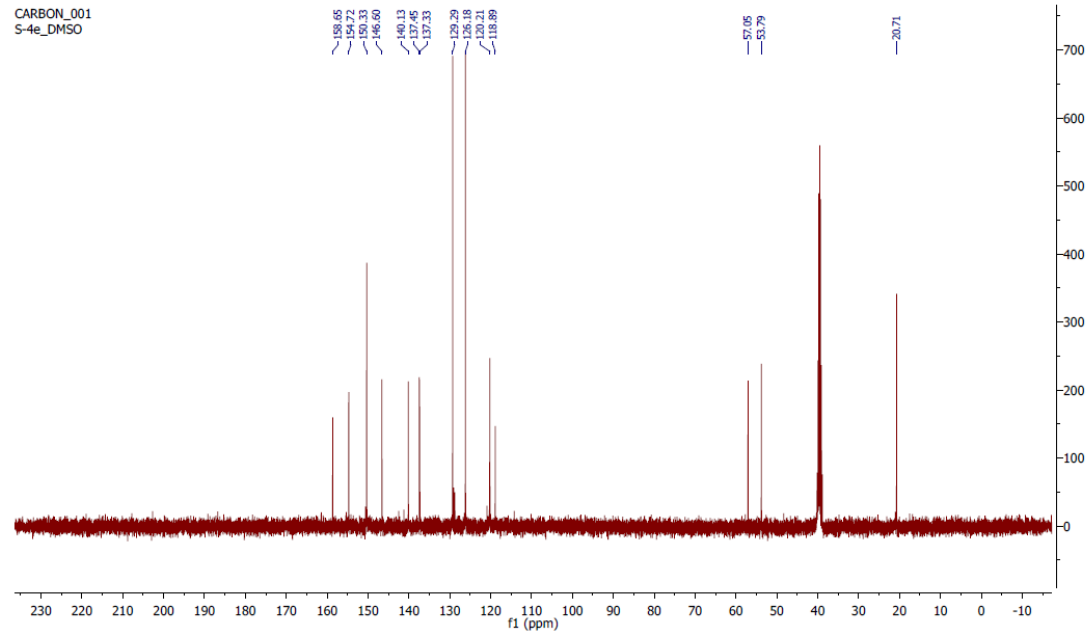

^{13}C NMR (101 MHz, dmso) δ 158.65, 154.72, 150.33, 146.60, 140.13, 137.45, 137.33, 129.29, 126.18, 120.21, 118.89, 57.05, 53.79, 20.71.

Fig. S18b: ^{13}C-NMR of compound 8i

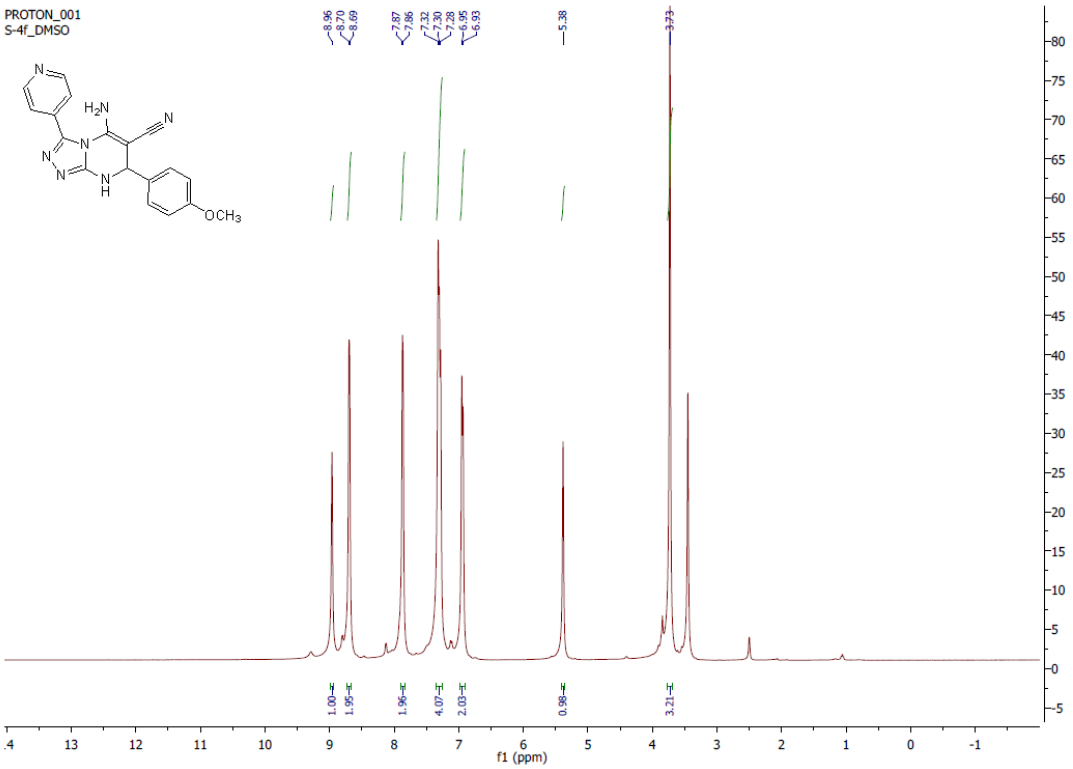

Fig. S19a: ^{1}H-NMR of compound 8j

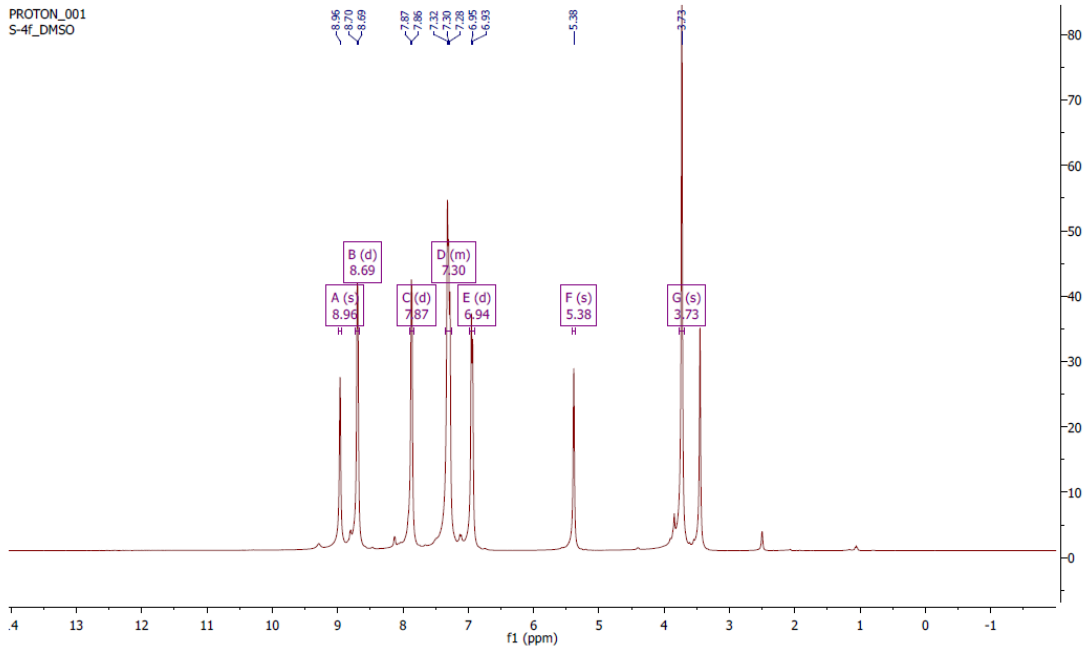

^{1}H NMR (400 MHz, DMSO-d_6) δ 8.96 (s, 1H), 8.69 (d, J = 5.1 Hz, 2H), 7.87 (d, J = 5.1 Hz, 2H), 7.34 – 7.25 (m, 4H), 6.94 (d, J = 8.3 Hz, 2H), 5.38 (s, 1H), 3.73 (s, 3H).

Fig. S19b: ^{1}H-NMR of compound 8j

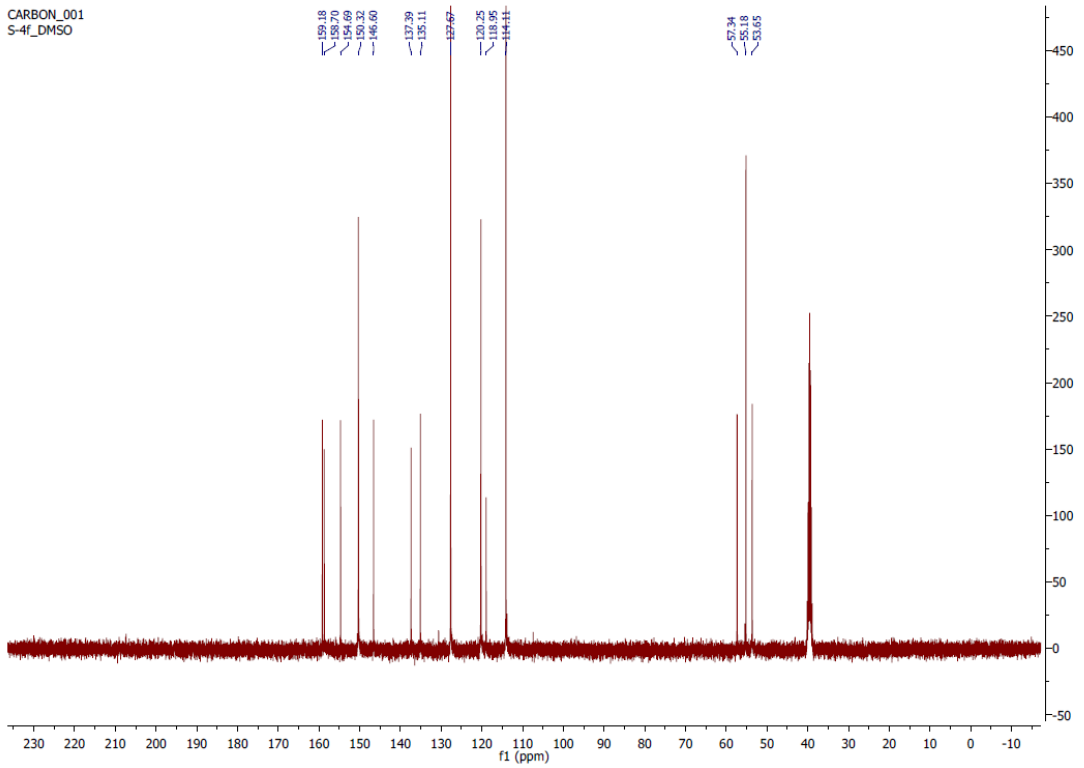

Fig. S20a: ^{13}C-NMR of compound 8j

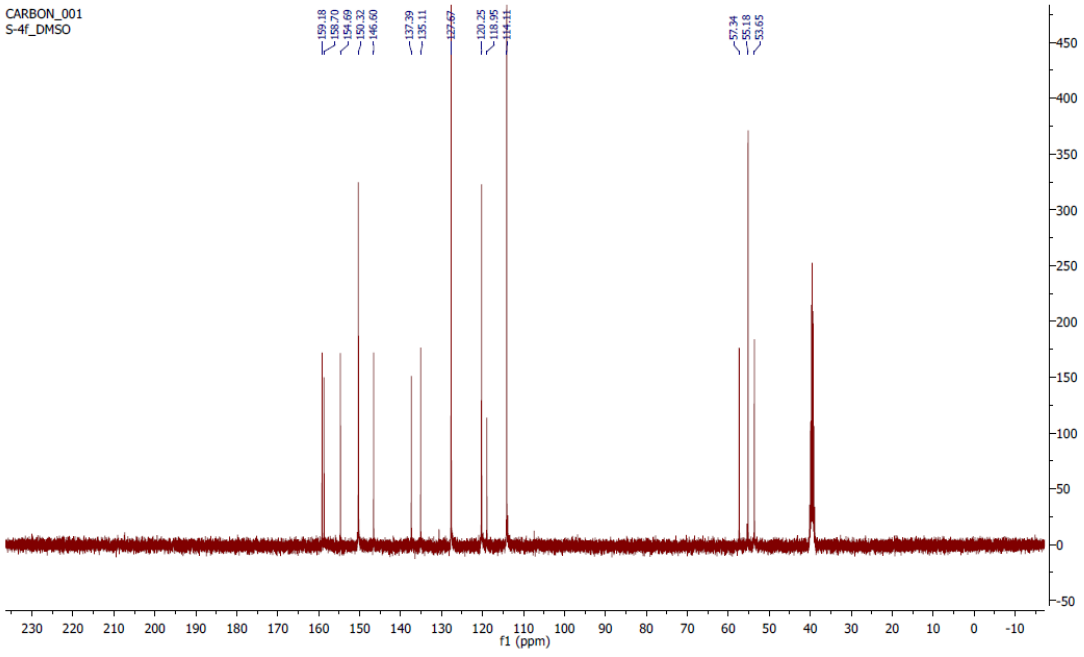

^{13}C NMR (101 MHz, dmso) δ 159.18, 158.70, 154.69, 150.32, 146.60, 137.39, 135.11, 127.67, 120.25, 118.95, 114.11, 57.34, 55.18, 53.65.

Fig. S20b: ^{13}C-NMR of compound 8j

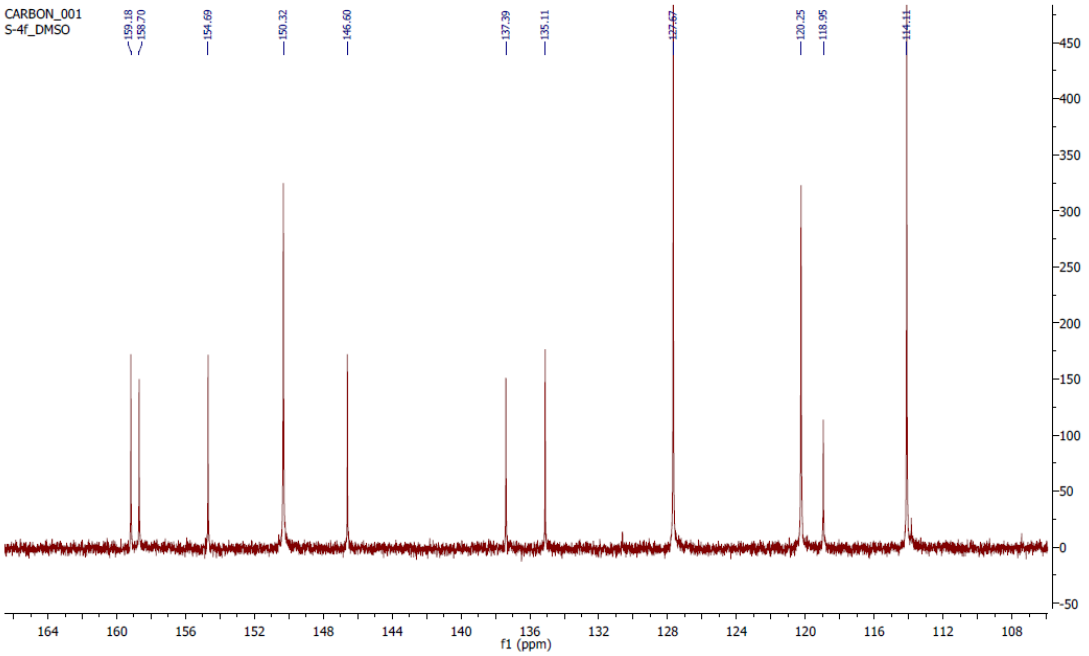

^{13}C NMR (101 MHz, dmso) δ 159.18, 158.70, 154.69, 150.32, 146.60, 137.39, 135.11, 127.67, 120.25, 118.95, 114.11, 57.34, 55.18, 53.65.

Fig. S20c: ^{13}C-NMR of compound 8j

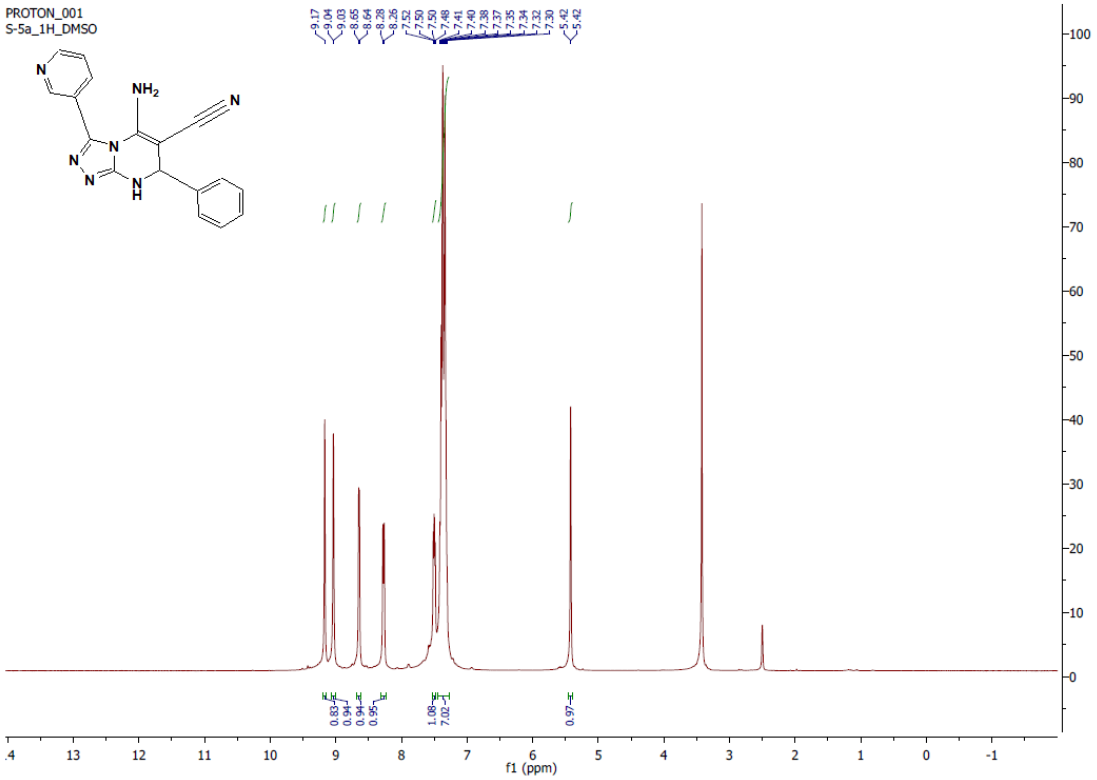

Fig. S21a: ^{1}H-NMR of compound 8k

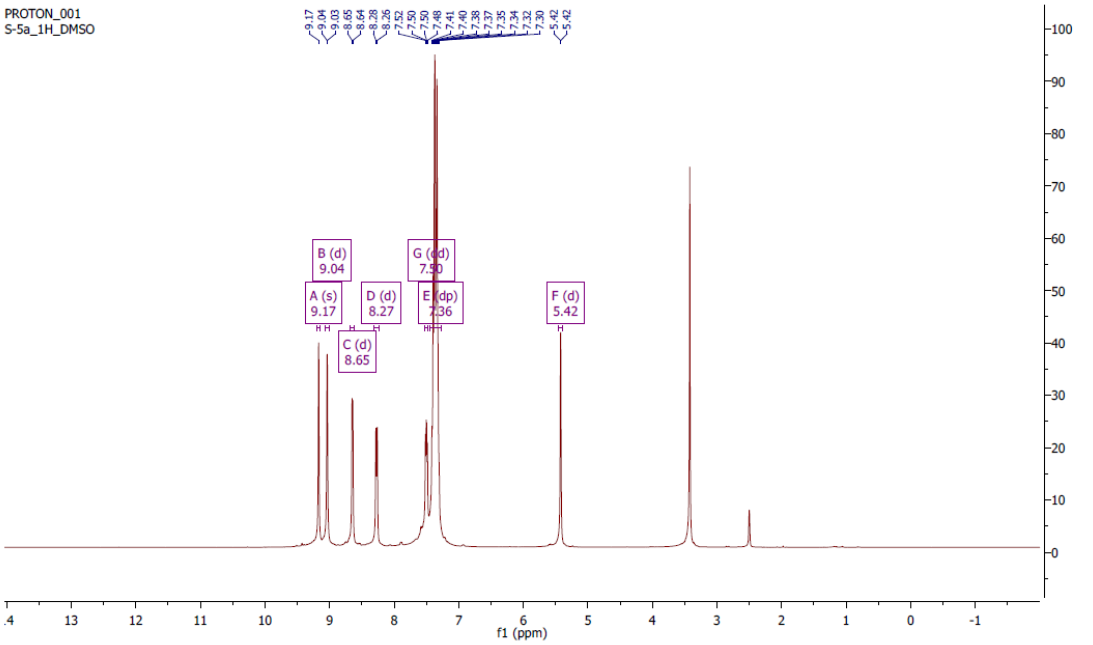

^{1}H NMR (400 MHz, DMSO-d_6) δ 9.17 (s, 1H), 9.04 (d, J = 2.6 Hz, 1H), 8.65 (d, J = 4.8 Hz, 1H), 8.27 (d, J = 8.0 Hz, 1H), 7.50 (dd, J = 8.0, 4.9 Hz, 1H), 7.43 - 7.29 (m, 7H), 5.42 (d, J = 2.4 Hz, 1H).

Fig. S21b: ^{1}H-NMR of compound 8k

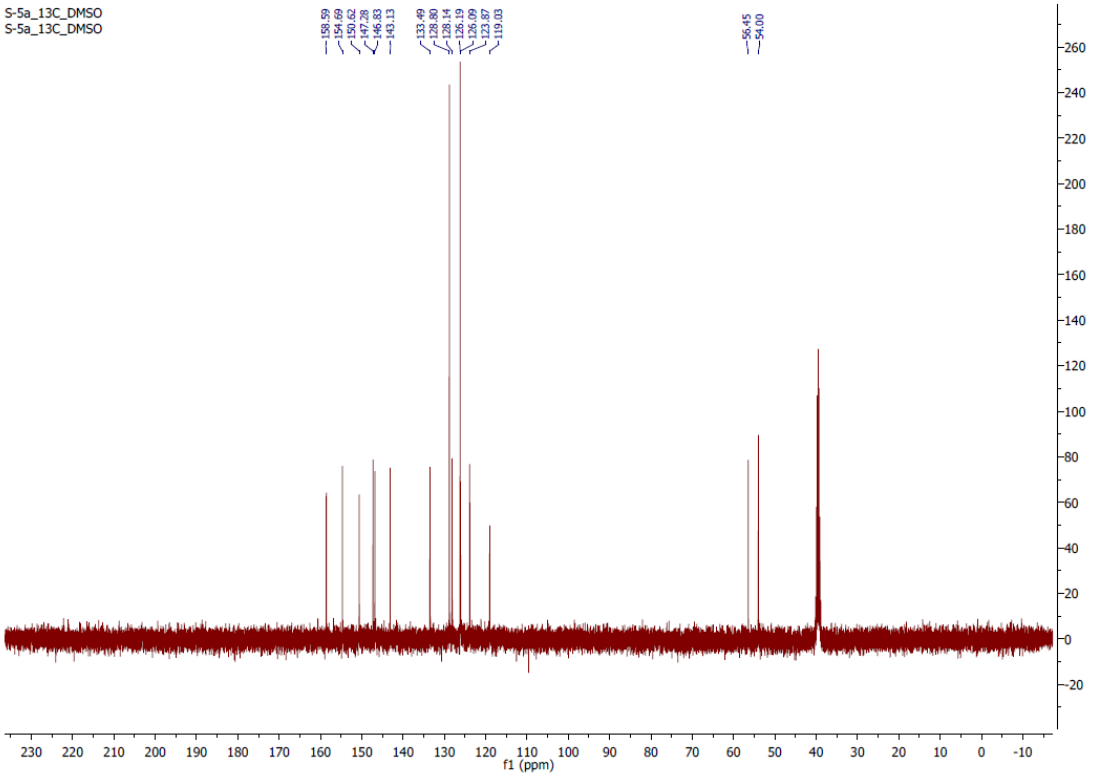

Fig. S22a: ^{13}C-NMR of compound 8k

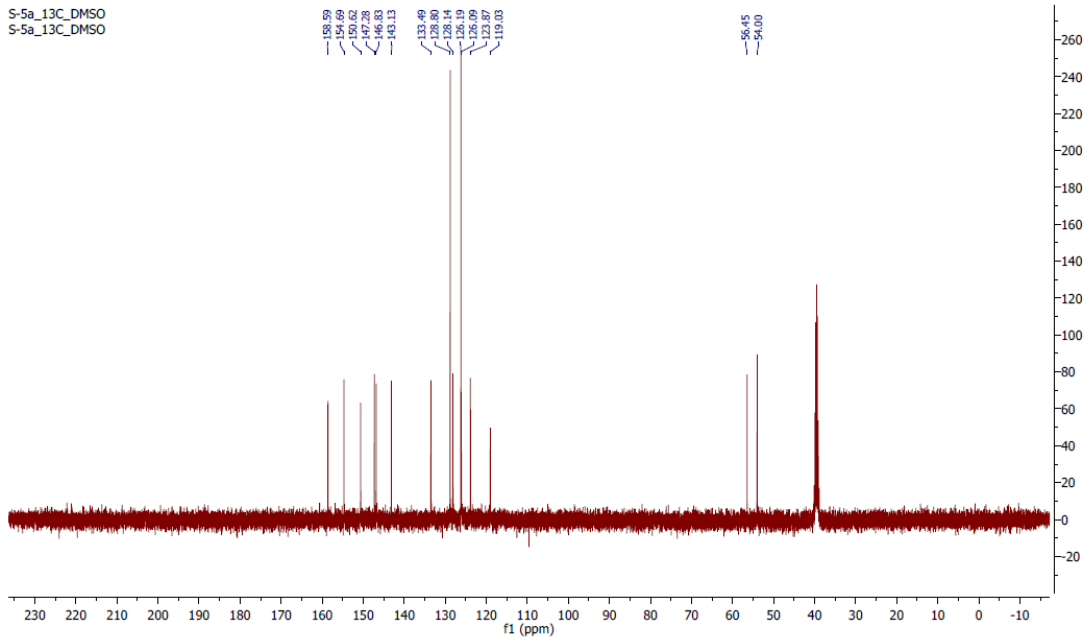

^{13}C NMR (101 MHz, dmso) δ 158.59, 154.69, 150.62, 147.28, 146.83, 143.13, 133.49, 128.80, 128.14, 126.19, 126.09, 123.87, 119.03, 56.45, 54.00.

Fig. S22b: ^{13}C-NMR of compound 8k

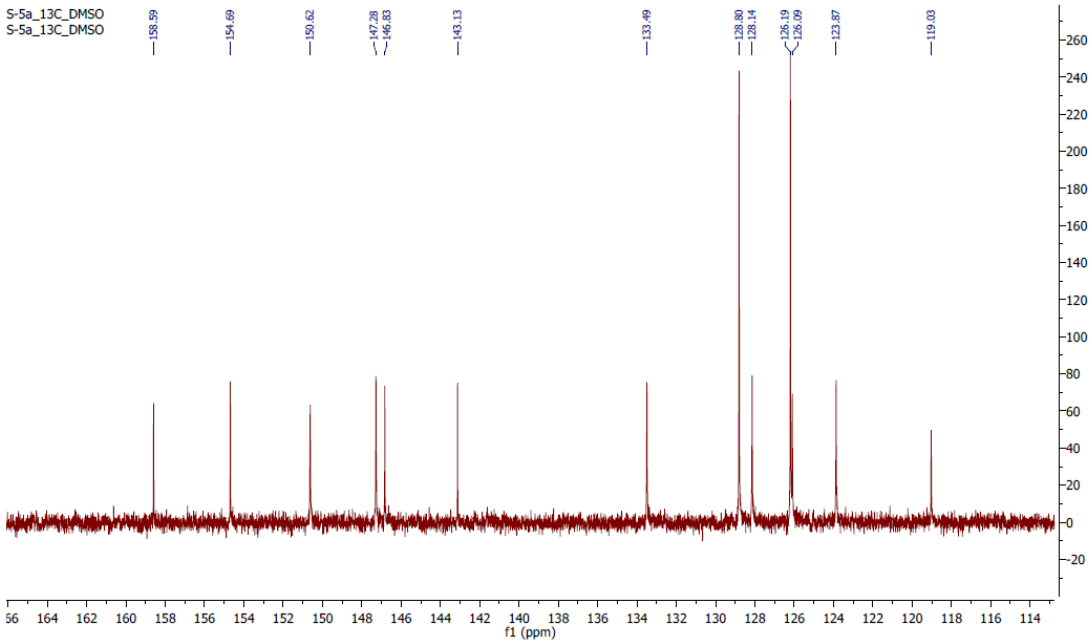

^{13}C NMR (101 MHz, dmso) δ 158.59, 154.69, 150.62, 147.28, 146.83, 143.13, 133.49, 128.80, 128.14, 126.19, 126.09, 123.87, 119.03, 56.45, 54.00.

Fig. S22c: ^{13}C-NMR of compound 8k

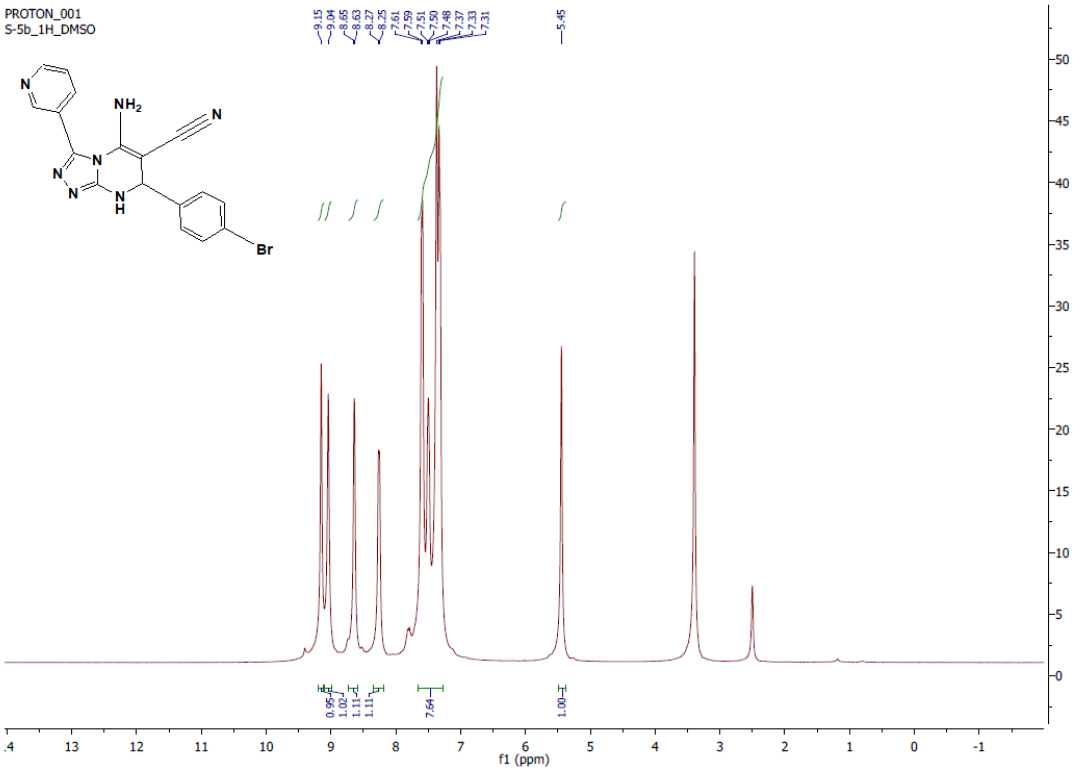

Fig. S23a: ^{1}H-NMR of compound 8l

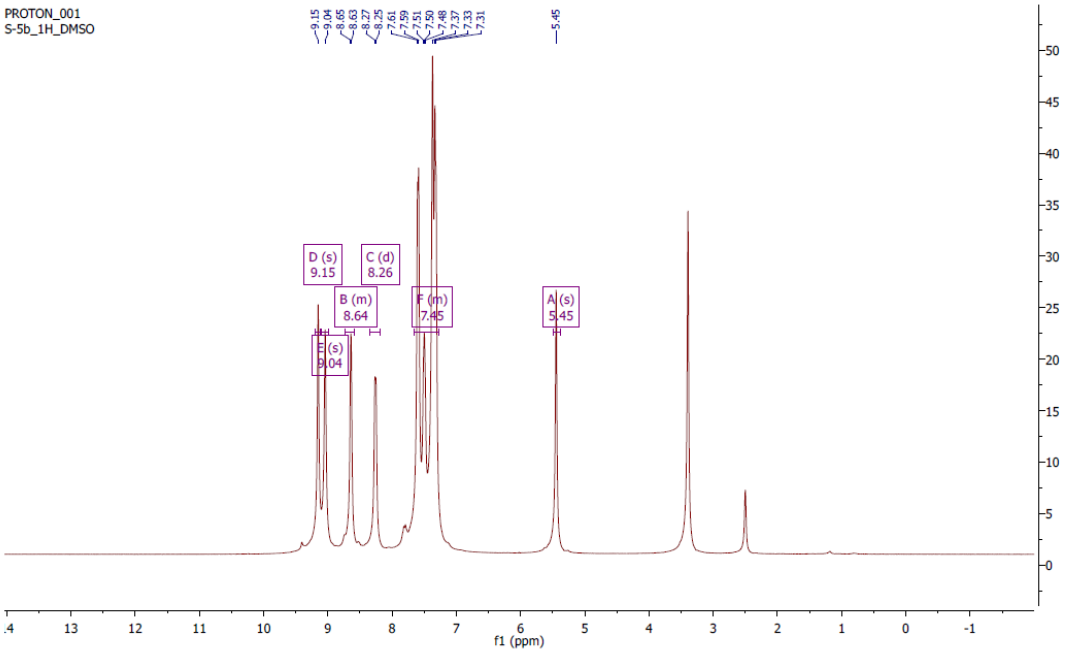

^{1}H NMR (400 MHz, DMSO-d_6) δ 9.15 (s, 1H), 9.04 (s, 1H), 8.64 (s, 1H), 8.26 (d, J = 7.9 Hz, 1H), 7.66 – 7.28 (m, 8H), 5.45 (s, 1H).

Fig. S23b: ^{1}H-NMR of compound 8l

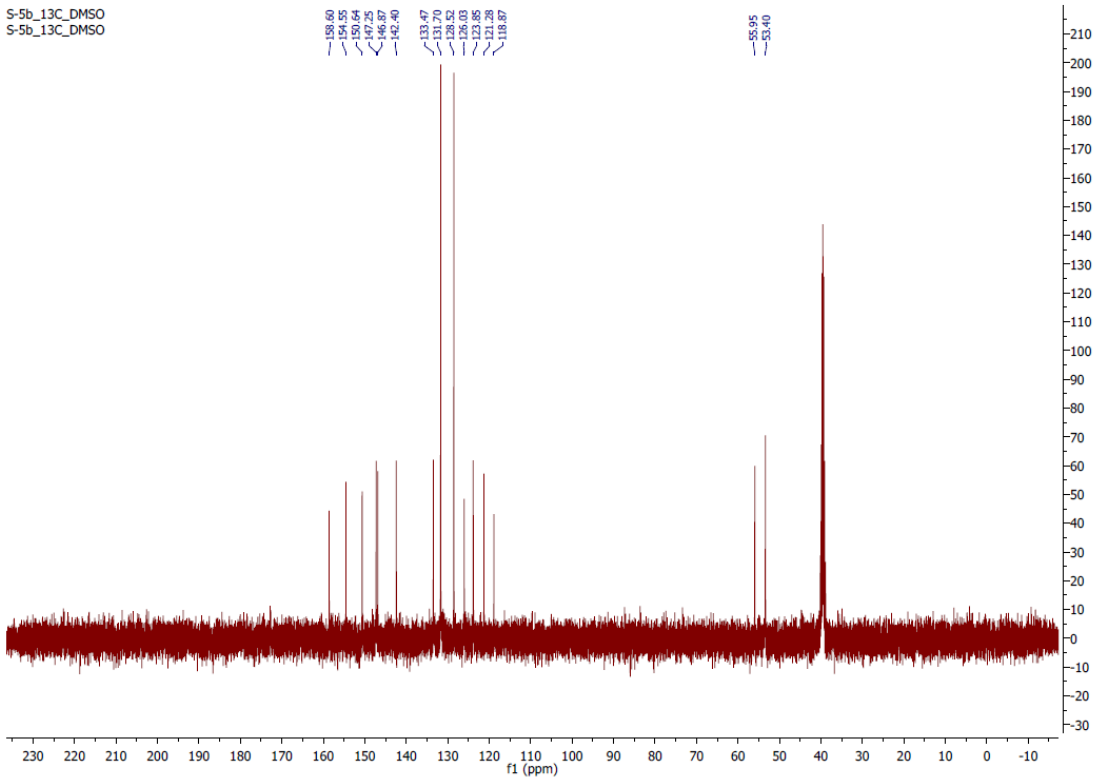

Fig. S24a: ^{13}C-NMR of compound 8l

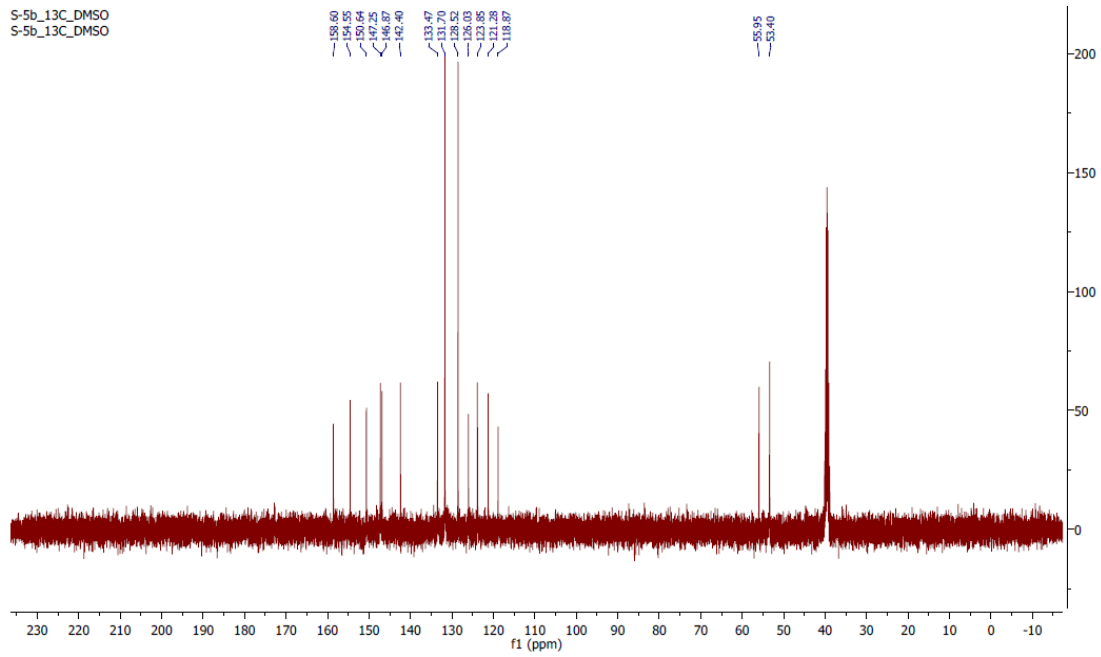

^{13}C NMR (101 MHz, dmso) δ 158.60, 154.55, 150.64, 147.25, 146.87, 142.40, 133.47, 131.70, 128.52, 126.03, 123.85, 121.28, 118.87, 55.95, 53.40.

Fig. S24b: ^{13}C-NMR of compound 8l

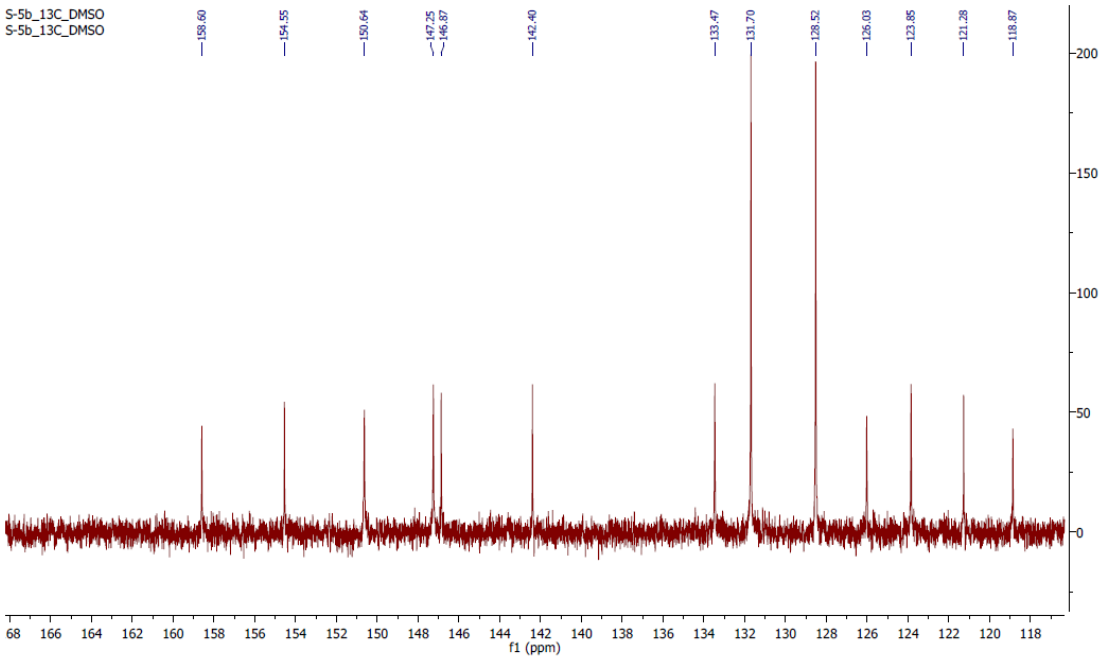

^{13}C NMR (101 MHz, dmso) δ 158.60, 154.55, 150.64, 147.25, 146.87, 142.40, 133.47, 131.70, 128.52, 126.03, 123.85, 121.28, 118.87, 55.95, 53.40.

Fig. S24c: ^{13}C-NMR of compound 8l

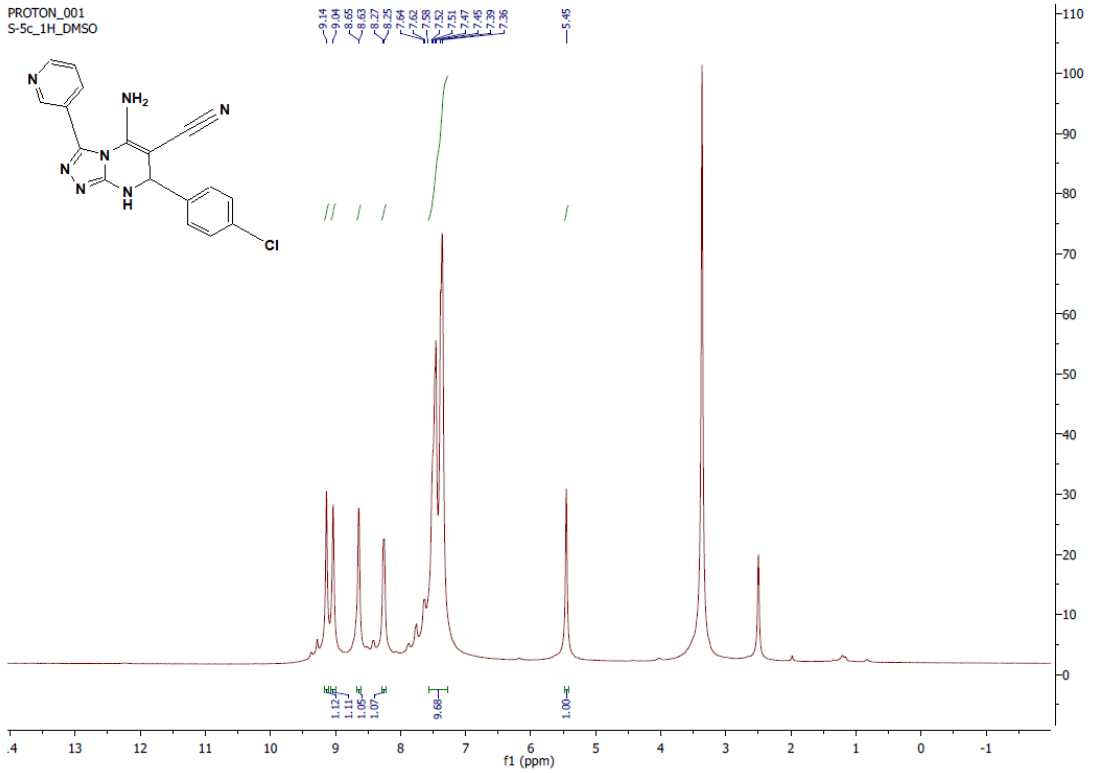

Fig. S25a: ^{1}H-NMR of compound 8m

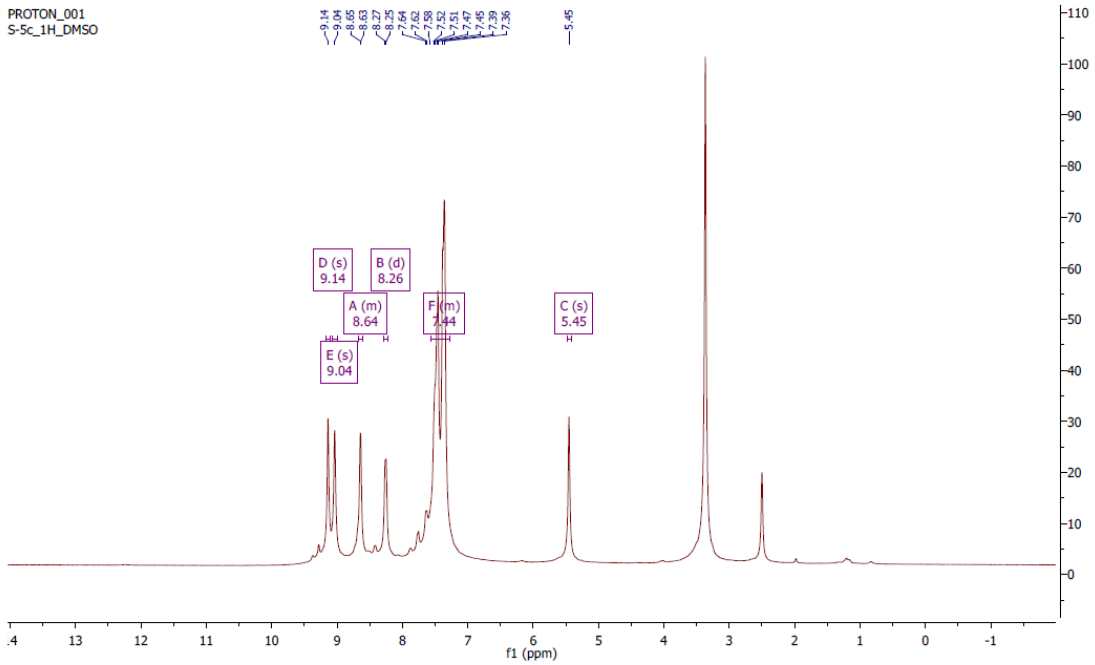

^{1}H NMR (400 MHz, DMSO-d_6) δ 9.14 (s, 1H), 9.04 (s, 1H), 8.64 (s, 1H), 8.26 (d, J = 8.0 Hz, 1H), 7.57 – 7.27 (m, 7H), 5.45 (s, 1H).

Fig. S25b: ^{1}H-NMR of compound 8m

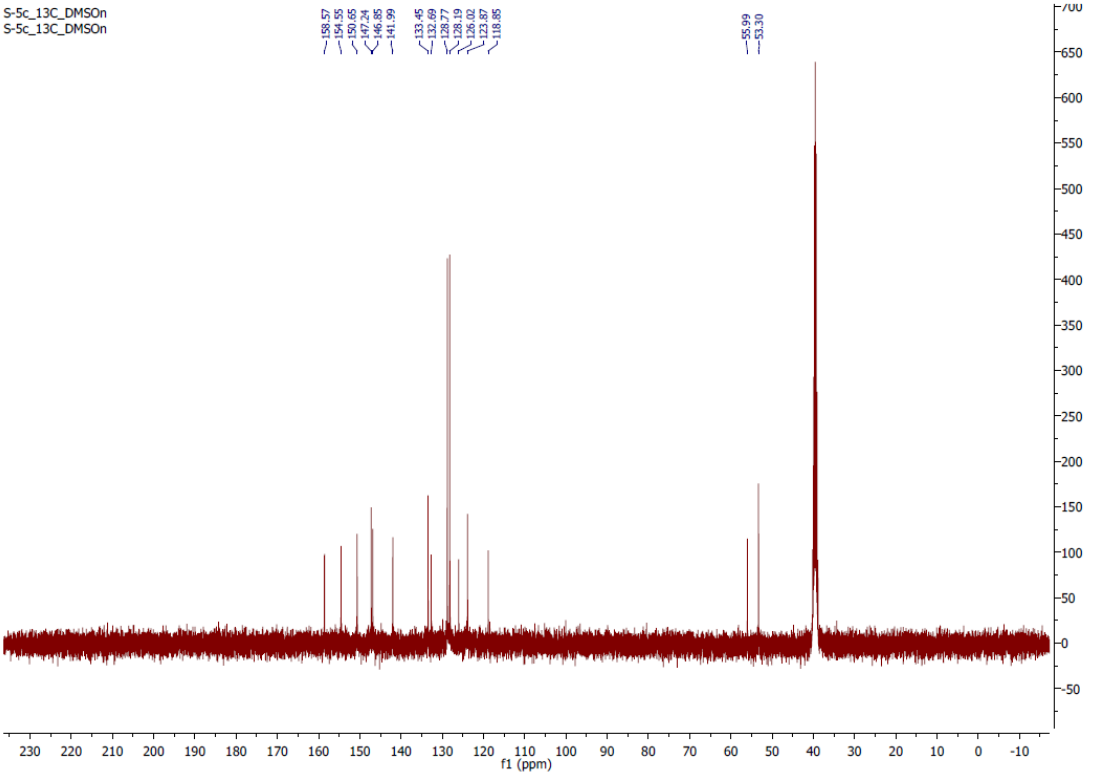

Fig. S26a: ^{13}C-NMR of compound 8m

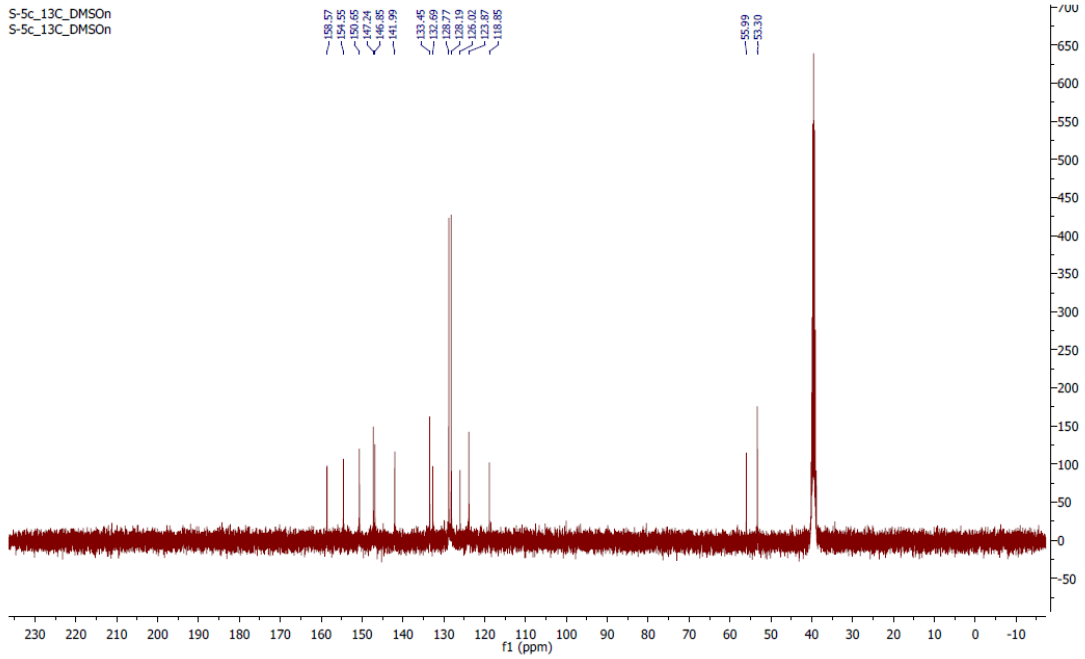

^{13}C NMR (101 MHz, dmso) δ 158.57, 154.55, 150.65, 147.24, 146.85, 141.99, 133.45, 132.69, 128.77, 128.19, 126.02, 123.87, 118.85, 55.99, 53.30.

Fig. S26b: ^{13}C-NMR of compound 8m

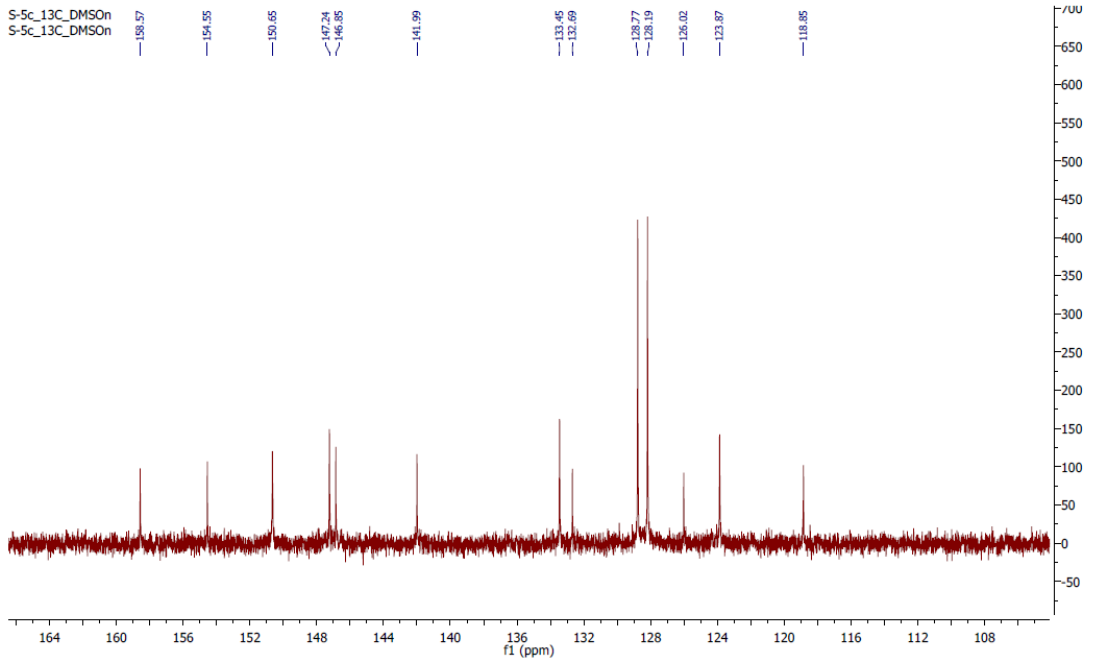

^{13}C NMR (101 MHz, dmso) δ 158.57, 154.55, 150.65, 147.24, 146.85, 141.99, 133.45, 132.69, 128.77, 128.19, 126.02, 123.87, 118.85, 55.99, 53.30.

Fig. S26c: ^{13}C-NMR of compound 8m

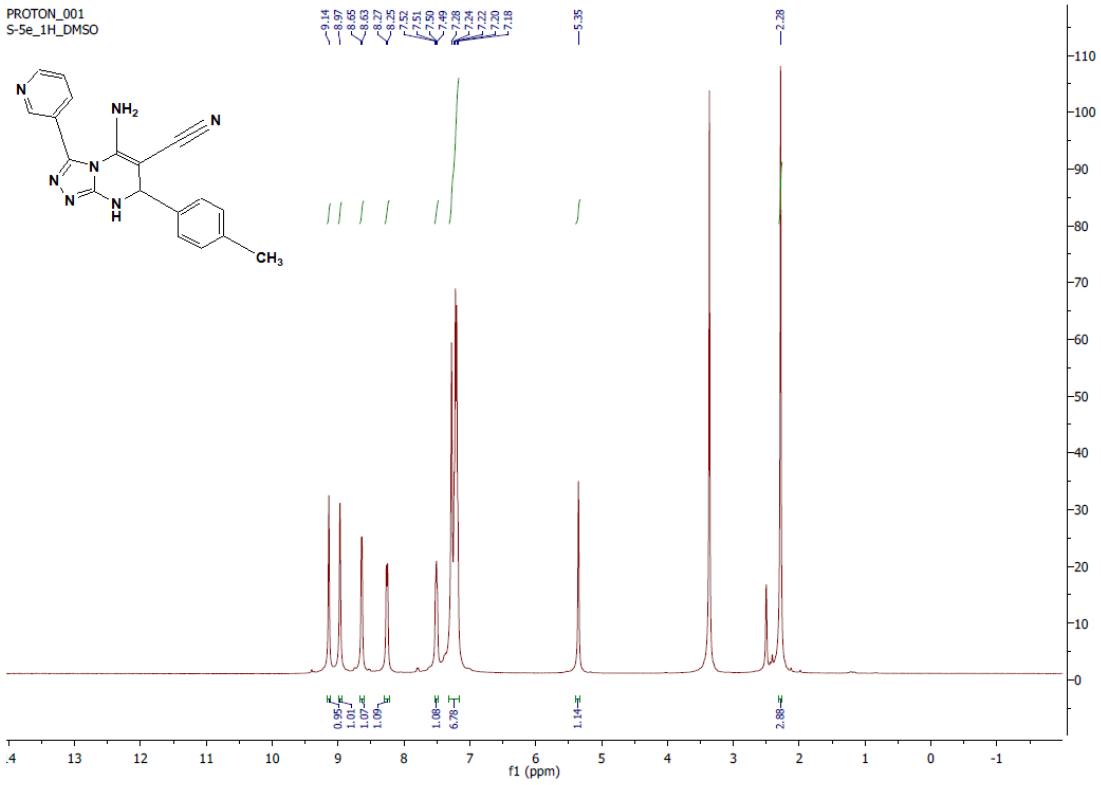

Fig. S27a: ^{1}H-NMR of compound 8n

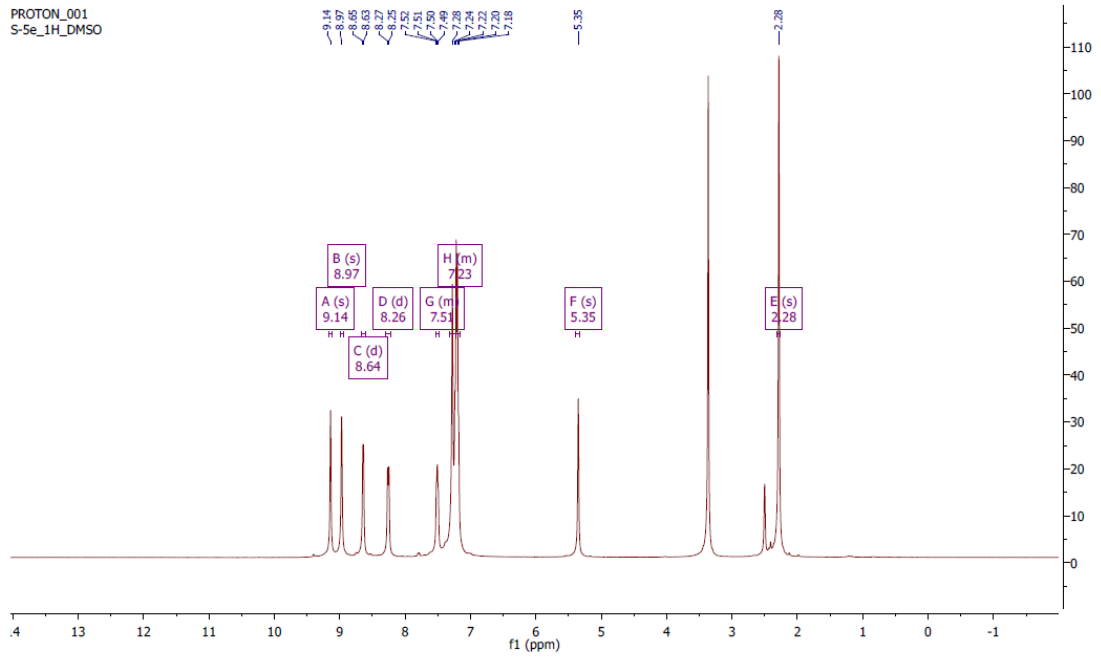

^{1}H NMR (400 MHz, DMSO-d_6) δ 9.14 (s, 1H), 8.97 (s, 1H), 8.64 (d, J = 4.8 Hz, 1H), 8.26 (d, J = 7.9 Hz, 1H), 7.54 – 7.48 (m, 1H), 7.31 – 7.17 (m, 6H), 5.35 (s, 1H), 2.28 (s, 3H).

Fig. S27b: ^{1}H-NMR of compound 8n

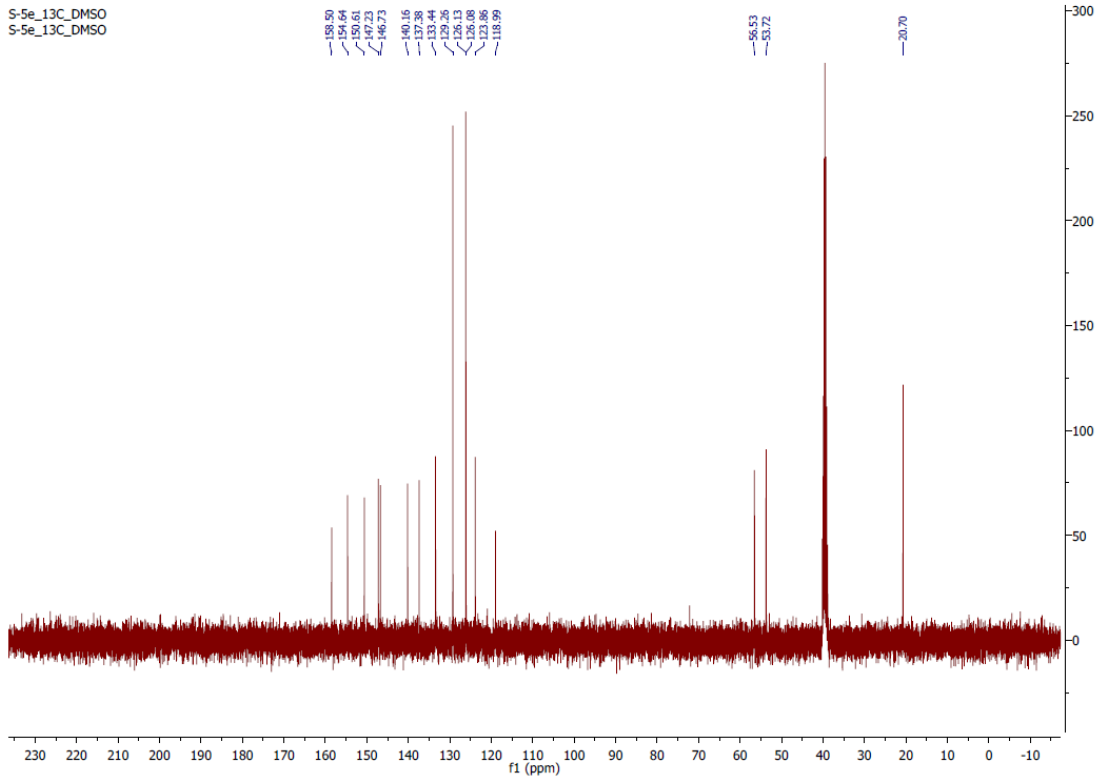

Fig. S28a: ^{1}H-NMR of compound 8n

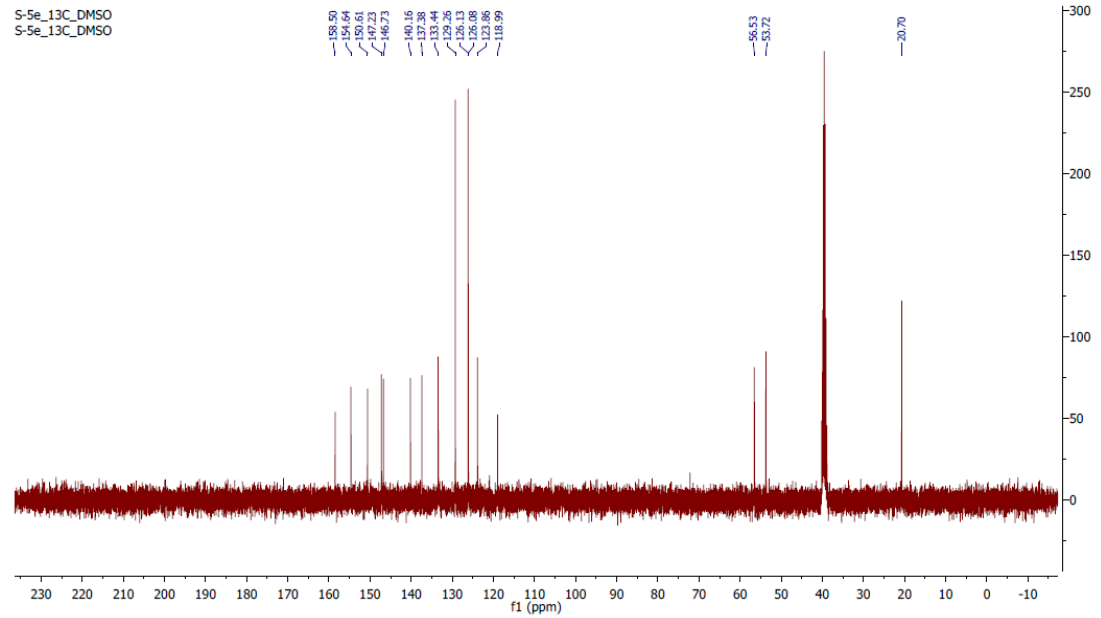

^{13}C NMR (101 MHz, dmso) δ 158.50, 154.64, 150.61, 147.23, 146.73, 140.16, 137.38, 133.44, 129.26, 126.13, 126.08, 123.86, 118.99, 56.53, 53.72, 20.70.

Fig. S28b: ^{1}H-NMR of compound 8n

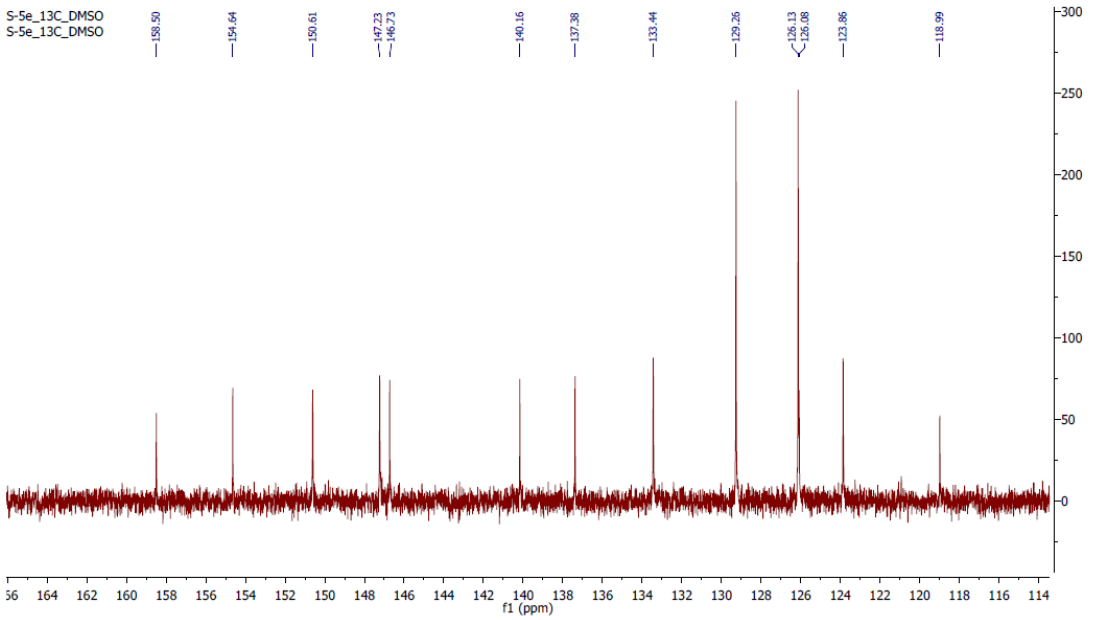

^{13}C NMR (101 MHz, dmso) δ 158.50, 154.64, 150.61, 147.23, 146.73, 140.16, 137.38, 133.44, 129.26, 126.13, 126.08, 123.86, 118.99, 56.53, 53.72, 20.70.

Fig. S28c: ^{1}H-NMR of compound 8n

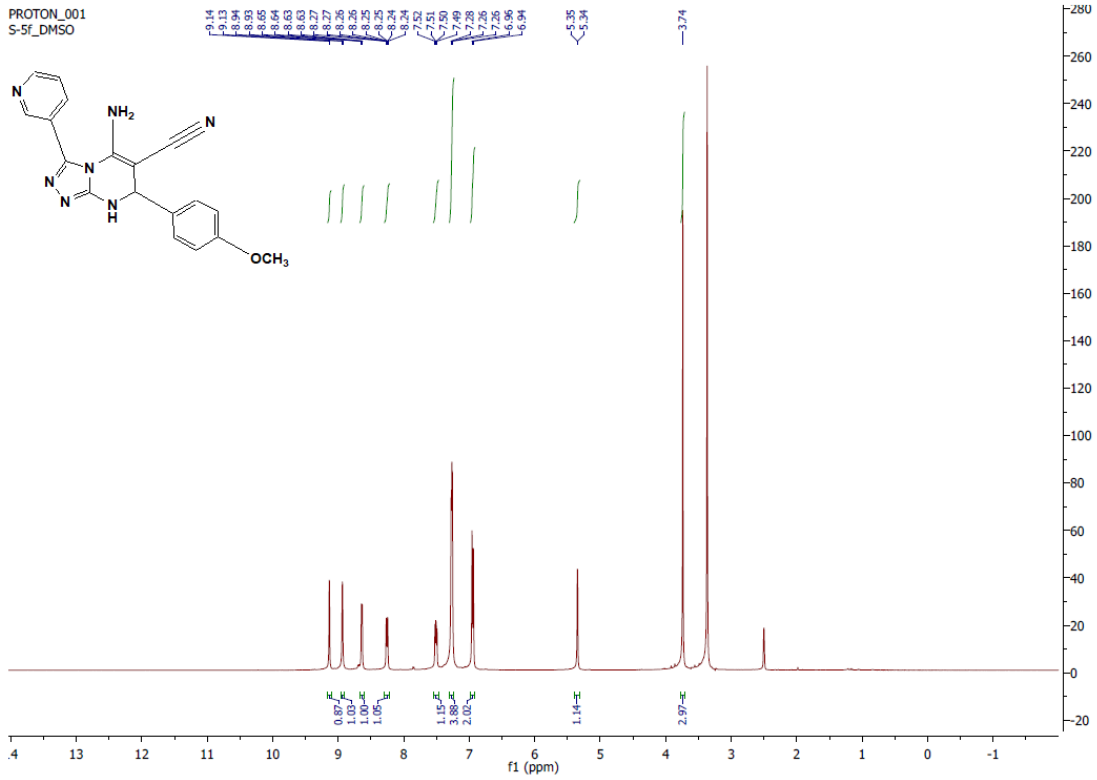

Fig. S29a: ^{1}H-NMR of compound 8o

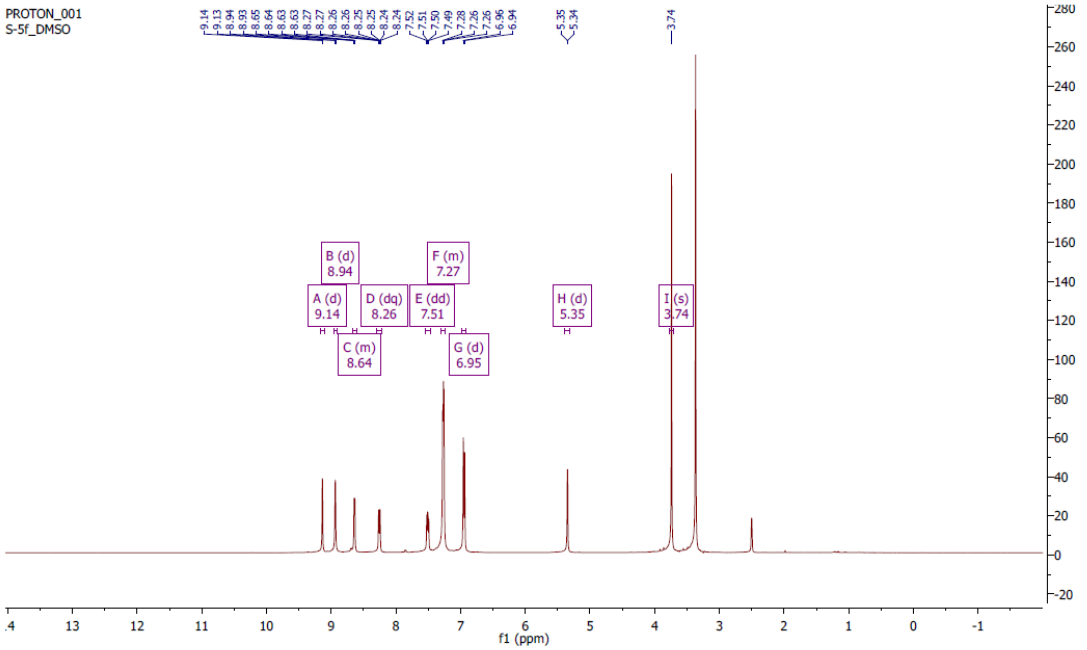

^{1}H NMR (400 MHz, DMSO-d_6) δ 9.14 (d, J = 2.1 Hz, 1H), 8.94 (d, J = 2.4 Hz, 1H), 8.67 – 8.60 (m, 1H), 8.26 (d, J = 8.2 Hz, 1H), 7.51 (dd, J = 7.9, 4.9 Hz, 1H), 7.30 – 7.23 (m, 4H), 6.95 (d, J = 8.3 Hz, 2H), 5.35 (d, J = 2.3 Hz, 1H), 3.74 (s, 3H).

Fig. S29b: ^{1}H-NMR of compound 8o

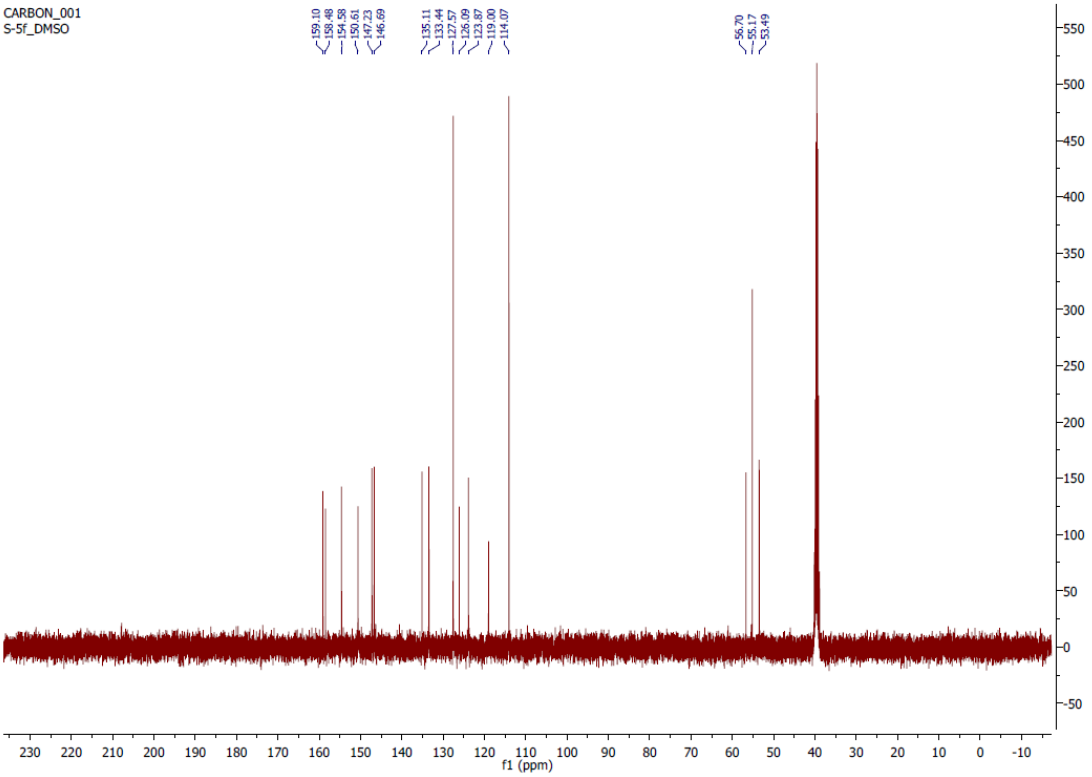

Fig. S30a: ^{13}C-NMR of compound 8o

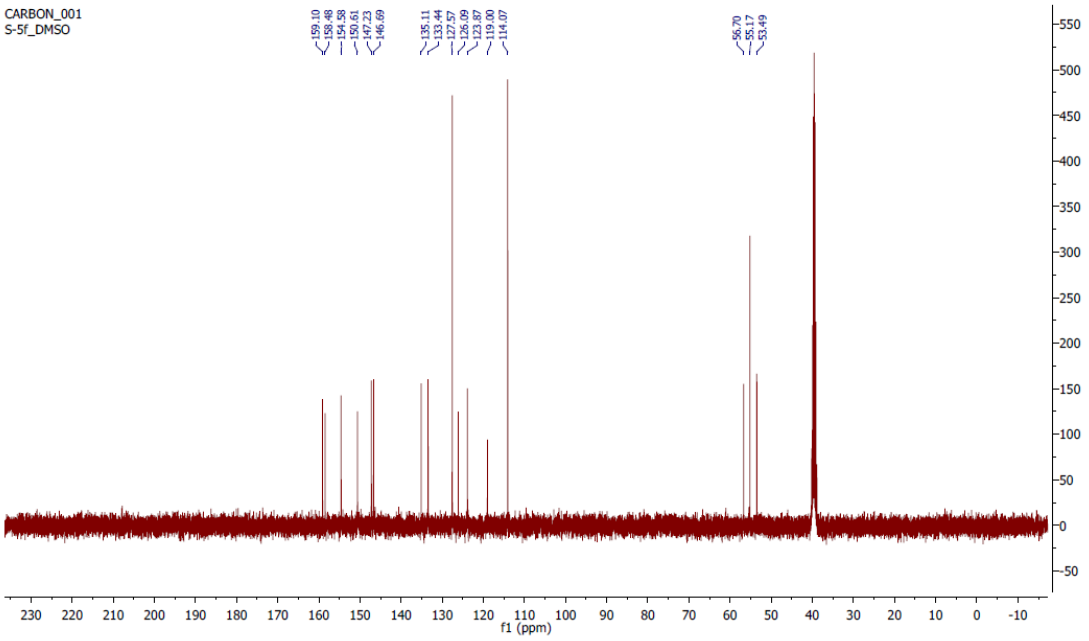

^{13}C NMR (101 MHz, dmso) δ 159.10, 158.48, 154.58, 150.61, 147.23, 146.69, 135.11, 133.44, 127.57, 126.09, 123.87, 119.00, 114.07, 56.70, 55.17, 53.49.

Fig. S30b: ^{13}C-NMR of compound 8o

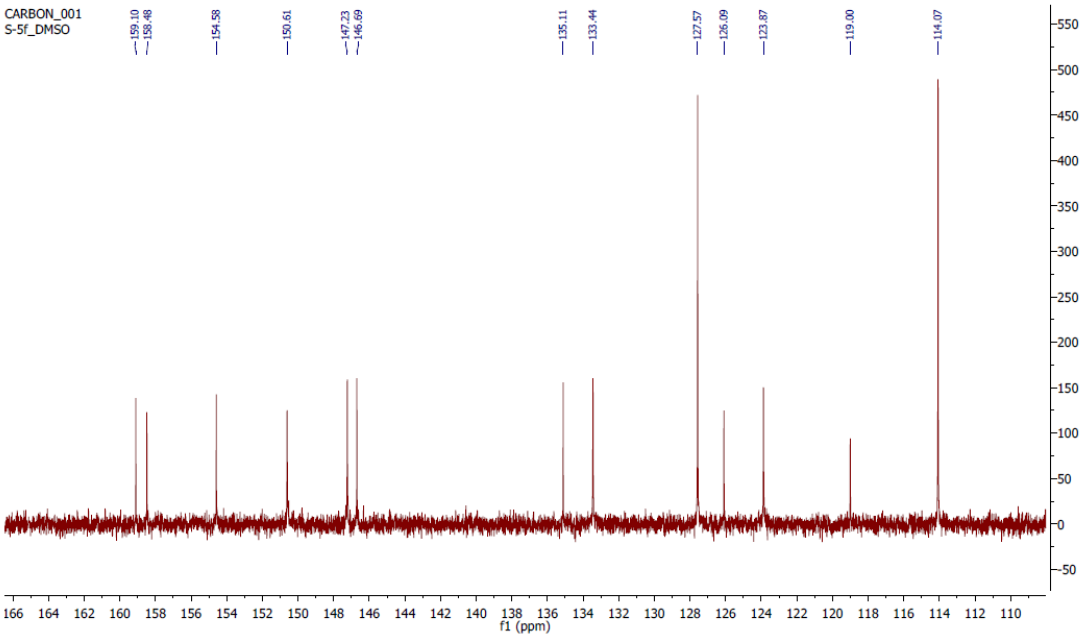

^{13}C NMR (101 MHz, dmso) δ 159.10, 158.48, 154.58, 150.61, 147.23, 146.69, 135.11, 133.44, 127.57, 126.09, 123.87, 119.00, 114.07, 56.70, 55.17, 53.49.

Fig. S30c: ^{13}C-NMR of compound 8o

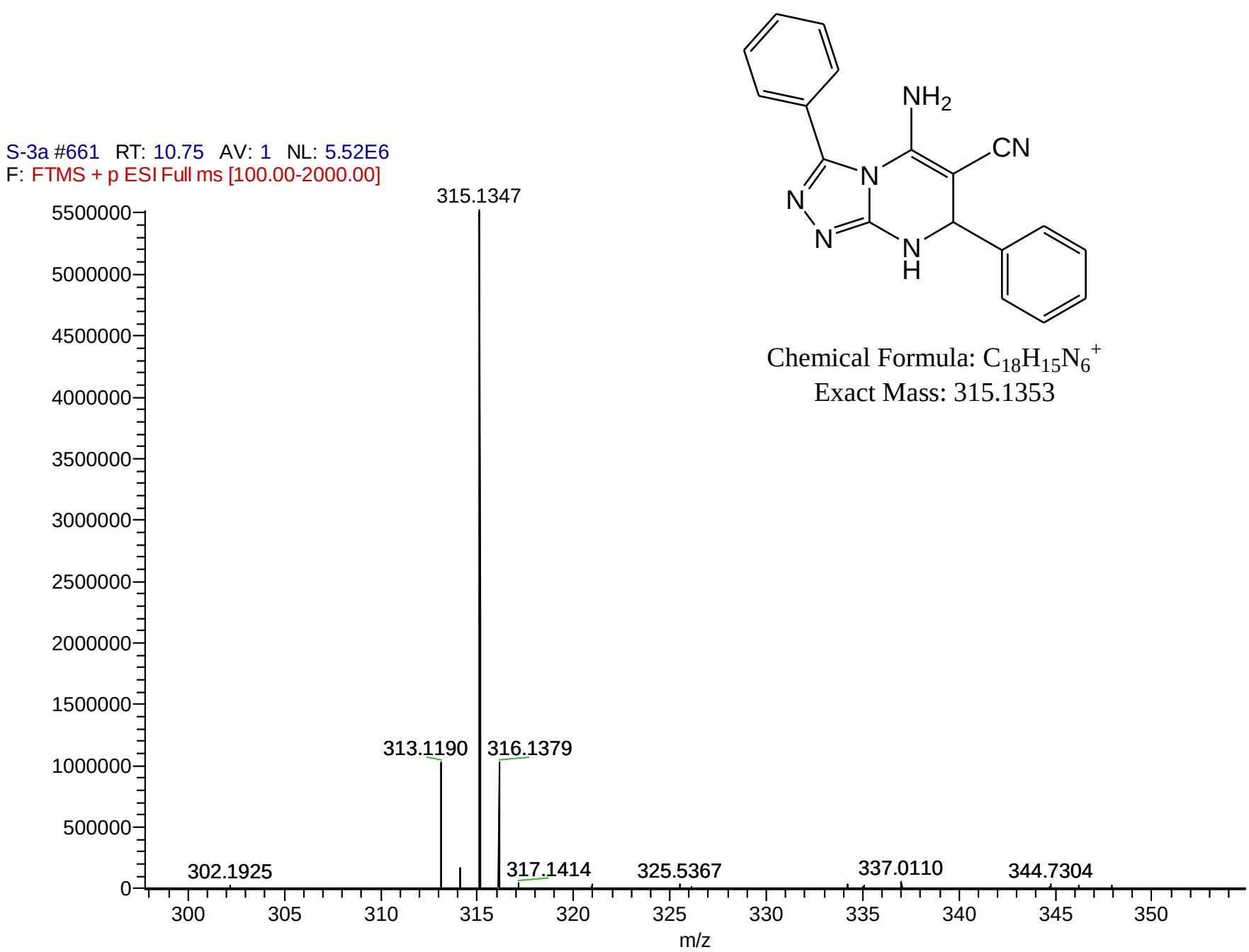

Chemical Formula: $C_{18}H_{15}N_6^+$

Exact Mass: 315.1353

Fig. S31a: LCMS of Compound 8a

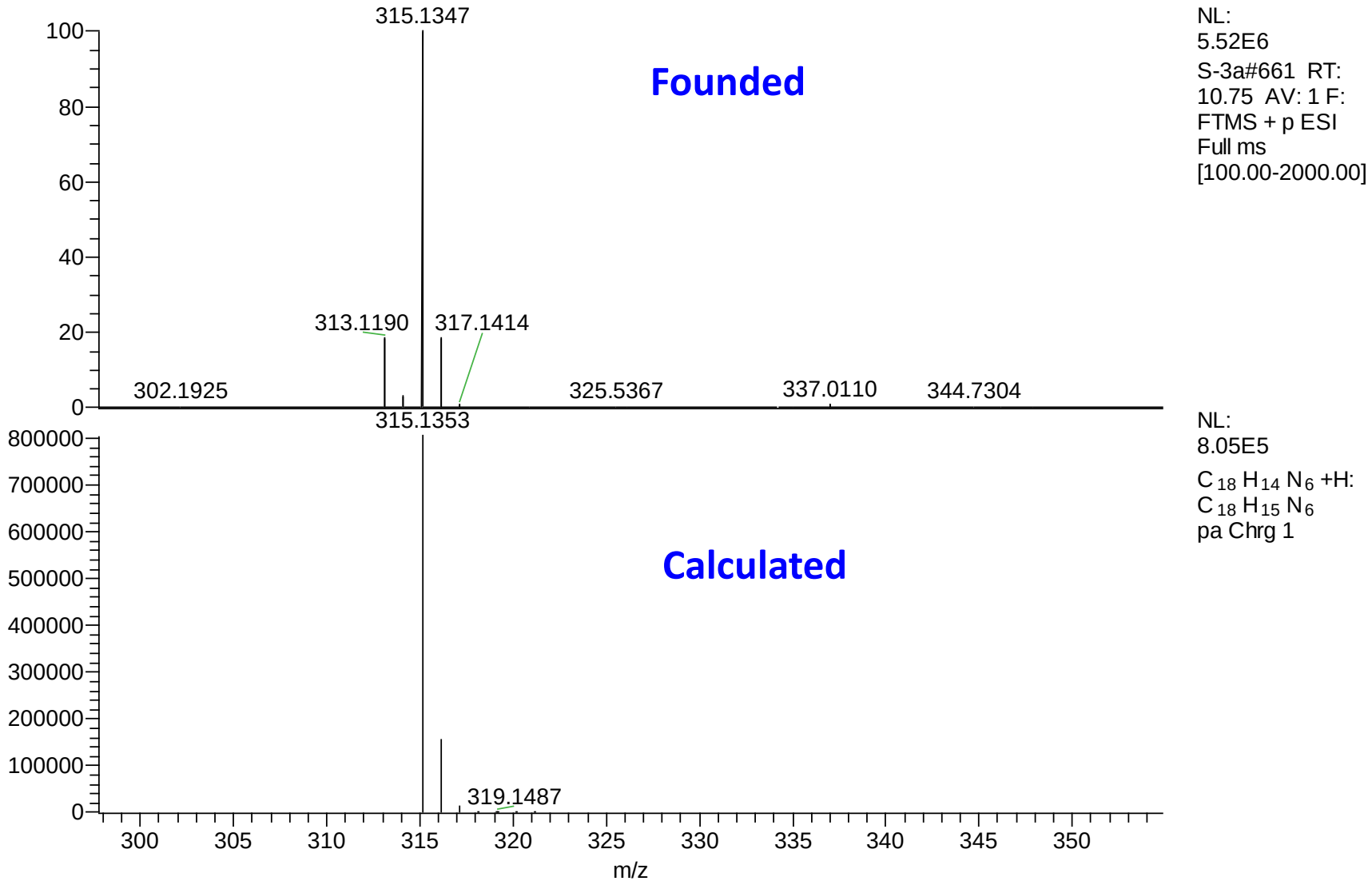

Fig. S31b: LCMS of Compound 8a

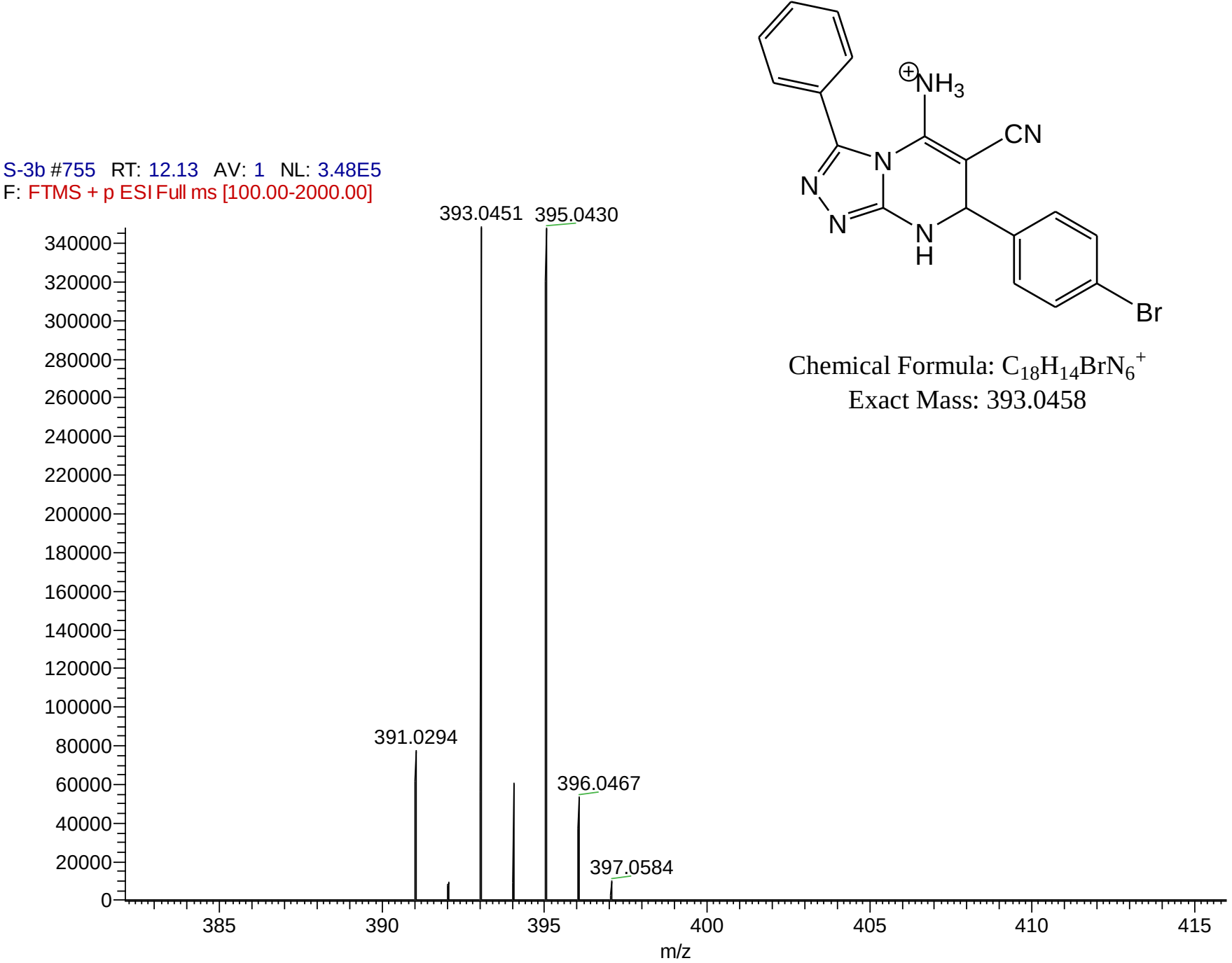

Fig. S32a: LCMS of Compound 8b

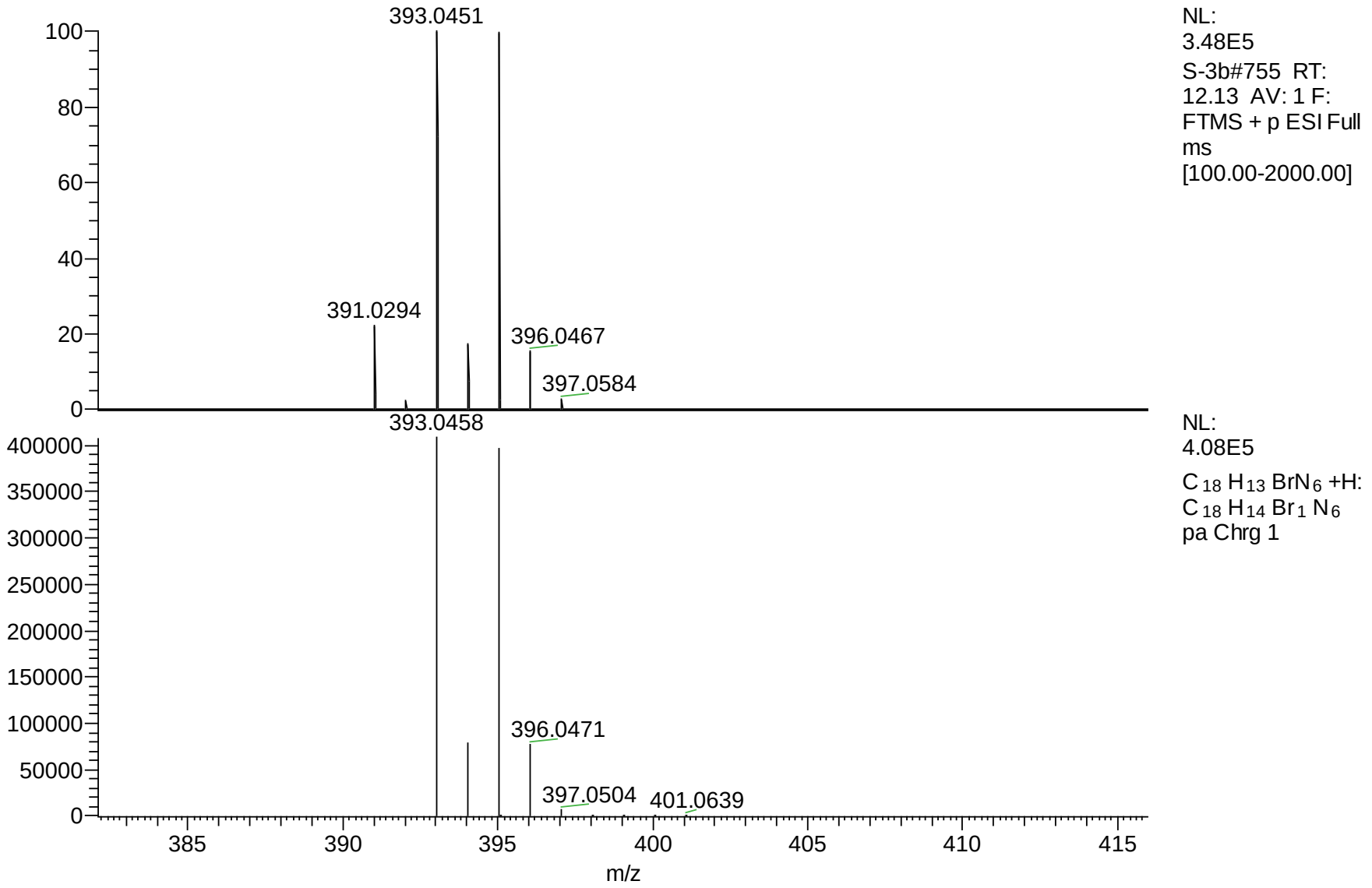

Fig. S32b: LCMS of Compound 8b

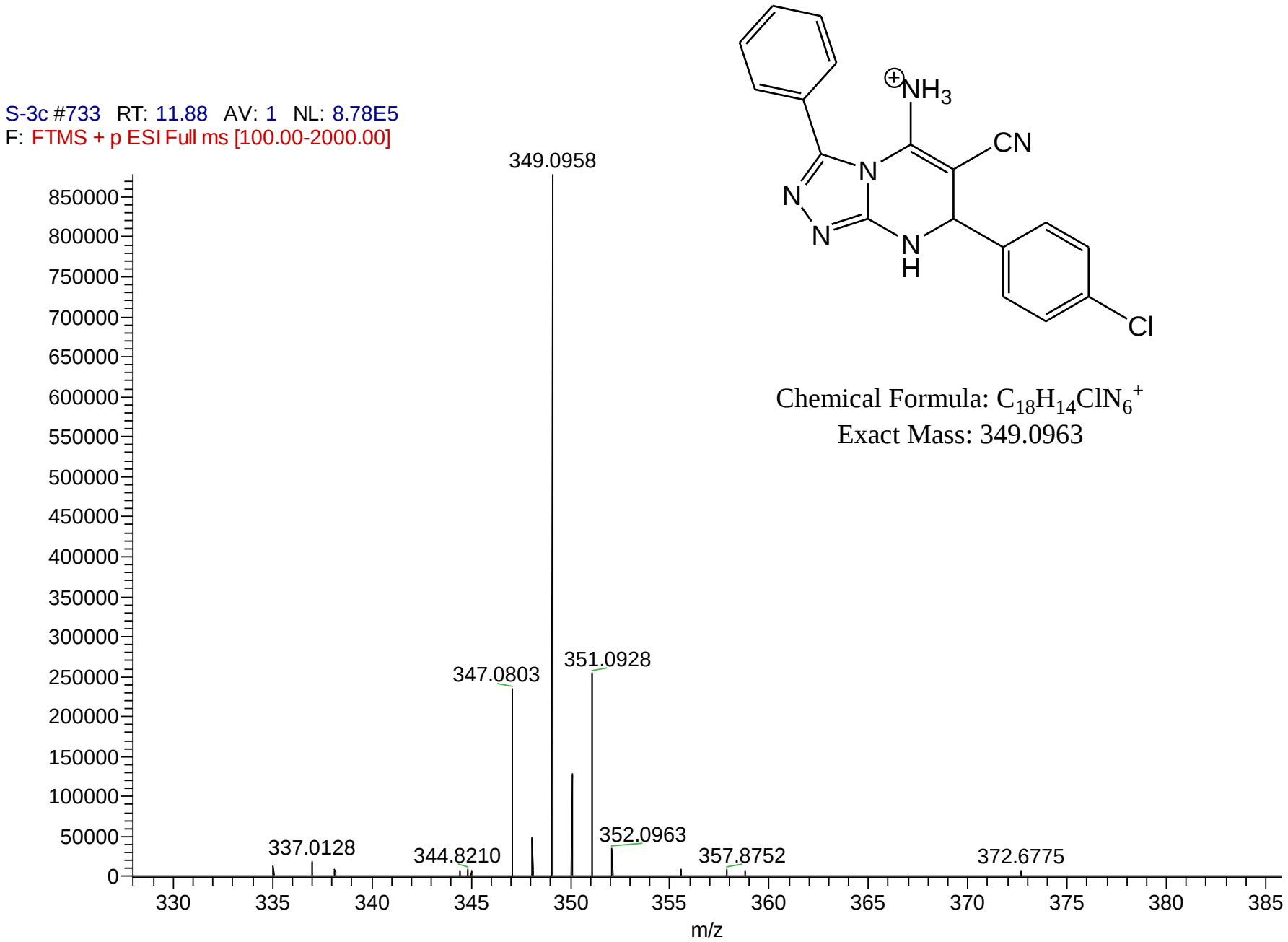

Chemical Formula: $C_{18}H_{14}ClN_6^+$

Exact Mass: 349.0963

Fig. S33a: LCMS of Compound 8c

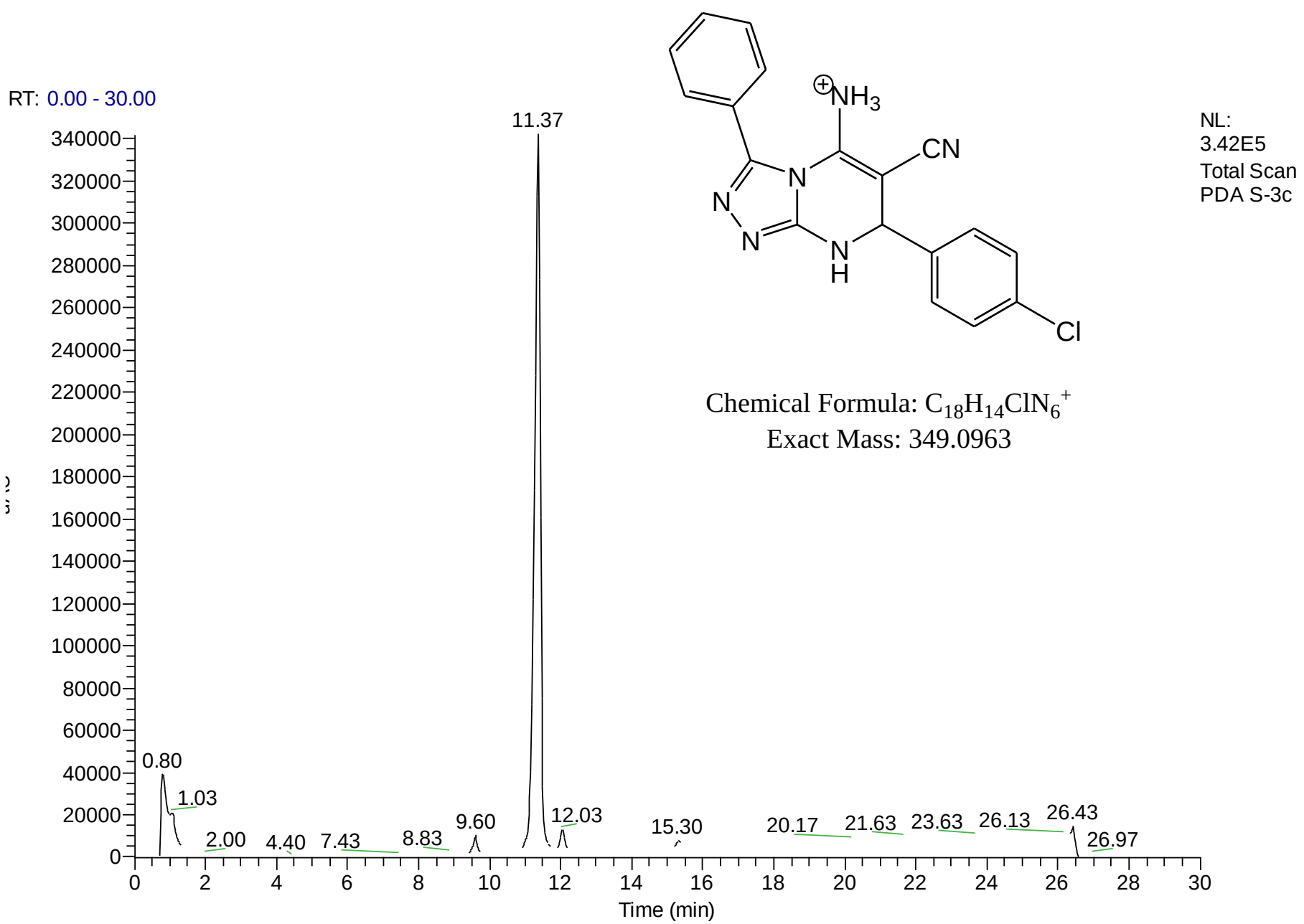

Fig. S33b: LCMS of Compound 8c

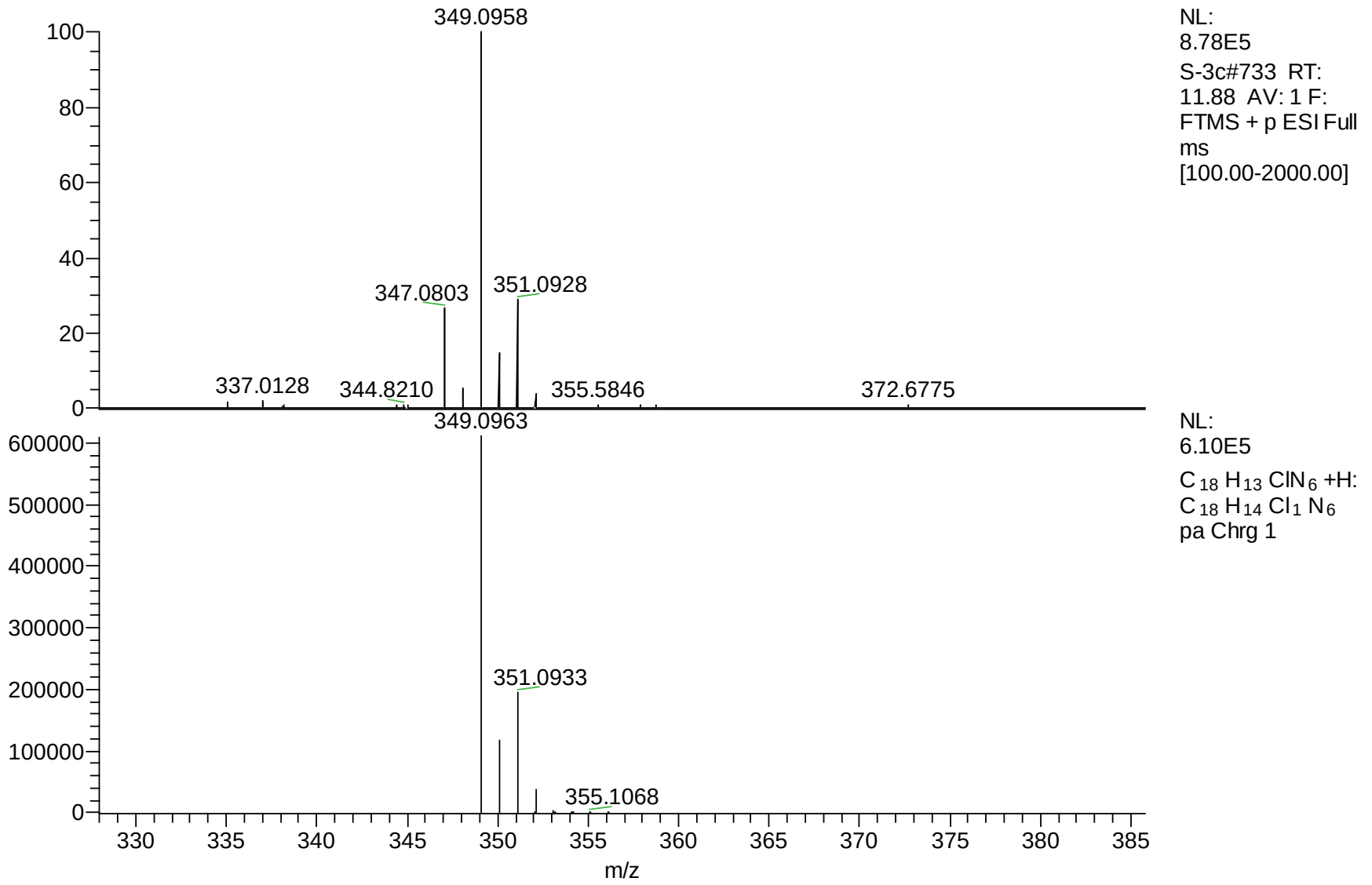

Fig. S33c: LCMS of Compound 8b

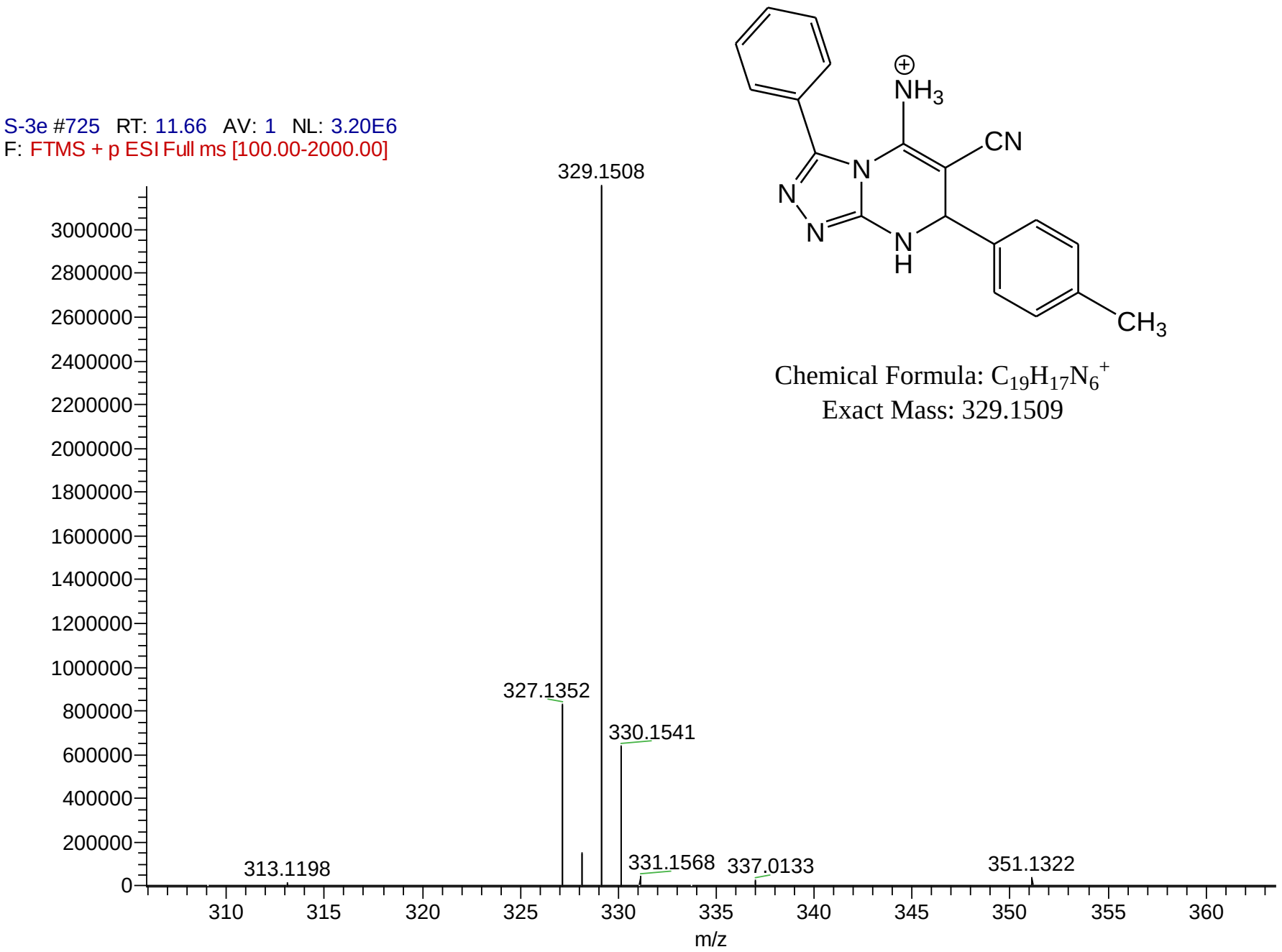

Fig. S34a: LCMS of Compound 8d

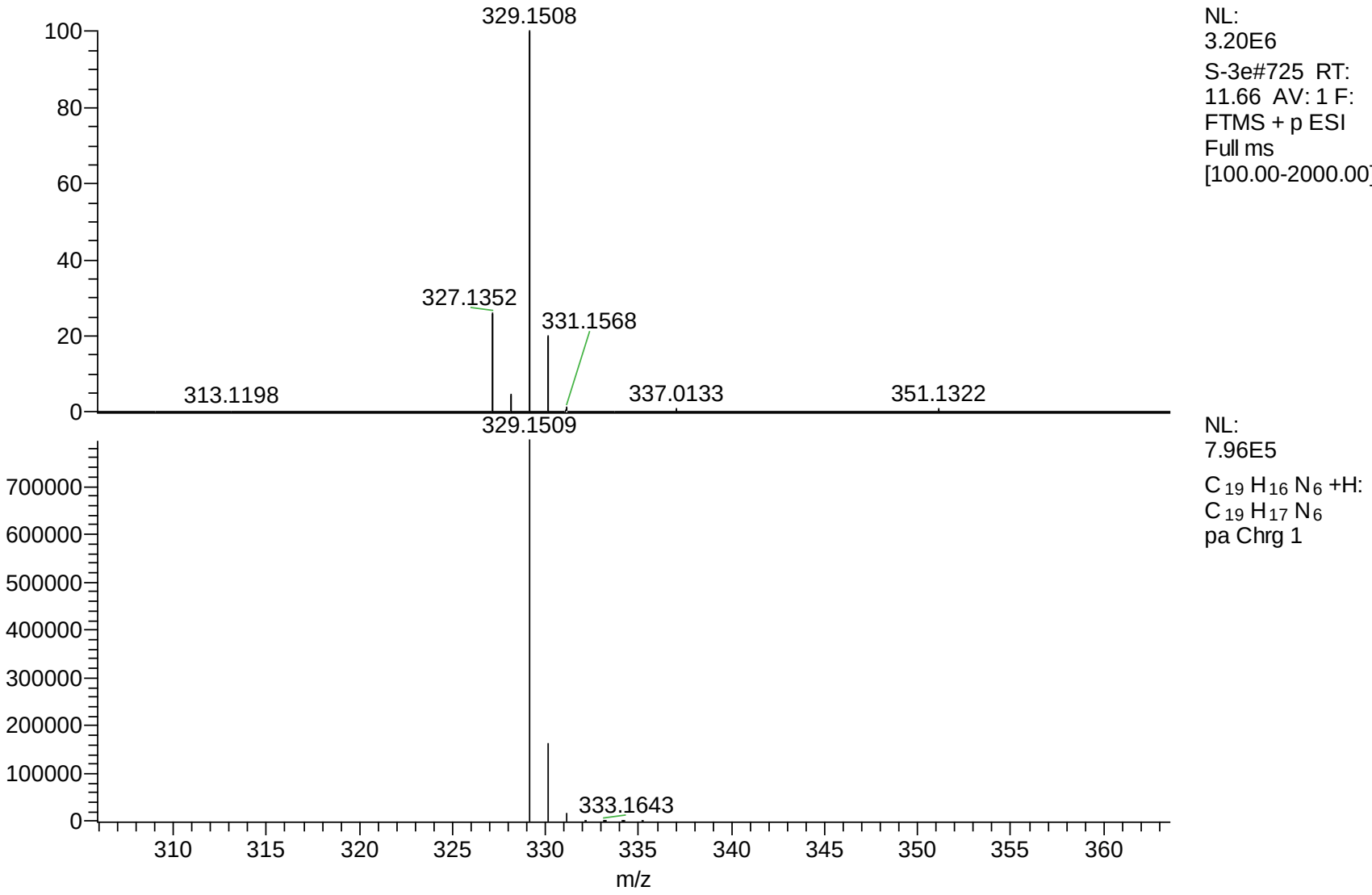

Fig. S34b: LCMS of Compound 8d

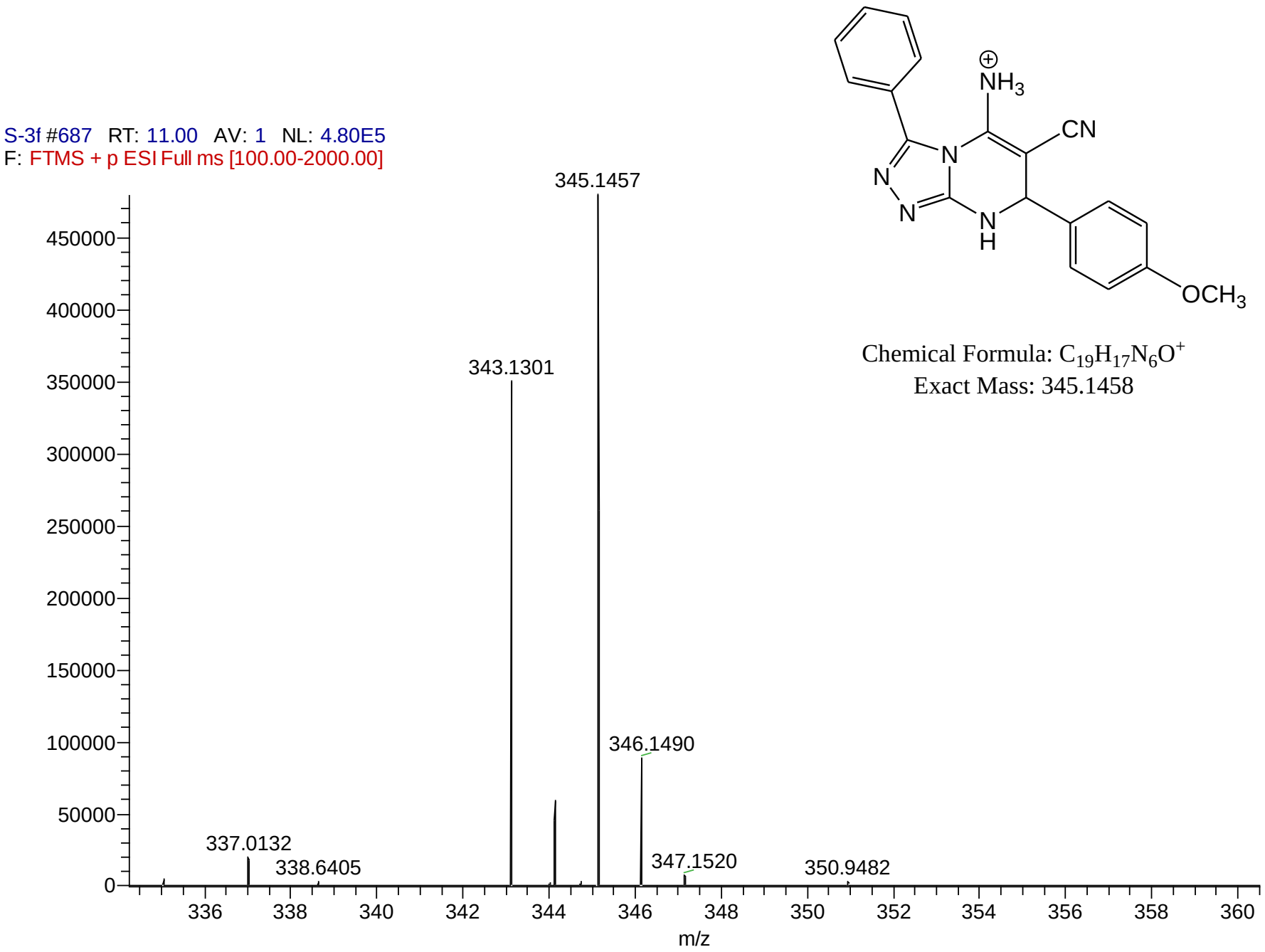

Fig. S35a: LCMS of Compound 8e

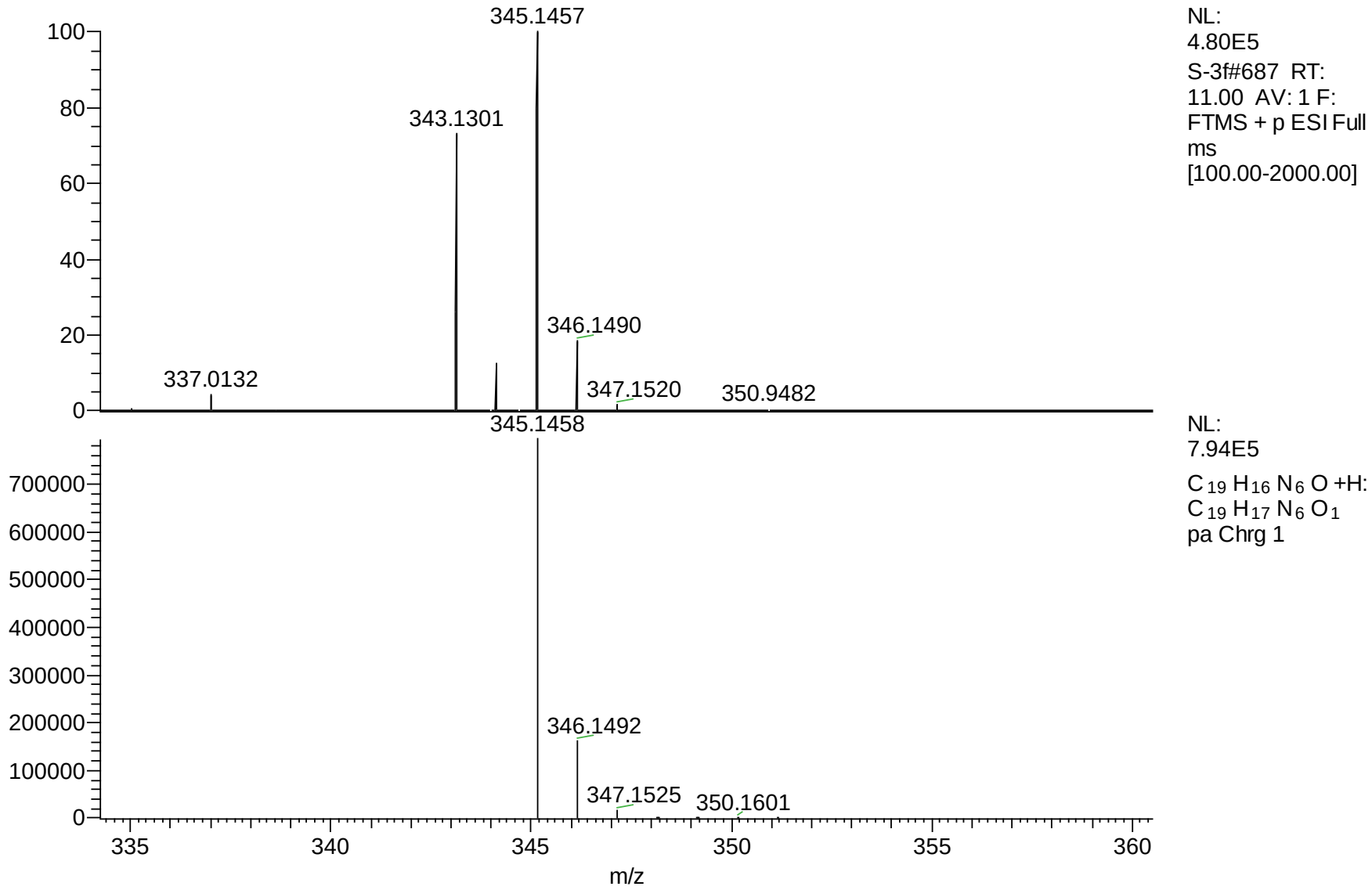

Fig. S35b: LCMS of Compound 8e

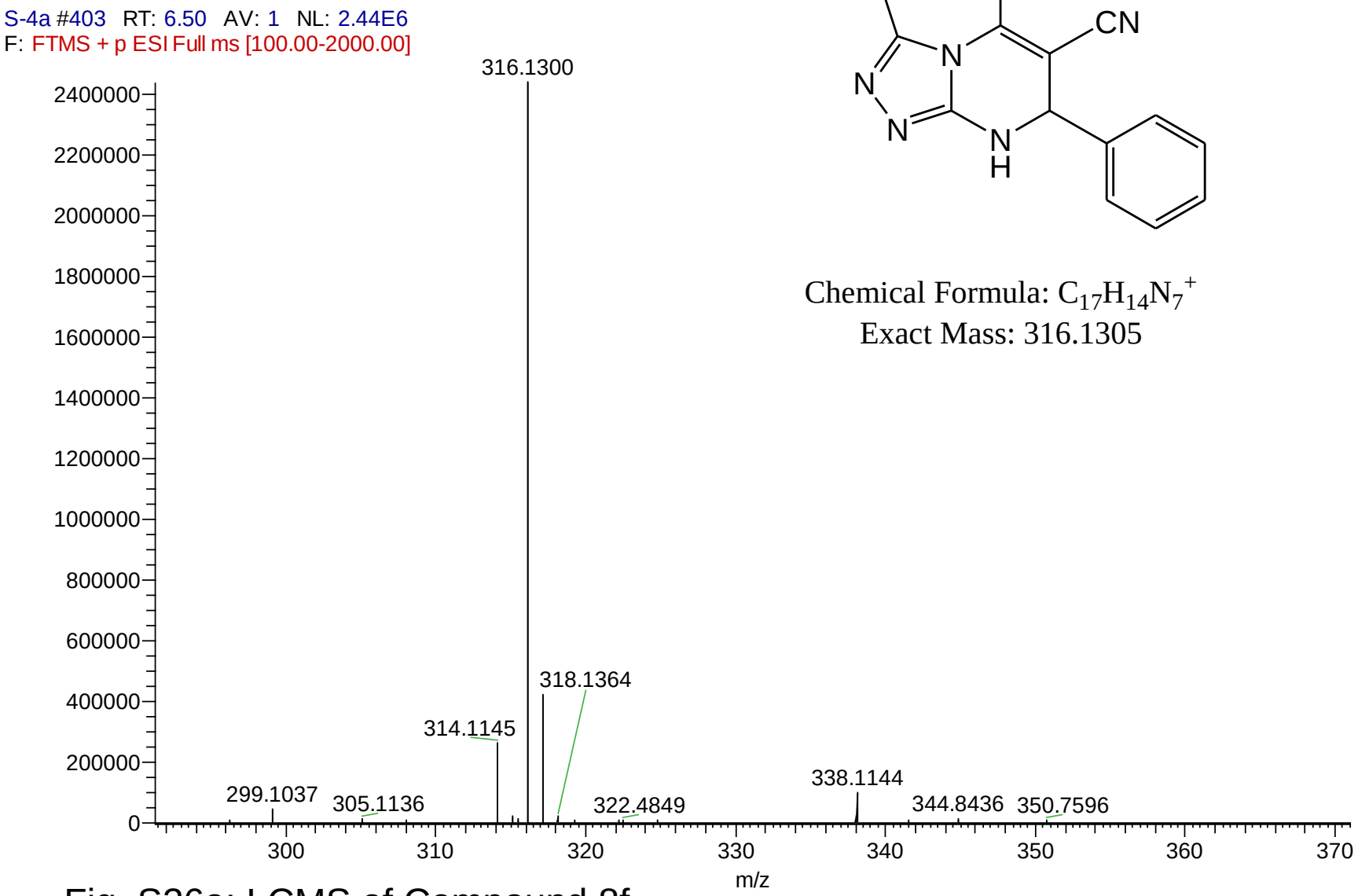

Chemical Formula: $C_{17}H_{14}N_7^+$
Exact Mass: 316.1305

Fig. S36a: LCMS of Compound 8f

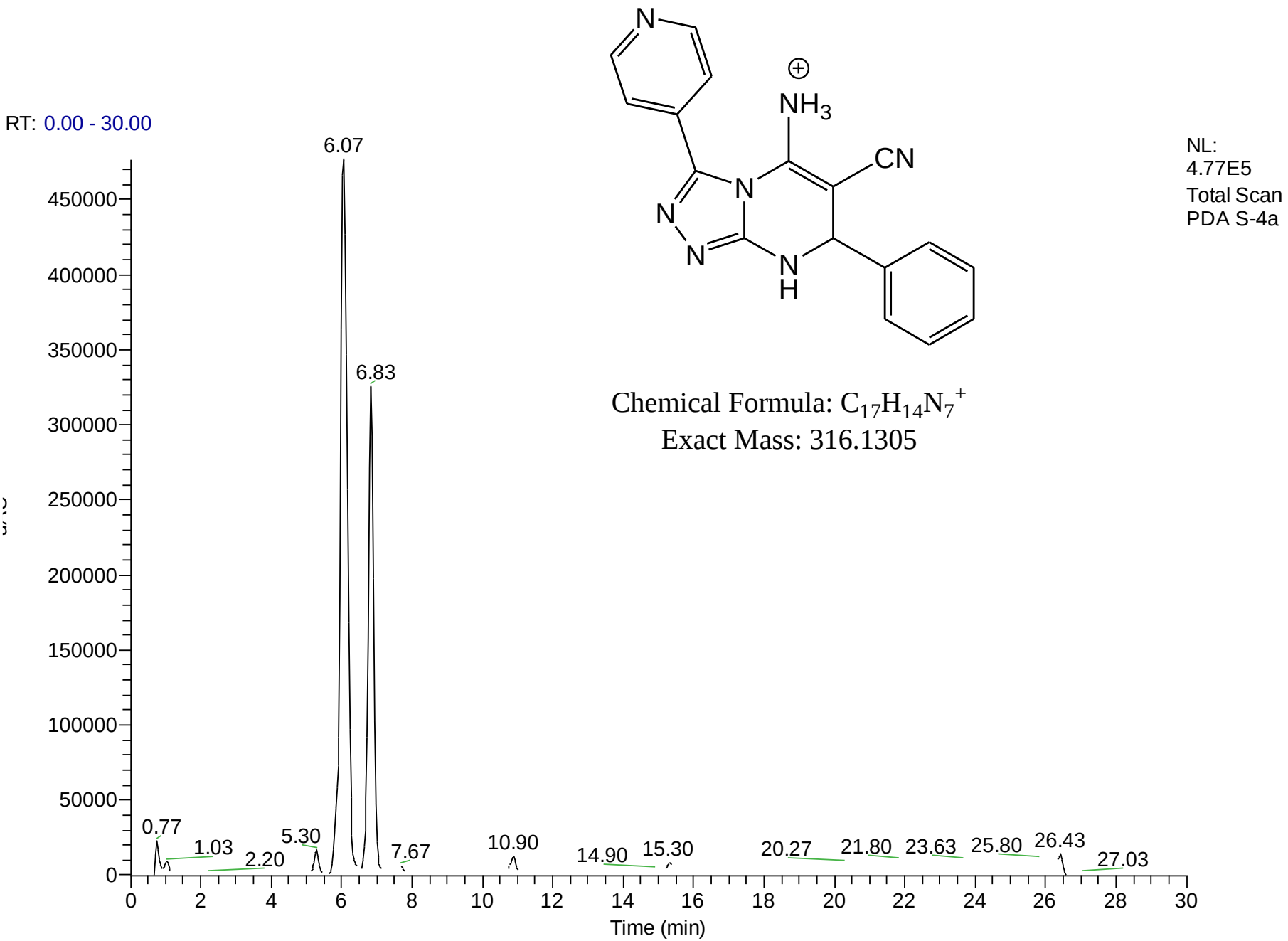

Fig. S36b: LCMS of Compound 8f

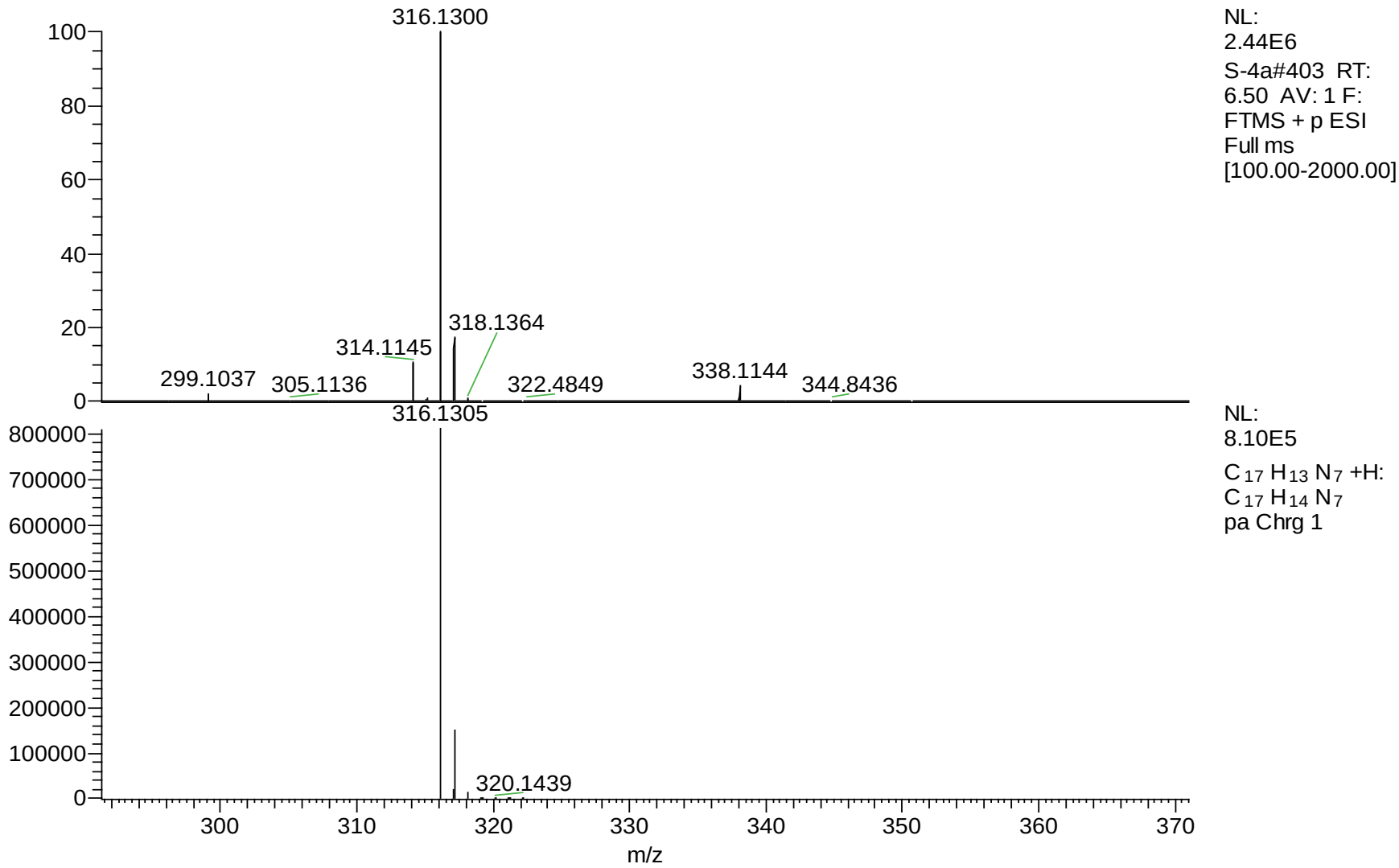

Fig. S36c: LCMS of Compound 8f

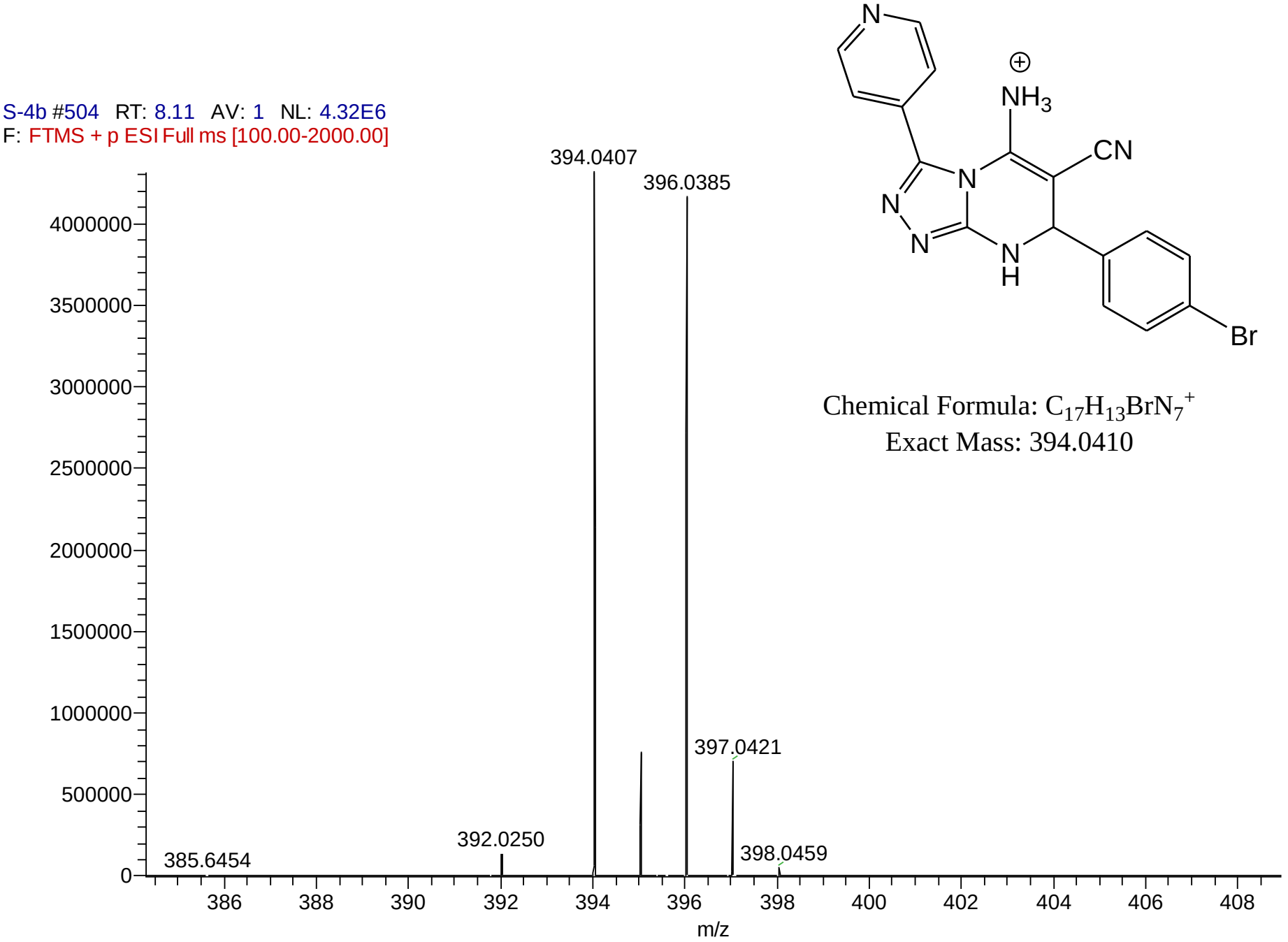

Fig. S37a: LCMS of Compound 8g

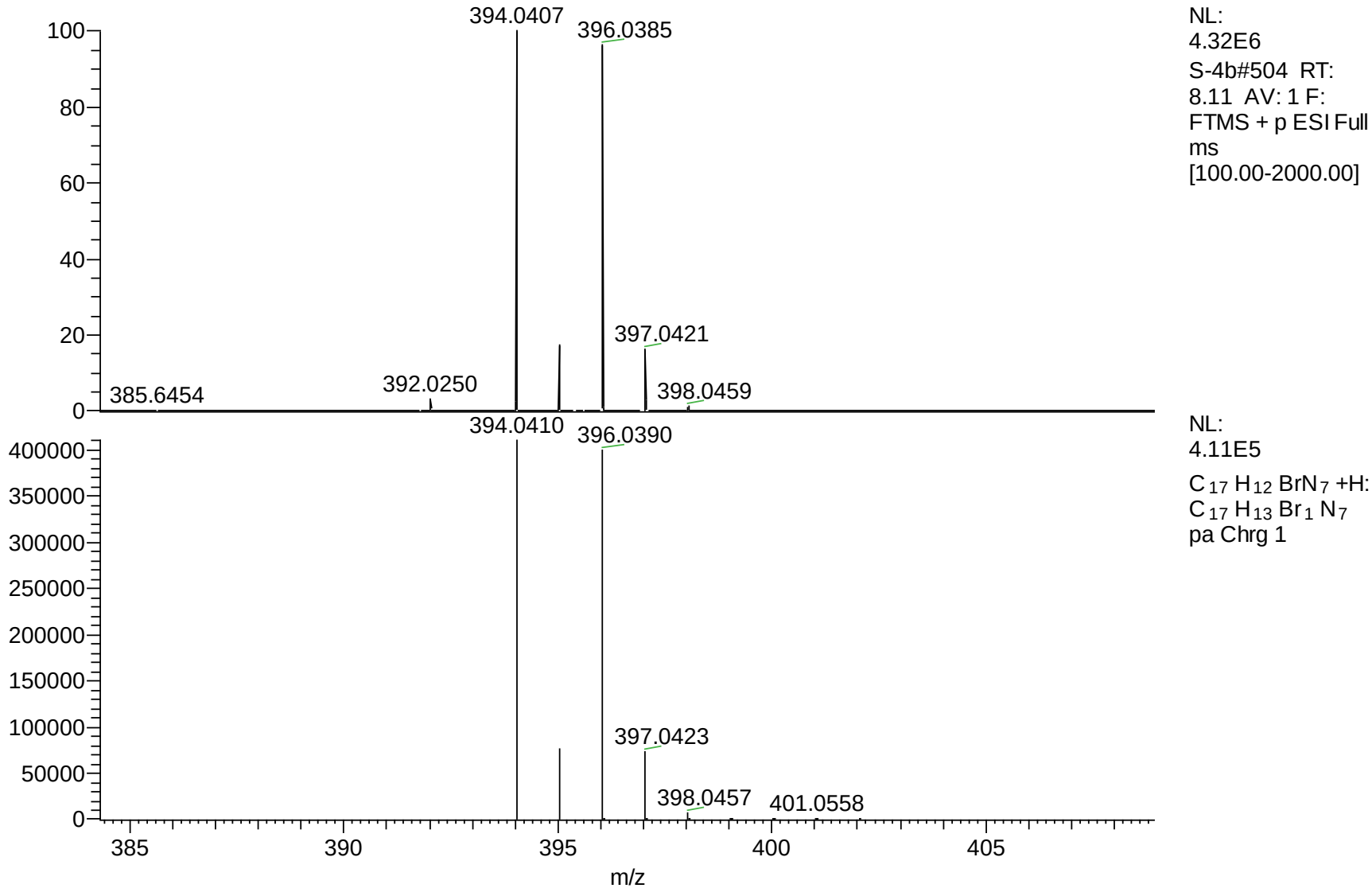

Fig. S37b: LCMS of Compound 8g

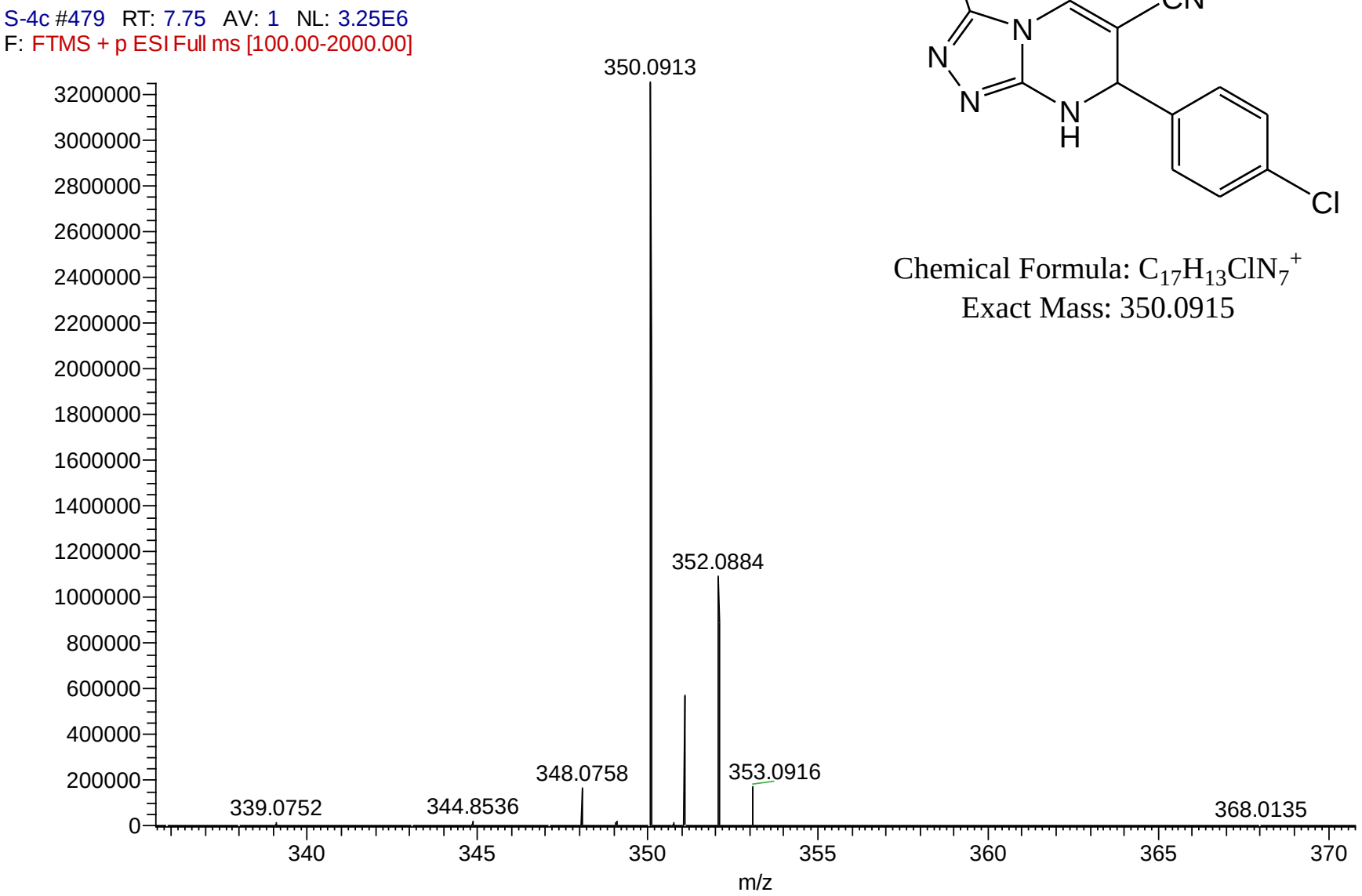

Chemical Formula: $C_{17}H_{13}ClN_7^+$
Exact Mass: 350.0915

Fig. S38a: LCMS of Compound 8h

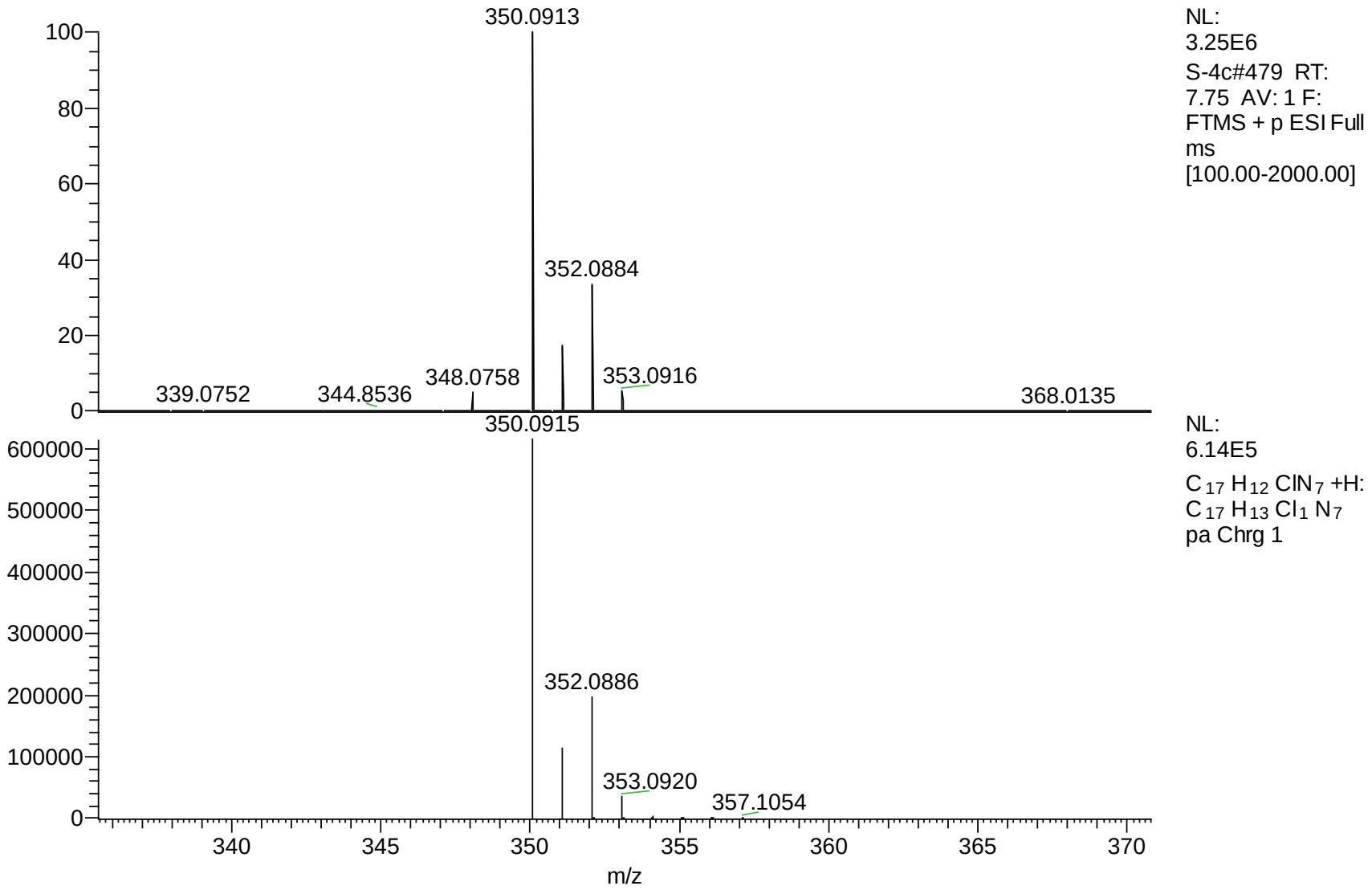

Fig. S38b: LCMS of Compound 8h

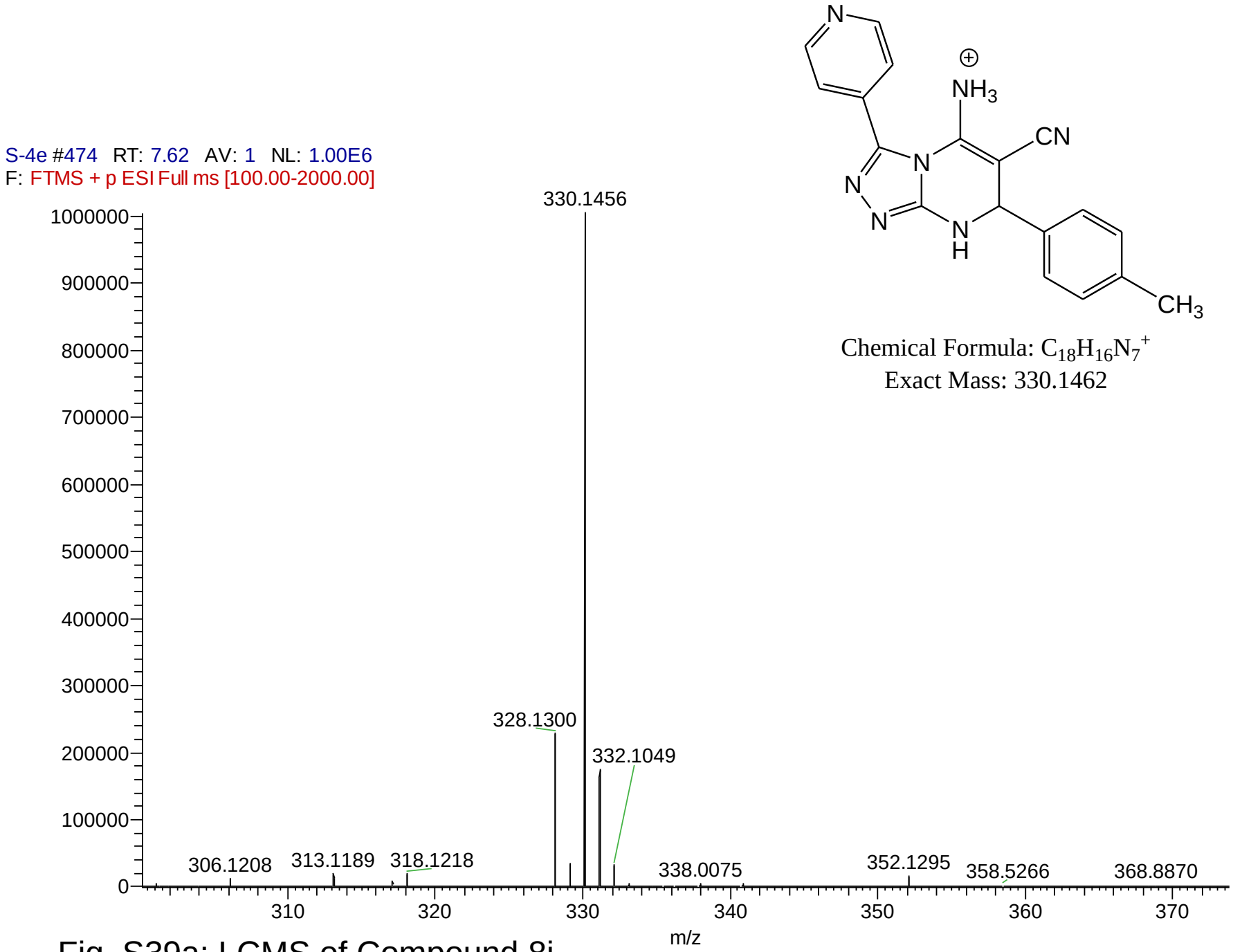

Chemical Formula: $C_{18}H_{16}N_7^+$

Exact Mass: 330.1462

Fig. S39a: LCMS of Compound 8i

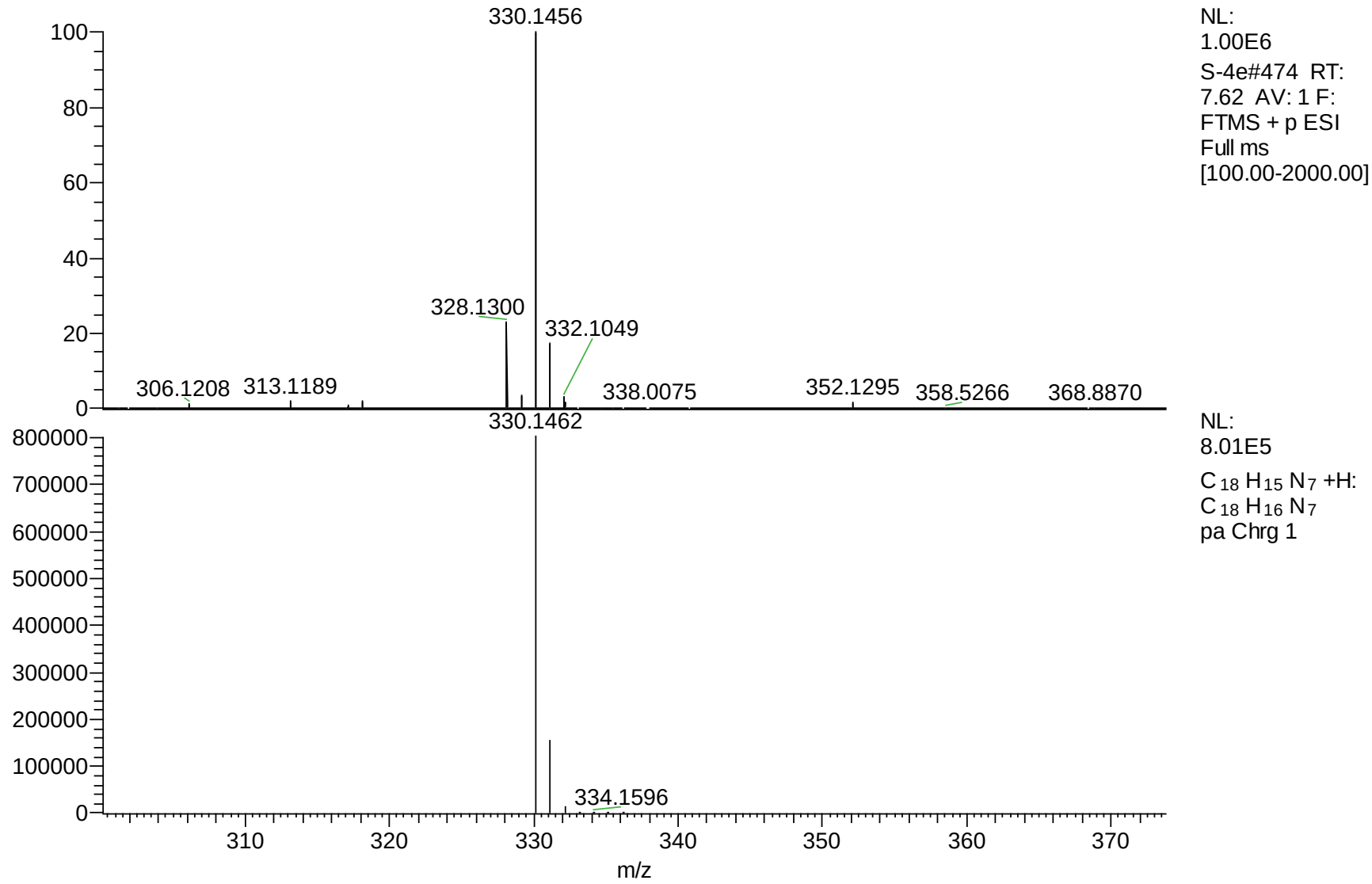

Fig. S39b: LCMS of Compound 8i

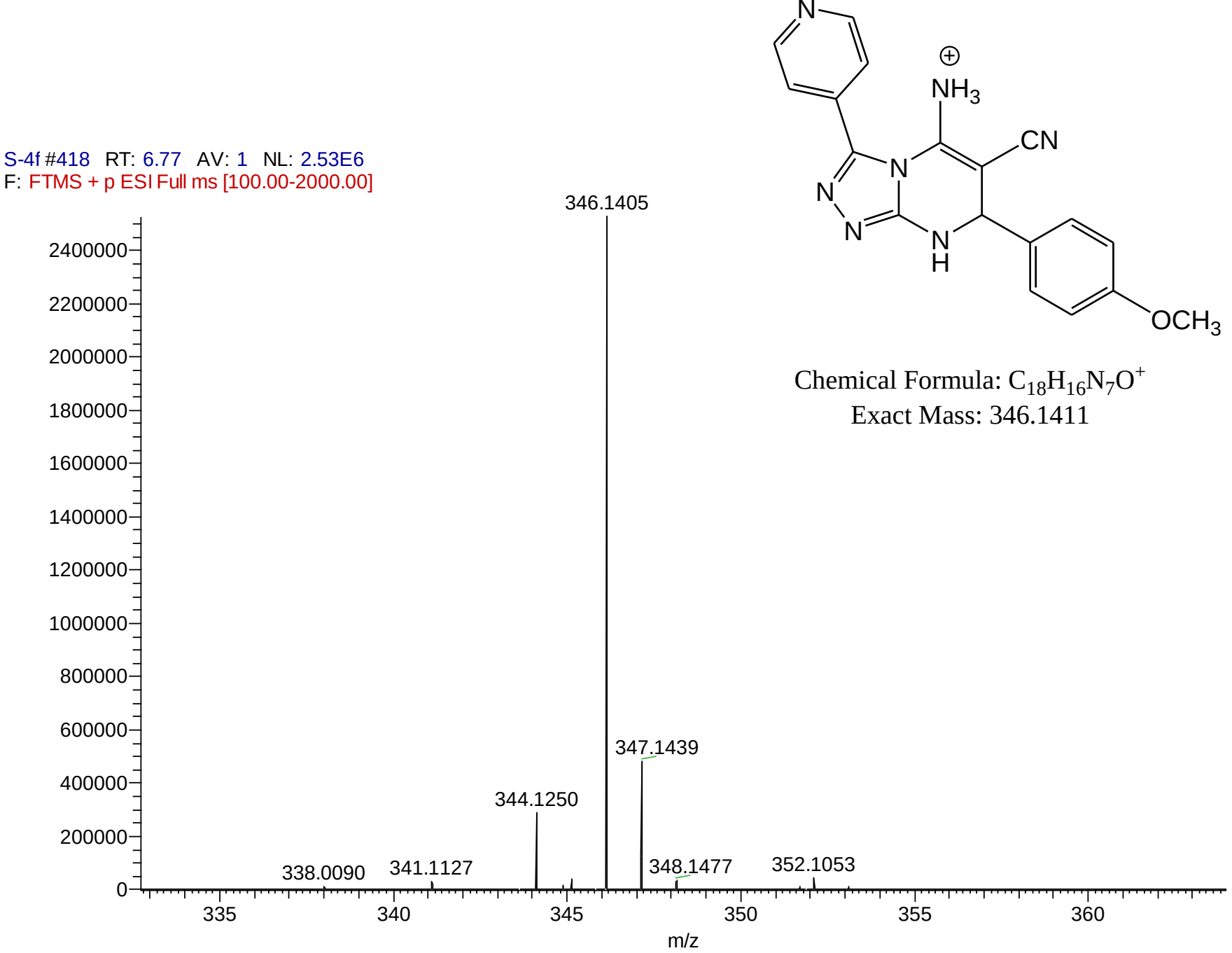

Fig. S40a: LCMS of Compound 8j

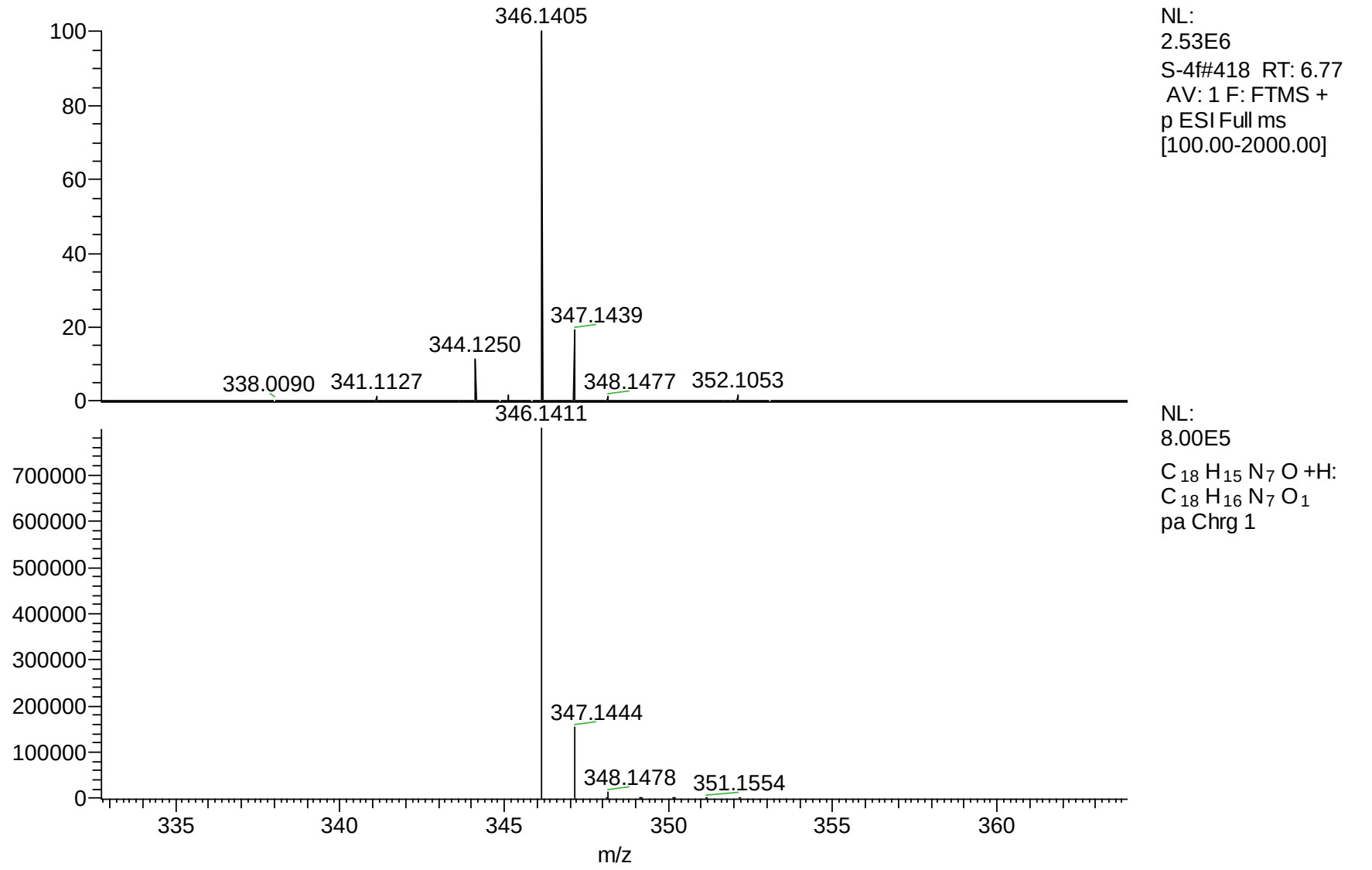

Fig. S40b: LCMS of Compound 8j

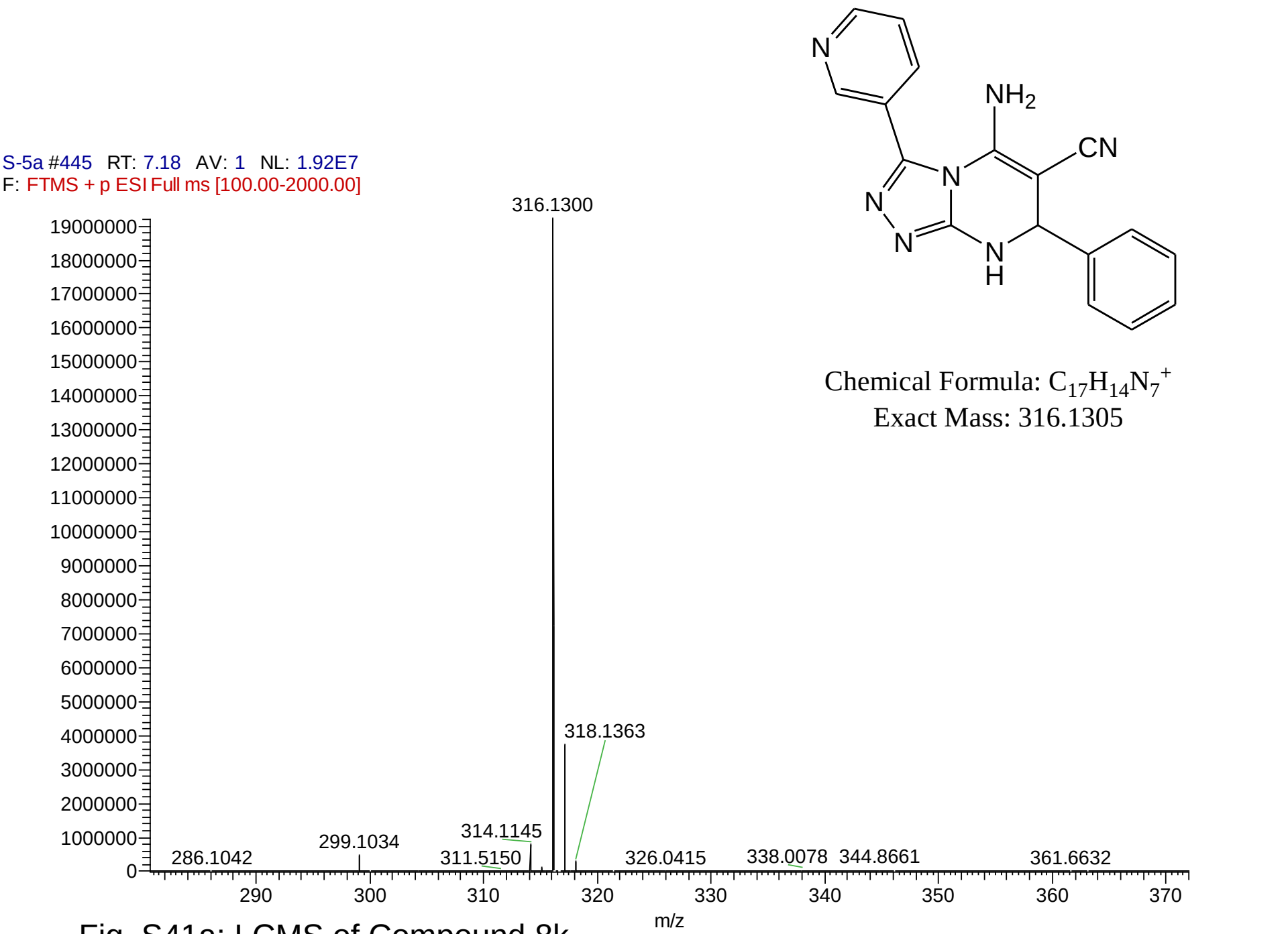

Fig. S41a: LCMS of Compound 8k

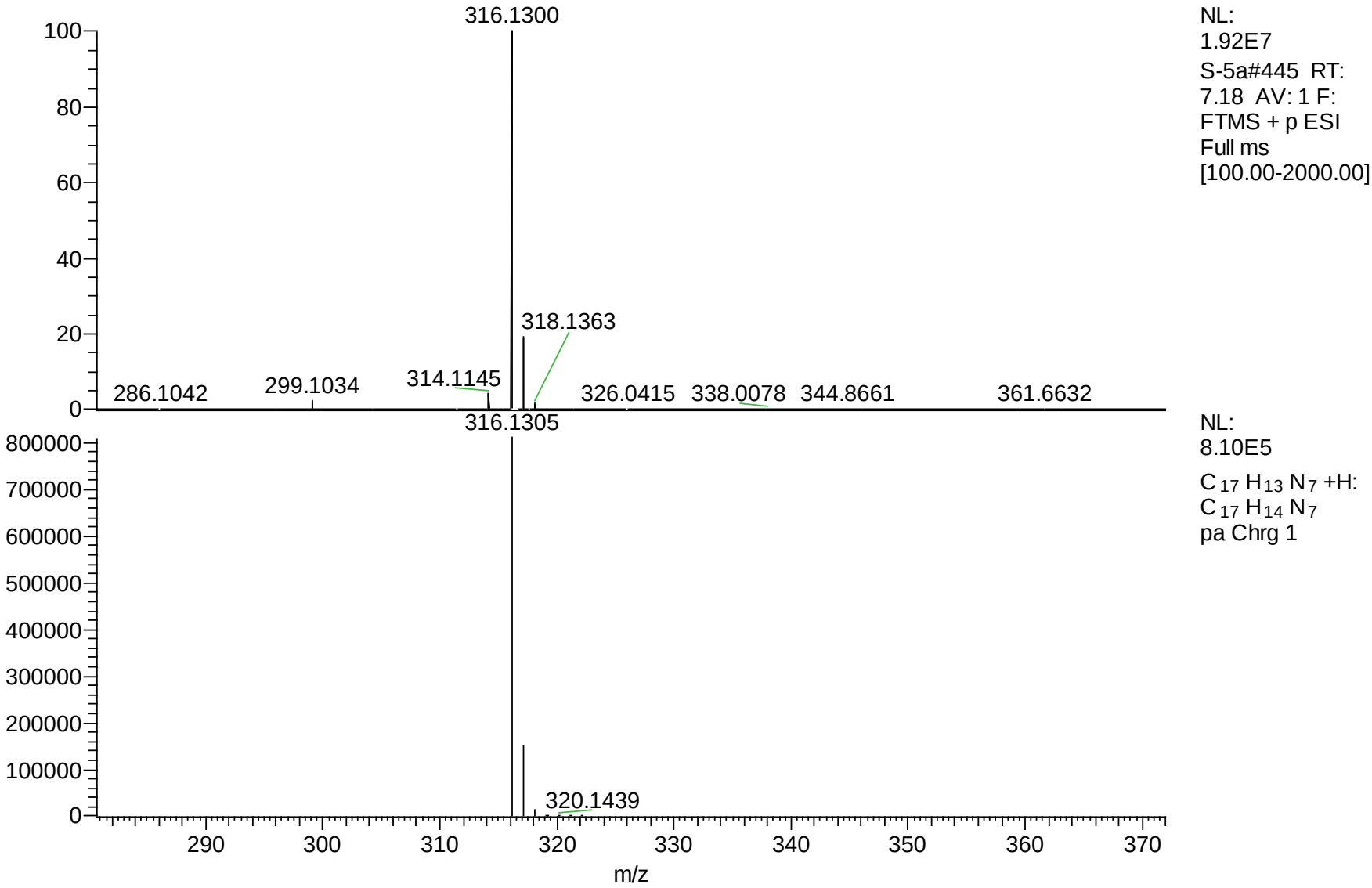

Fig. S41b: LCMS of Compound 8k

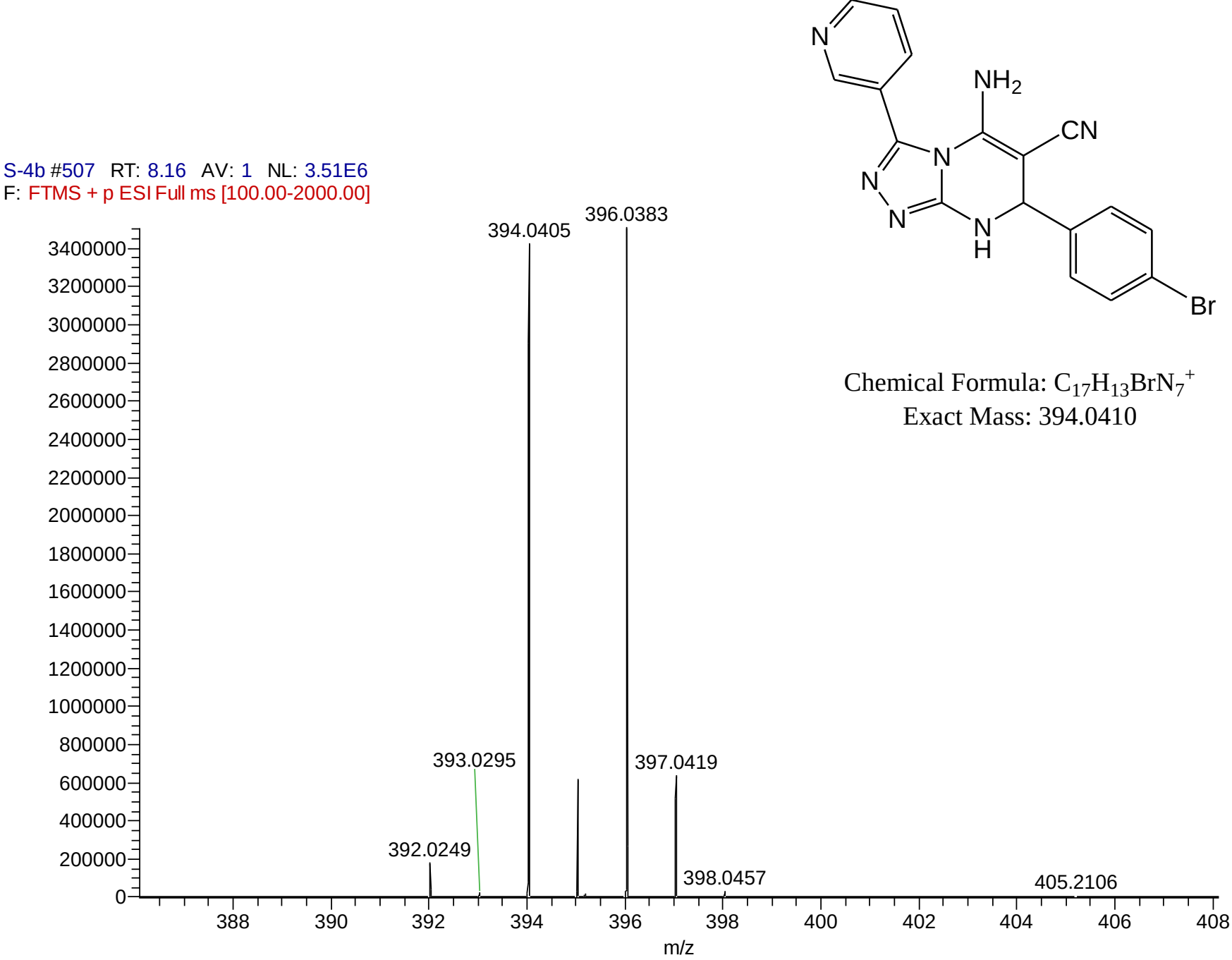

Fig. S42a: LCMS of Compound 8l

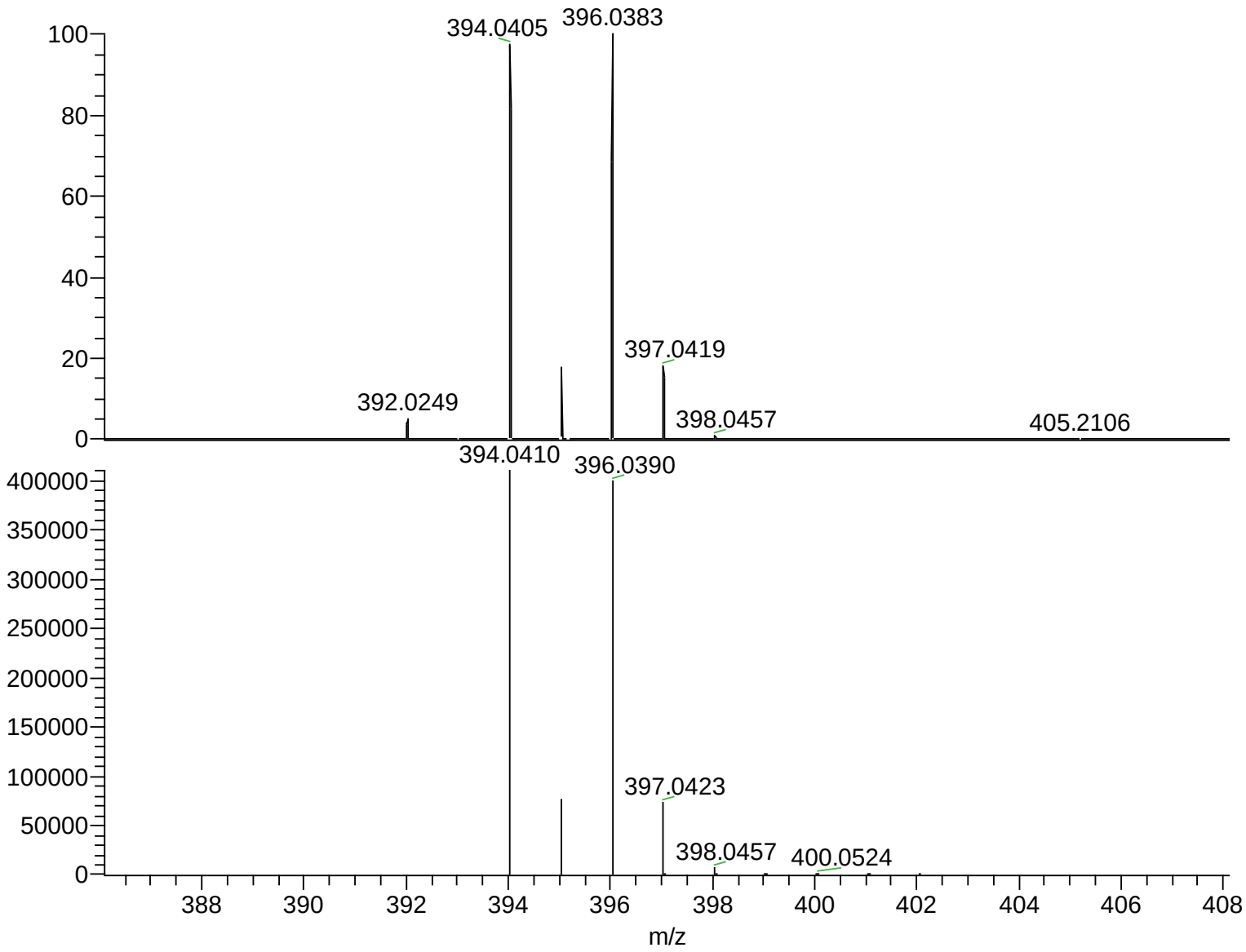

Fig. S42b: LCMS of Compound 8l

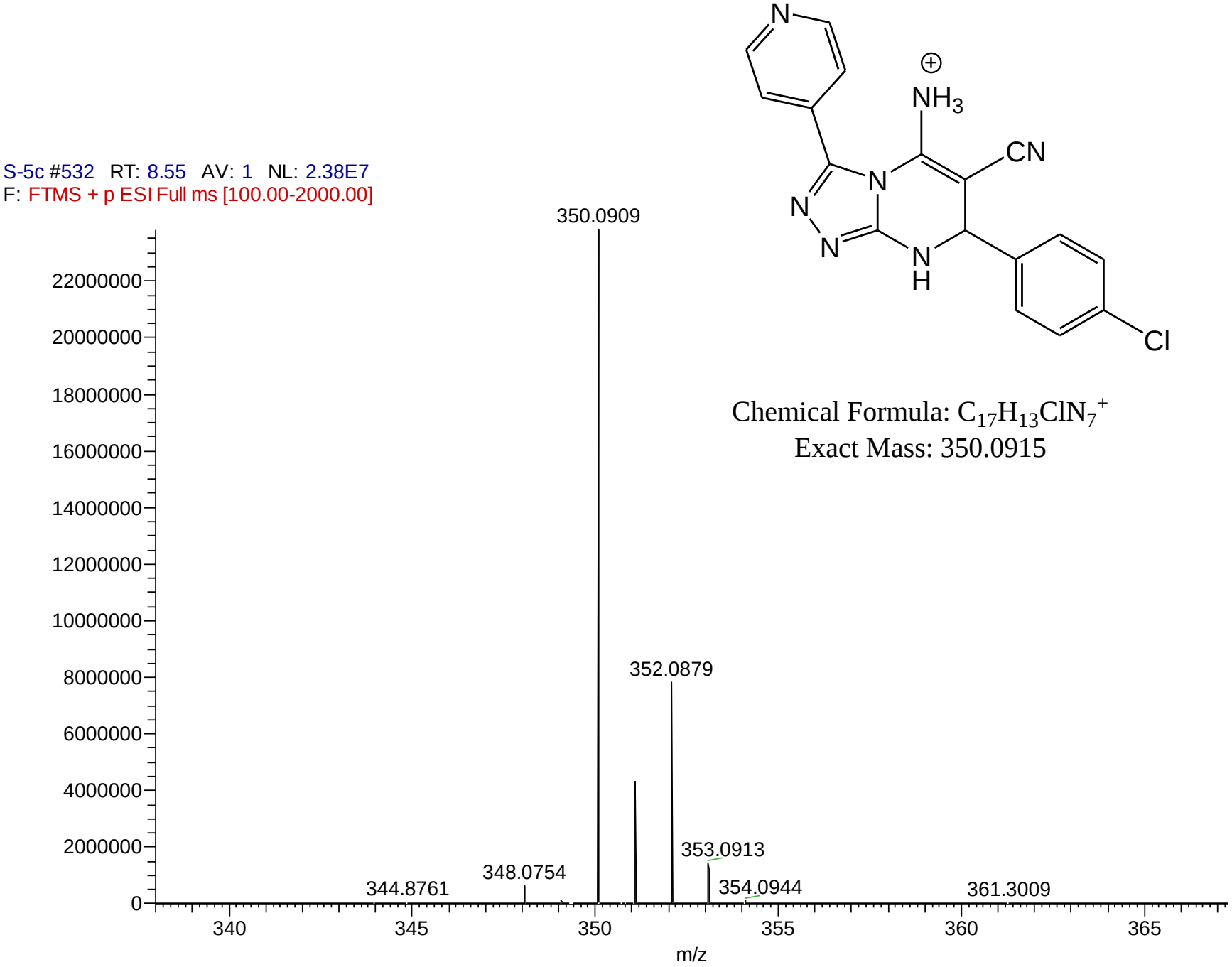

Fig. S43a: LCMS of Compound 8m

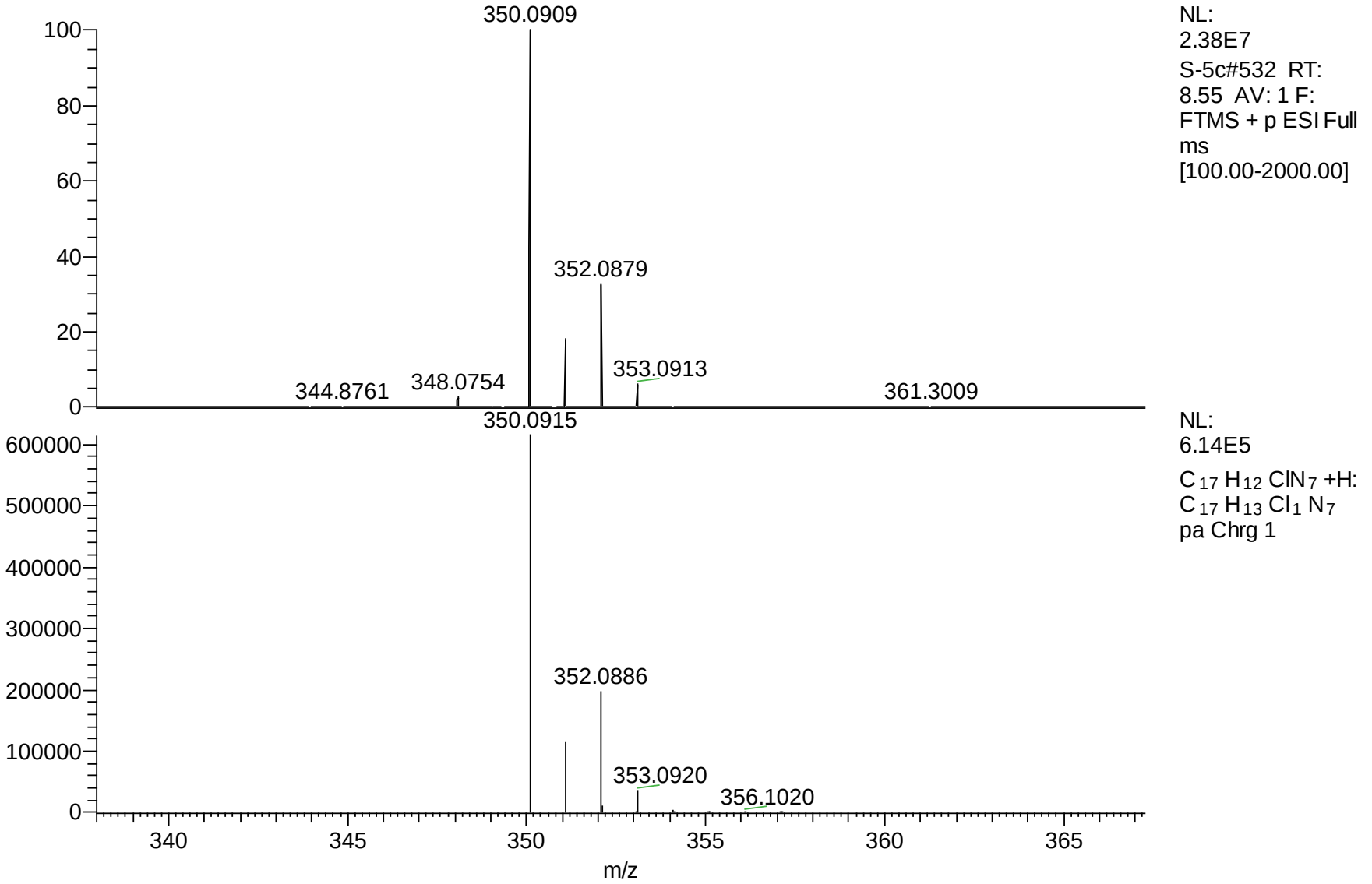

Fig. S43b: LCMS of Compound 8m

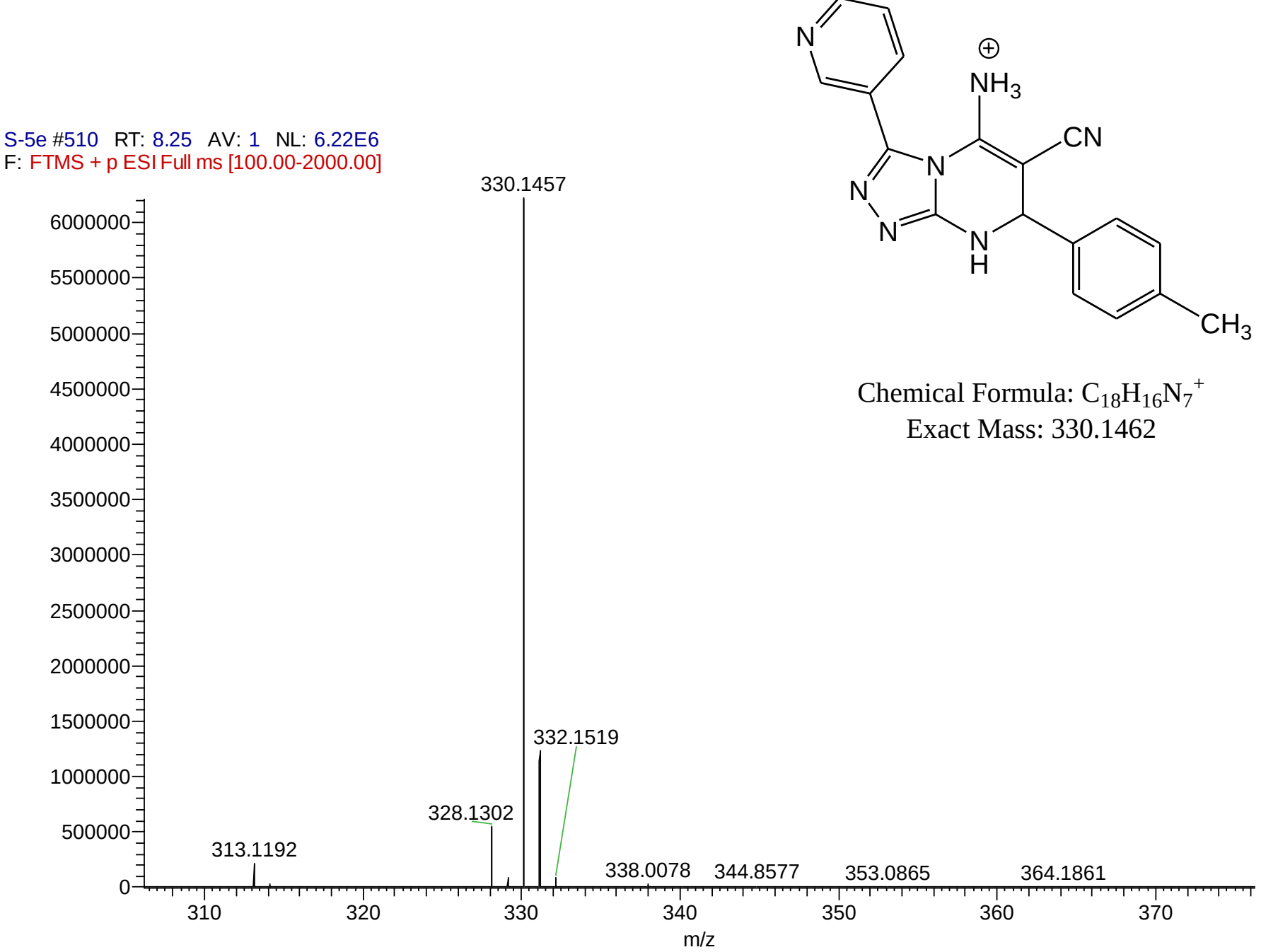

Fig. S44a: LCMS of Compound 8n

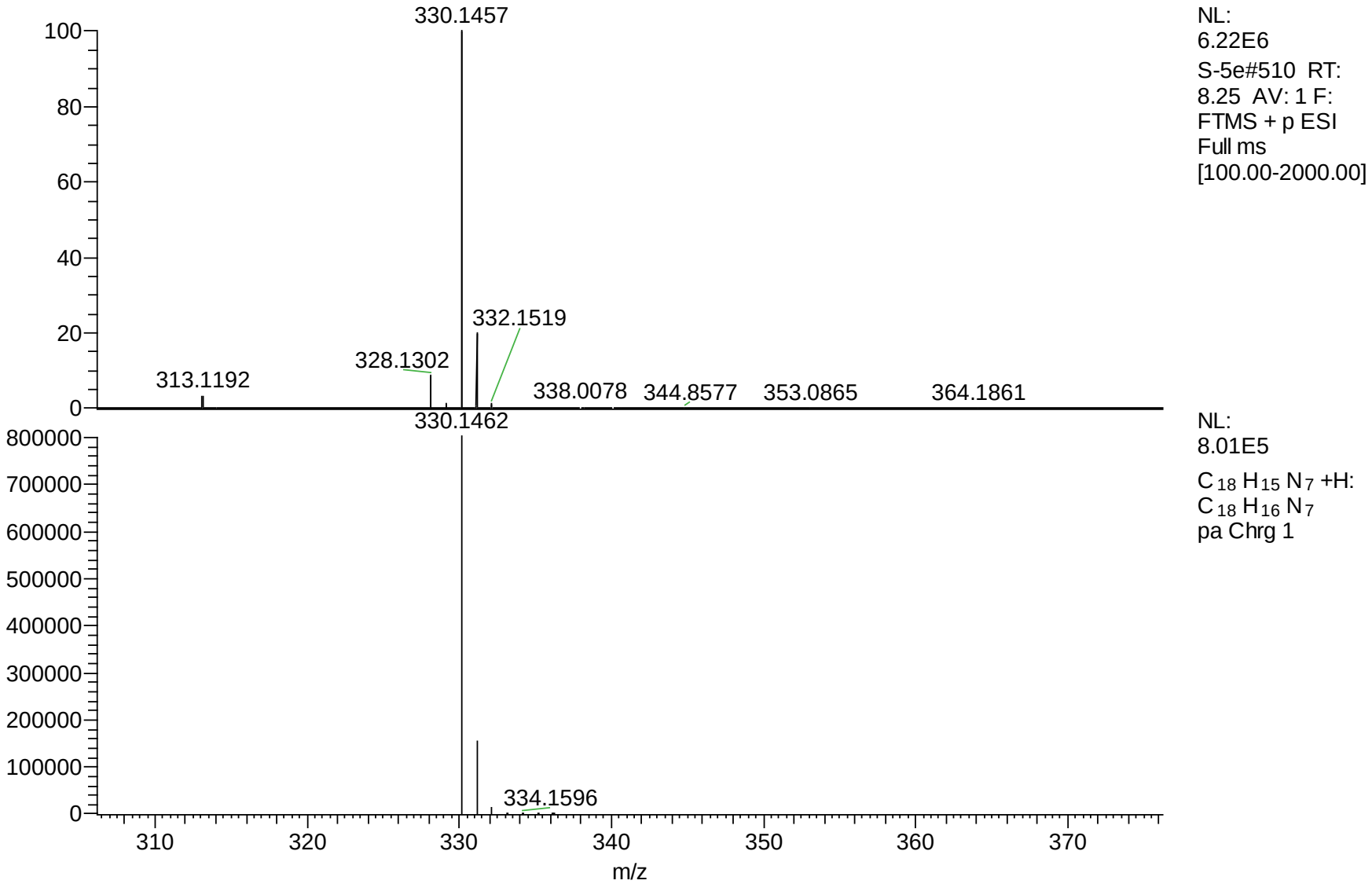

Fig. S44b: LCMS of Compound 8n

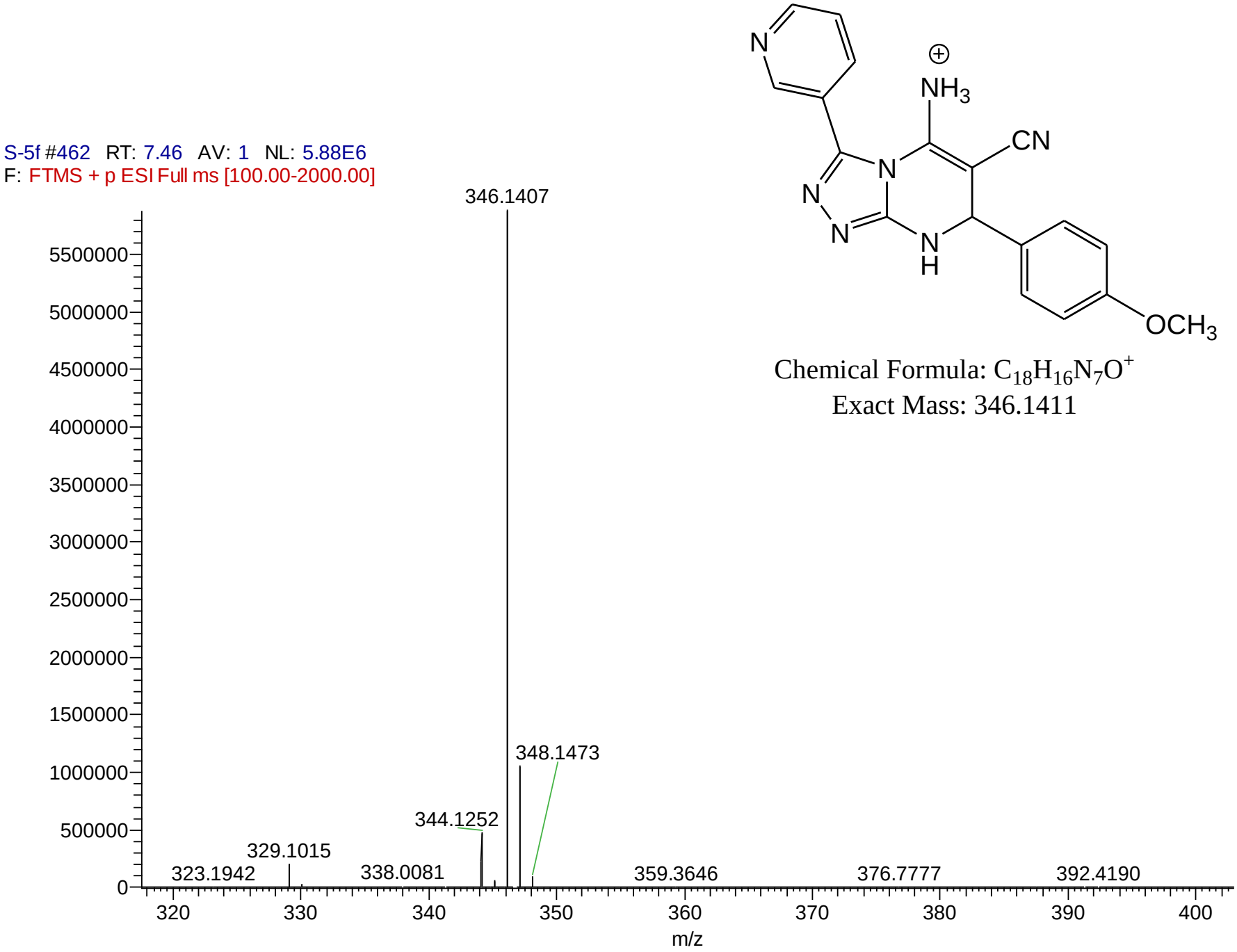

Chemical Formula: $C_{18}H_{16}N_7O^+$

Exact Mass: 346.1411

Fig. S45a: LCMS of Compound 8o

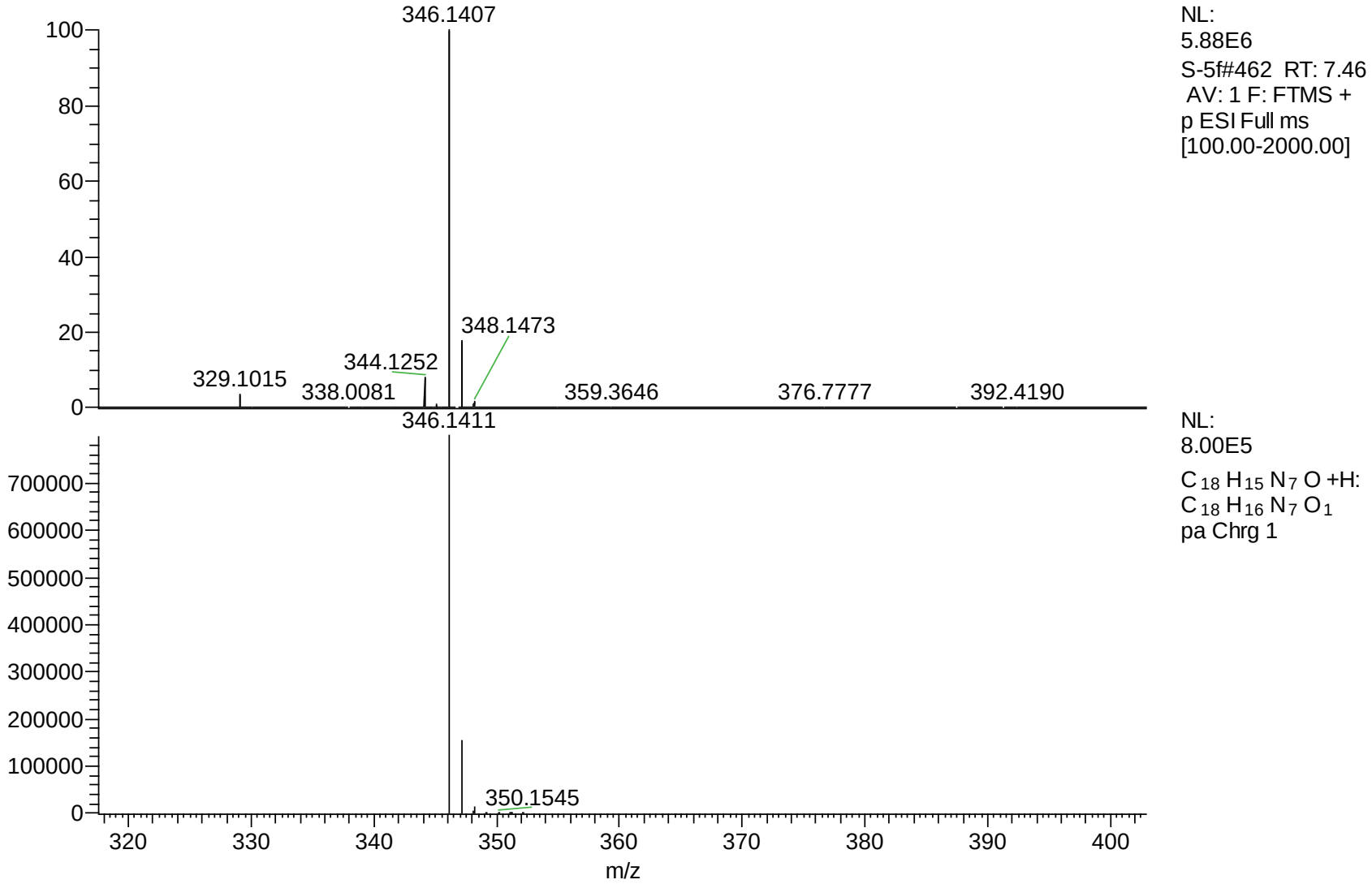

Fig. S45b: LCMS of Compound 8o

Appendix A

4. Experimental

4.1. Chemistry

General details:

Melting points were determined on an electrothermal melting point apparatus (Stuart Scientific Co.) and were uncorrected. Pre-coated silica gel plates (kieselgel 0.25 mm, 60G F254, Merck, Darmstadt, Germany) were used for TLC monitoring of reactions. The developing solvent systems of $CHCl_3/CH_3OH$ (9:1 v/v) were used and the spots were detected at 254 nm wavelength using ultraviolet lamp (Spectroline, model CM-10, Seattle, USA). ^{1}H-NMR and 13C-NMR spectra were recorded using Varian Unity INOVA 400 MHz at university of Aberdeen, United Kingdom. ^{1}H-NMR operating at 400 MHz and ^{13}C-NMR operating at 100 MHz. Chemical shifts are expressed in δ-value (ppm) relative to DMSO-d_6 as internal standard. ^{1}H NMR data are recorded as follows: chemical shift (δ) [multiplicity, coupling constant (s) J (Hz) and relative integral, where multiplicity is defined as: s= singlet; d= doublet; t= triplet; q= quartet; m= multiplet or combinations of the above. High resolution mass spectrometric data were obtained using the EPSRC mass spectrometry Centre in Swansea and Thermo Instruments MS system (LTQ XL/LTQ Orbitrap Discovery) coupled to a Thermo Instruments HPLC system (Accela PDA detector, Accela PDA autosampler and Pump) at university of Aberdeen, UK. Compounds yields given are those of crude products. All solvents were obtained from commercial suppliers and used without further purification.

4.2. Biological Evaluations

4.2.1. *In vitro* COX-1 and COX-2 inhibition assays

All the newly synthesized compounds were screened for their ability to inhibit COX-1 and COX-2 enzymes using ten folds serial dilutions (1, 0.1, 0.01, 0.001 mg/mL). This was carried out using the COX 1(human) Inhibitor Screening Assay Kit and COX 2 (human) Inhibitor Screening Assay Kit (supplied by Cayman chemicals (catalog no. 560131), Ann Arbor, MI, USA). The preparation of reagents and testing procedures were according to the instructions recommended by the supplier. COX catalyzes the first step in the biosynthesis of arachidonic acid to PGH2. The PGF2α produced from PGH2 by reduction with stannous chloride is measured by enzyme-linked immunosorbent assay (ELISA). In brief, the compounds were dissolved in dimethyl sulfoxide (DMSO). The enzyme COX-1 and COX-2 (10 mL), heme (10 mL), and samples (20 mL) were added to the supplied reaction buffer solution (160 mL, 0.1M Tris-HCl, pH 8 containing 5 mM ethylenediaminetetraacetate (EDTA), and 2 mM phenol) and pre-incubated for 10 min in a water bath (37 ^{o}C). After that, COX reactions were initiated by the addition of arachidonic acid (10 mL, final concentration in reaction mixture 100 mM). After 2 min, The COX reactions were stopped by the addition of saturated stannous chloride (30 mL) followed by incubation for 5 min at room temperature. The PGF2α formed in the samples by COX reactions was quantified by ELISA. Following transfer to a 96-well plate, the plate was incubated with samples for 18 h at room temperature. After incubation, the plate was washed to remove any unbound reagent, and then Ellman's reagent (200 mL), which contains substrate to acetylcholinesterase, was added and incubated at room temperature for 60-90 min until the absorbance of Bo well is in the range 0.3e0.8 AU. at 410 nm. The plate was then read by an ELISA plate reader. The IC_{50} of inhibition of COX-

1 and COX-2 was calculated by the comparison of the sample treated incubations to control incubations. Celecoxib was used as the reference standard drug in the study.

4.2.2. In vitro 5-LOX inhibitory assay

The newly synthesized compounds were screened for their ability to inhibit lipoxygenase enzymes. This was carried out using Abnova lipoxygenase inhibitor screening assay kit (Catalog No. 760700) according to reported method.

4.2.1.2. *In vitro* sEH assay

IC_{50} values were determined using a cell-based assay system of 96-well format [35]. Epoxy Flour 7, a sensitive fluorescent substrate, was utilized to monitor the activity of the enzyme through its hydrolysis by sEH to the fluorescent 6-methoxy-2-naphthaldehyde that could be monitored (λem = 330 nm, λex = 465 nm). Briefly, the assay was carried out through incubation of 10 mL of compounds buffer or 10 mL of the AUDA solution to appropriate wells. For positive control wells, 100 mL of the 10 ng/mL sEH positive control (substrate) was prepared for two wells. Then, 200 mL of 6-methoxy-2-Naphthaldehyde was added. Standards were prepared above to corresponding wells of the black plate. 100 mL of the substrate solution was added to each well, except the standards, and the plate was allowed to incubate at 37 ^{o}C for 30 min. The fluorescent intensity of each well (excitation = 330 nm; emission = 465 nm) was read.

4.2.2. *In vivo* assays

Animals

Thirty-two adult male Wistar rats (150-200 g) were purchased from the animal breeding unit at the National Research Centre. Standard conditions as the 12:12 light-dark cycle and well-ventilated rooms have been established for housing the animals. Appropriate dealings were taken to minimize the pain or distress of the animals. Animals were kept in sanitary cages and given

clean standard pellet diet food and water ad-libitum. One week before the experiment, all the animals were shifted to be adapted to the laboratory environment. This study was conducted according to the National Regulations on Animal Welfare and Institutional Animal Ethical Committee (IAEC).

Chemicals and kits

Carrageenan and Celecoxib were purchased from Sigma Aldrich, Germany. ELISA kits were used assessment of prostaglandin E_2 (PGE_2; Kamiya Biomedical Company, USA), interleukin-6 (IL-6; Cloud-Clone, USA), tumor necrosis factor-alpha (TNF-α; Abbexa Ltd, UK), and Total antioxidant capacity (TAC; Life span Bioscience Inc., USA) according to the manufacturer's instructions. All chemicals used were of the highest commercial grade available.

4.2.2.1. Anti-inflammatory assay (**carrageenan induced rat paw edema)**

Forty male Wistar rats (150-200 b) were divided randomly into eight groups (n=5). Group1 was kept as control negative (1ml saline per os), Group 2 served as control +ve injected with 0.1 ml carrageenan (1% w/v) at sub plantar region of the left hind paw according to the method of **winter et al. (1962)**, Group 3-8 were given oral administration of celecoxib (2mg/kg) **(El-Awdan et al.,2015)**, compounds **20**, **21**, **22**, **24** and drug **29** respectively in a dose of (2mg/kg) and thirty minutes later, groups 3-8 were injected with carrageenan. After 1, 3, and 5 hours of carrageenan injection, paw thickness was measured for all the rats using MNT-150 vernier calliper (Jiangsu Goldmoon Industry Co., Ltd.- Shanghai, China) and expressed in milliliters according to the method of **Ou et al. (2019)**. Edema rate and inhibition rate were calculated at the mentioned intervals using the following equations **(Khalifa et al., 2015)**:

Edema rate (%) = Tt - To/ To

Inhibition rate (%) = Ec - Et/ Ec

Where:

To is the thickness before carrageenan injection (ml).

Tt is the thickness at t hour after carrageenan injection (ml).

Ec is the edema rate of control group.

Et is the edema rate of treated group.

Four hours after 1% carrageenan injection, blood samples were collected from the retro-orbital plexus under anesthesia with a low dose of ketamine from the overnight fasted animals into sampling tubes. The blood samples were centrifuged at 3000 x g for 10 minutes at 4 ^{o}C. The sera were then kept at -80 ^{o}C until the assessment of inflammatory cytokines; PGE, IL-6, and TNF-α.

4.2.2.2. Assessment of inflammatory cytokines

PGE_2, IL-6 and TNF-α were determined using specific ELISA kits according to the manufacturer's instructions. All the parameters are measured using OD 450 nm.

4.3. Gastric ulcerogenic activity

Compounds **20**, **22**, and **29** were also evaluated for acute gastric ulcerogenic effect in the adult male albino rat. Rats were starved for 18 h prior and were divided into seven groups of six rats each and tested compounds, references (celecoxib and indomethacin), or saline as control were administered orally at a dose of 10 mg/kg body weight. Four hours after the treatment the animals were sacrificed, and their stomachs were removed and examined macroscopically using a magnifying lens. A longitudinal incision along the greater curvature was made with a fine scissor. The presence of single or multiple lesions, erosion, ulcer, or perforation was evaluated [38]. The number of ulcers and the occurrence of hyperemia were noted. The gastric lesions were stretched out and scored from 0 (no lesion) to 5 (3 or more marked ulcers), according to the method of Clementi et al.

4.4. Cardiovascular evaluation

The experiments were carried out on adult male albino Wister rats (170-200 g) obtained from the animal breeding unit at the National Research Centre. The animals were split into four groups with six animals in each one after housing at controlled temperature 25 ± 2 ^{o}C with normal light/dark cycles, where the applied protocol of caring and treatment was approved by the Research Ethical Committee of National Research Centre, which is a member of the Egyptian Network of Research Ethics Committees (ENREC) and which followed the recommendations of the National Institutes of Health (NIH) Guide for Care and Use of Laboratory Animals (NIH Publication No. 8023, revised 1978). A suspension of the tested compounds 22, 29, and celecoxib in 1% tween in saline was given orally to the groups at a dose of 100 mg/kg body weight. Only one group received saline to act as a control group. Administration of the drugs was continued for 2 weeks and, on the 15th day, collection of the blood samples from the retro-orbital plexus vein of all rats were executed. The clotting of the blood samples was carried out at room temperature followed by centrifugation at 1500 rpm for 10 min for serum separation. Storage of the serum samples was performed at -20 ^{o}C for analysis of LDH, CK-MB, and cTn-I [47-49]. Subsequently, the animals were sacrificed via cervical dislocation and cautiously dissected. The hearts were exposed by making an incision along the thorax followed by washing with ice-cold normal saline solution and dried with filter papers.

Rat Cardiac Troponin-I (cTn-I) ELISA kit was supplied by CusaBio, USA, with Catalog number CSB-E08594r, detection range 31.25-2000 pg/mL, detection wavelength 450 nm, inter-assay variability 10%, and intra-assay variability 8%. A Lactate dehydrogenase (LDH) kit was purchased from SPINREACT S.A.U. Spain. Detection wavelength of 340 nm. Creatine kinase-MB (CKMB) was obtained from SPINREACT S.A.U. Spain. Detection wavelength 340 nm. All other chemicals and reagents used were of analytical grade while celecoxib was purchased as Celebrex 100 mg

capsule. The biochemical parameters were assayed as following; Troponin-I (cTn-I) was measured in serum using ELISA kits according to the reported method [56-58]. While LDH and CK-MB levels were determined spectrophotometry according to reported procedures [59,60].

Statistical method

Statistical analysis was done by one-way analysis of variance (ANOVA) followed by Turkey test for confirmation and multiple comparison. $P < 0.05$ was assumed to denote statistical significance.

4.5. Docking Study

Docking the original ligand has been performed to validate the docking processes through determining the root mean square deviation (RMSD). COX 2 enzyme was prepared for docking process as follows: 1) the B chain and other co-crystallized ligand were removed. 2) The enzyme was 3D protonated, where hydrogen atoms were added at their standard geometry, surfaces and maps were computed and the system was optimized. Flexible ligand–rigid receptor docking of the most stable conformers was done with MOE-DOCK using triangle matcher as placement method and London dG as a scoring function. The obtained poses were subjected to forcefield refinement using the same scoring function. Ten of the most stable docking models for each ligand were retained with the best scored conformation.

4.6. Molecular Dynamics Simulation

NAMD 3.0.0. software was used for performing MD simulation. This software applies the Charmm-36 force field. Protein systems were built using the QwikMD toolkit of the VMD software, where the protein structure was checked for any missing hydrogens, the protonation states of the amino acid residues were set (pH = 7.4), and the co-crystalized water molecules were removed. Thereafter, the whole structure was embedded in an orthorhombic box of TIP3P water together with 0.15 M Na^+ and Cl^- ions in 20 Å solvent buffer. Afterward, the prepared systems

were energy minimized and equilibrated for 5 ns. For protein-ligand complexes, the top-scoring pose (8o) was used as a starting point for simulation. The parameters and topologies of the compounds were calculated by using the VMD plugin Force Field Toolkit (ffTK). Afterward, the generated parameters and topology files were loaded to VMD to readily read the protein–ligand complexes without errors and then conduct the simulation steps.

2. Binding Free Energy Calculations

Molecular Mechanics Poisson-Boltzmann Surface Area (MM-PBSA) embedded in the MMPBSA.py module of AMBER18 was utilized to calculate the binding free energy of the docked complex. 100 frames were processed from the trajectories in total, and the system's net energy was estimated using the following equation:

$$\Delta G_{\text{Binding}} = \Delta G_{\text{Complex}} - \Delta G_{\text{Receptor}} - \Delta G_{\text{Inhibitor}}$$

Each of the aforementioned terms requires the calculation of multiple energy components, including van der Waals energy, electrostatic energy, internal energy from molecular mechanics, and polar contribution to solvation energy.